

# Culturable fungi from urban soils in China II, with the description of 18 novel species in Ascomycota (Dothideomycetes, Eurotiomycetes, Leotiomycetes and Sordariomycetes)

Zhi-Yuan Zhang<sup>1,2</sup>, Xin Li<sup>1</sup>, Wan-Hao Chen<sup>3</sup>, Jian-Dong Liang<sup>3</sup>, Yan-Feng Han<sup>1</sup>

1 Institute of Fungus Resources, College of Life Sciences, Guizhou University, Guiyang 550025, China

2 College of Eco-Environmental Engineering, Guizhou Minzu University, Guiyang 550025, China

3 Basic Medical School, Guizhou University of Traditional Chinese Medicine, Guiyang 550025, China

Corresponding author: Yan-Feng Han (swallow1128@126.com)

## Abstract

As China's urbanisation continues to advance, more people are choosing to live in cities. However, this trend has a significant impact on the natural ecosystem. For instance, the accumulation of keratin-rich substrates in urban habitats has led to an increase in keratinophilic microbes. Despite this, there is still a limited amount of research on the prevalence of keratinophilic fungi in urban areas. Fortunately, our group has conducted in-depth investigations into this topic since 2015. Through our research, we have discovered a significant amount of keratinophilic fungi in soil samples collected from various urban areas in China. In this study, we have identified and characterised 18 new species through the integration of morphological and phylogenetic analyses. These findings reveal the presence of numerous unexplored fungal taxa in urban habitats, emphasising the need for further taxonomic research in urban China.



Academic editor: Huzeifa Raja

Received: 1 March 2023

Accepted: 14 June 2023

Published: 29 June 2023

**Citation:** Zhang Z-Y, Li X, Chen W-H, Liang J-D, Han Y-F (2023) Culturable fungi from urban soils in China II, with the description of 18 novel species in Ascomycota (Dothideomycetes, Eurotiomycetes, Leotiomycetes and Sordariomycetes). MycoKeys 98: 167–220. <https://doi.org/10.3897/mycokes.98.102816>

**Copyright:** © Zhi-Yuan Zhang et al.

This is an open access article distributed under terms of the Creative Commons Attribution License (Attribution 4.0 International – CC BY 4.0).

## Introduction

Biodiversity has always been a hot area of research in ecology and biology. Fungi represent one of the most diverse groups of microorganisms on the planet, with an essential role in ecosystem processes and functioning (Hyde et al. 2020a). At the same time, fungi have a significant influence on human society. On the one hand, they are able to produce a large number of secondary metabolites that can be used by humans, such as various antibiotics and enzymes (Uchida et al. 2005; Hoffmeister and Keller 2007; El-Gendi et al. 2022; Mapook et al. 2022). They also infect humans, animals and plants, bringing great harm to human health and the national economy (Fisher et al. 2012; Fisher et al. 2020; Fones et al. 2020). To date, the total number of fungal species is still a prolonged debate. While numerous studies have explored fungal diversity in marine, cave, forest, volcanic, mountain, desert, freshwater aquatic systems, lakes, grasslands and indoor environments (Hyde et al. 2020a), their distribution in urban environments seems to have been overlooked.

Urbanisation is an inevitable trend in humanity's development and is an important symbol of the progress made in science and technology (Wang et al. 2018). Urbanisation has swept across the globe over the last several decades (Berry 2008). The rate of urban expansion is currently at an unprecedented level and the migration of people from rural to urban regions leads to increased anthropogenic changes to the urban environment. These changes may include alterations in land use, the establishment of transportation networks and the management of urban soil and vegetation (Hoyt 1939; McDonnell and Pickett 1990; Antrop 2004). As urbanisation continues to expand worldwide (as noted by Rydin et al. 2012), urban soil fungi have become increasingly important in relation to human health and environmental concerns (Grimm et al. 2008). Due to the variety of urban soils, diverse habitats, rapid urbanisation and high population density, the study and investigation of the diversity of soil fungi in different cities in China will provide valuable scientific data for understanding their ecological functions and maintaining public health safety.

As the foundation of all fungal research, accurate identification and taxonomy for the fungal species are the primary and important task. Morphology is the traditional method for species classification. However, with the dramatic increase in species, it is very difficult to identify the fungal species from morphology alone. Recently, there has been an increase in the use of DNA barcoding or DNA classification methods to address the identification of specific taxa (Hebert et al. 2003; Tautz et al. 2003). ITS rDNA has been the common barcoding marker of fungal species (Schoch et al. 2012; Stielow et al. 2015; Vu et al. 2016). Polygenic phylogeny also has been used widely for species identification; for example, Wang et al. (2019) studied phylogenetic re-evaluation of *Thielavia* and proposed a new family and many new species. Hou et al. (2023) redisposition of acremonium-like fungi in Hypocreales combined morphological characterisation and multilocus phylogenetic analysis. Peng et al. (2023) reported eight new species of *Acrophialophora*, based on multilocus phylogenetic analysis. Therefore, the fungal taxonomy combining DNA-based approaches and morphological characterisation has been a widely accepted and used method (Orr et al. 2020).

In our investigation of keratinophilic fungi from urban soils in southern China, we have isolated and identified a large number of these fungi after using hair baiting enrichment treatment and reported several new taxa, for example, *Plectosphaerella guizhouensis* and *P. nauculaspora* (Zhang et al. 2019a), *Gongronella sichuanensis* (Zhang et al. 2019b), *Ctenomyces albus*, *C. obovatus* and *C. peltricolor* (Zhang et al. 2019c), *Geomycetes obovatus*, *Pseudogymnoascus sinensis* and *Solomyces sinensis* etc. (Zhang et al. 2020b), *Cunninghamella guizhouensis* (Zhang et al. 2020c), *Pseudogymnoascus catenatus*, *Solomyces guizhouensis* and *Zongqia sinensis* etc. (Zhang et al. 2021b), *Arthrographis multiformispora* (Li et al. 2022a), *Keratinophyton chongqingense* and *K. sichuanense* (Li et al. 2022b), *Pseudogeomyces lindneri* and *Pseudogymnoascus campensis* (Zhang et al. 2023a), *Paraneoaraneomyces sinensis* and *Pochonia sinensis* (Zhang et al. 2023b). Following our previous studies, based on morphological characters and polygenic analysis, 18 new species were identified and described in this study. The new taxa belong to six orders (Eurotiales, Hypocreales, Onygenales, Thelebolales, Venturiales and Xylariales), eight families (Arthrodermataceae, Aspergillaceae, Bionectriaceae, Microdochiaeae, Nectriaceae, Niessliaceae,

Sympoventuriaceae and Thelebolaceae) and 11 genera (*Aspergillus*, *Clonostachys*, *Cyanonectria*, *Echinocatena*, *Fusarium*, *Idriella*, *Nannizzia*, *Niesslia*, *Penicillium*, *Pseudogymnoascus* and *Talaromyces*) in the Pezizomycotina. This study helps in determining their ecological roles in the ecosystem and also contributes to the accumulation of new scientific resources for future research.

## Materials and methods

### Sample collection and fungal isolation

Soil samples were collected from the green belts of hospitals, parks and university campuses in some cities in southern China. Samples were collected from 3–10 cm below the soil surface, placed in Ziploc plastic bags, brought back to the laboratory and processed immediately. The soil samples were mixed with clean, sterile, chicken feathers, approximately 2 cm long and moistened with sterile water (Li et al. 2022b). The samples were then incubated in the dark at 23–27 °C for 1 month. For fungi isolation, 2 g of each of the collected samples was suspended in 20 ml of sterile water in a 50 ml sterile conical flask. The conical flasks were thoroughly shaken using a Vortex vibration meter. The suspension was then diluted to a concentration of 10<sup>-4</sup>. Then, 1 ml of the diluted sample was transferred to a sterile Petri dish and modified Sabouraud's dextrose agar (SDA; peptone 10 g/l, dextrose 40 g/l, agar 20 g/l, 3.3 ml of 1% Bengal red aqueous solution) medium containing 50 mg/l penicillin and 50 mg/l streptomycin was added and mixed. The plates were incubated at 25 °C for 1–2 weeks and single colonies were selected from the plates and inoculated to new potato dextrose agar (PDA, potato 200 g/l, dextrose 20 g/l, agar 20 g/l) plates. The ITS regions of all isolates were sequenced and BLASTn searched in NCBI and assigned to a potential genus and species. According to Zhang et al. (2021a), the strains whose ITS sequences are less than 97% in the similarities to the closest strain were recognised as potential new species, which were further identified by combining morphological characterisation and phylogenetic analyses.

### Morphological study

Strains of potentially new species were transferred to new plates of potato dextrose agar (PDA, Bio-way, China), malt extract agar (MEA, Bio-way, China) and oatmeal agar (OA, Bio-way, China) and were incubated at 25 °C for examining their colony morphology and microscopic morphology. The colony diameters and morphologies were determined after 14 days and the colony colours on the surface and reverse of inoculated Petri dishes were assessed according to the Methuen Handbook of Colour (Kornerup and Wanscher 1978). The characterisation and measurement of fungal microscopic characteristics were performed in 25% lactic acid. Images were obtained using an optical microscope (OM; DM4 B, Leica, Germany) with differential interference contrast (DIC). Taxonomic descriptions and nomenclature were deposited in MycoBank (<https://www.mycobank.org>; accessed on 25 May 2022). Type collections of the novel species are deposited in the Mycological Herbarium of the Institute of Microbiology, Chinese Academy of Sciences, Beijing, China (HMAS; (<https://nmdc.cn/fungarium/>). The ex-type living cultures and other isolates are deposited in the

China General Microbiological Culture Collection Center (CGMCC; <https://www.cgmcc.net/english/>; accessed on 7 April 2022) or at the Institute of Fungus Resources, Guizhou University (GZAC), Guiyang City, Guizhou, China.

### DNA extraction, PCR amplification and sequencing

Total genomic DNA was extracted from fungal mycelia using a BioTeke fungus genomic DNA extraction kit (DP2032, BioTeke, Beijing, China) following the manufacturer's instructions. The internal transcribed spacers (ITS) are widely used in fungal biodiversity and phylogenetic studies (Schoch et al. 2012; Stielow et al. 2015; Vu et al. 2016) and combining ITS and LSU improves species discrimination (Heeger et al. 2018; Vu et al. 2019); thus, ITS and the 28S nrRNA locus (LSU) sequences of all isolates were sequenced. In addition, more loci are often needed for specific taxa to obtain higher accuracy, so this study also amplified different loci for different taxa, such as  $\beta$ -tubulin (*TUB*), RNA polymerase II subunit (*RPB2*) and Twenty S rRNA accumulation (*TSR1*), translation elongation factor 1-alpha gene region (*EF1A*), calmodulin gene (*CaM*), partial  $\gamma$ -actin (*ACT*), DNA replication licensing factor (*MCM7*), translation elongation factor 3 (*TEF3*) and 60S ribosomal protein L10 (*RP 60S L1*) etc. (Table 1). The amplification reactions were performed in 25  $\mu$ l final volumes consisted of 2  $\mu$ l DNA template (10 ng/ $\mu$ l), 1  $\mu$ l forward primer (10  $\mu$ M), 1  $\mu$ l reverse primer (10  $\mu$ M), 12.5  $\mu$ l 2 $\times$  SanTaq PCR Master Mix (containing Taq polymerase, dNTP and Mg<sup>2+</sup>; Sangon Biotech Co., Ltd, Shanghai, China) and 8.5  $\mu$ l sterile water. The PCR was run using a T100 (Bio-Rad, California, USA) Thermal Cycler and the resulting amplified PCR products were sequenced in both directions using PCR primers. After amplification, the PCR products were visualised on a 1% agarose gel stained with ethidium bromide and the positive PCR products were then sent for sequencing to Sangon Biotech (Shanghai, China). The primer pairs and amplification conditions for each of the above-mentioned gene regions are provided in Table 1. All of the new sequences generated were deposited to GenBank (Suppl. material 1).

### Phylogenetic analysis

The collation of sequences (including name simplification and renaming) was performed using TBtools software (Chen et al. 2020). The sequence set was aligned by MAFFT v.7.037v (Katoh and Standley 2013), with sequence editing and trimming implemented in MEGA v.6.06 (Tamura et al. 2013). The "Concatenate Sequence" function in PhyloSuite v.1.16 (Zhang et al. 2020a) was used for the concatenation of loci. All concatenate data are provided in Suppl. material 3. For the phylogenetic construction of each loci dataset, both the Maximum Likelihood (ML) and the Bayesian Inference (BI) methods were used. The best-fit substitution model was selected using the Akaike Information Criterion correction (AICc), in ModelFinder (Kalyaanamoorthy et al. 2017). The ML analysis was implemented in IQ-TREE v.1.6.11 (Nguyen et al. 2015) with 10<sup>4</sup> bootstrap tests using the ultrafast algorithm (Minh et al. 2013). For Bayesian Inference, MrBayes v.3.2 (Ronquist et al. 2012) was used and Markov Chain Monte Carlo (MCMC) simulations were run for 5  $\times$  10<sup>7</sup> generations with

**Table 1.** Sequences of primers were used for the amplification of molecular markers in this study.

Molecular marker	Primer name	Primer sequence (5'-3')	Optimised PCR protocols	Reference
<i>ACT</i>	ACT-512F	ATGTGCAAGGCCGGTTCGC	94 °C: 5 min, (94 °C: 30 s, 55 °C: 50 s, 72 °C: 1 min) × 35 cycles 72 °C: 10 min	Carbone and Kohn (1999)
	ACT-783R	TACGAGTCCTCTGGCCCAT		
<i>CaM</i>	CF1	GCCGACTCTTGACYGARGAR	94 °C: 5 min, (94 °C: 30 s, 55 °C: 30 s, 72 °C: 1 min) × 35 cycles, 72 °C: 10 min	Peterson et al. (2005)
	CF4	TTTYTGCATCATRAGYTGGAC		
	CAL-CL1	GARTWCAAGGAGGCCTTCTC	94 °C: 5 min, (94 °C: 45 s, 55 °C: 45 s, 72 °C: 1 min) × 35 cycles, 72 °C: 10 min	O'Donnell et al. (2000)
	CAL-CL2A	TTTTTGCATCATGAGTTGGAC		
<i>EF1A</i>	983F	GCYCCYGGHCAUCGTGAYTTYAT	94 °C: 5 min, (94 °C: 30 s, 58 °C: 1 min 20 s, 72 °C: 1 min) × 35 cycles, 72 °C: 10 min	Rehner and Buckley (2005)
	2218R	ATGACACCRACRGCRACRGTYTG		
	EF-1	ATGGGTAAGGARGACAAGAC	94 °C: 5 min, (94 °C: 45 s, 55 °C: 45 s, 72 °C: 1 min) × 35 cycles, 72 °C: 10 min	O'Donnell et al. (1998)
	EF-2	GGARGTACCAAGTSATCATG		
<i>ITS</i>	ITS1	TCCGTAGGTGAACCTCGC	94 °C: 5 min, (94 °C: 30 s, 51 °C: 50 s, 72 °C: 45 s) × 35 cycles, 72 °C: 10 min	White et al. (1990)
	ITS4	TCCTCCGCTTATTGATATGC		
<i>LSU</i>	LR0R	ACCCGCTGAACCTAAC	94 °C: 5 min, (94 °C: 30 s, 51 °C: 1 min, 72 °C: 2 min) × 35 cycles, 72 °C: 10 min	Vilgalys and Hester (1990)
	LR7	TACTACCACCAAGATCT		
<i>MCM7</i>	Mcm7-709f	ACNMNGNTNTCVGAYGTHAARCC	94 °C: 5 min, (94 °C: 1 min, 55 °C: 1 min, 72 °C: 1 min 40 s) × 35 cycles 72 °C: 10 min	Schmitt et al. (2009)
	Mcm7-1348r	GAYTTDGCNACNCCNGGRTCWCCCAT		
<i>RP 60S L1</i>	60S-506F	GHGACAAGCGTTCTCNGG	94 °C: 5 min, (94 °C: 45 s, 55 °C: 50 s, 72 °C: 1 min) × 35 cycles 72 °C: 10 min	Stielow et al. (2015)
	60S-908R	CTTVAVYTGAACTTGATGGT		
<i>RPB2</i>	fRPB2-5F	GAYGAYMGWGATCAYTTYGG	94 °C: 5 min, (94 °C: 30 s, 54 °C: 40 s, 72 °C: 1 min 20 s) × 35 cycles, 72 °C: 10 min	Liu et al. (1999)
	RPB2-7cR	CCCATRGCTTGYTTRCCCAT		
	fRPB2-7cF	ATGGGYAARCAAGCYATGGG	94 °C: 5 min, (94 °C: 1 min, 50 °C: 2 min, 72 °C: 2 min 10 s) × 35 cycles 72 °C: 10 min	Liu et al. (1999)
	RPB2-3053bR	TGRATYTTRTCRTCSACCAT		
<i>TEF3</i>	EF3-3185F	TCYGGWGGHTGGAAGATGAAG	94 °C: 5 min, (94 °C: 45 s, 55 °C: 50 s, 72 °C: 1 min) × 35 cycles 72 °C: 10 min	Stielow et al. (2015)
	EF3-3188F	GGHGGHTGGAAGATGAAG		
	EF3-3538R	YTTGGTCTTGACACCNTC		
	EF3-3984R	TCRTAVSWGTTCTGAACCTT		
<i>TSR1</i>	F1526Pc	GARTAYCCBCARTCNGAGATGT	94 °C: 5 min, (94 °C: 30 s, 50 °C: 30 s, 72 °C: 1 min) × 35 cycles, 72 °C: 10 min	Houbraken et al. (2011b)
	R2434	ASAGYTGVARDGCCTTRAACCA		
<i>TUB</i>	BT-2a	GGTAACCAAATCGGTGCTGCTTC	94 °C: 5 min, (94 °C: 30 s, 58 °C: 50 s, 72 °C: 1 min) × 35 cycles 72 °C: 10 min	Glass and Donaldson (1995)
	Bt-2b	ACCCTCAGTGTAGTGACCCCTGGC		
	TUB2Fd	GTBCACCTYCARACCGGYCARTG	94 °C: 5 min, (94 °C: 30 s, 52 °C: 30 s, 72 °C: 30 s) × 35 cycles 72 °C: 10 min	Woudenberg et al. (2009)
	TUB4Fd	CCRGAYTGRCCRAARACRAAGTTGC		
	Btub526_F	CGAGCGYATGAGYGTACTT	94 °C: 5 min, (94 °C: 30 s, 53 °C: 45 s, 72 °C: 1 min 30 s) × 35 cycles 72 °C: 10 min	Jewell and Hsiang (2013)
	Btub1332_R	TCATGTTCTGGGGTCGAA		

a sampling frequency of every 10<sup>3</sup> generations and a burn-in of 25%. The above analyses were carried out in PhyloSuite v.1.16 (Zhang et al. 2020a). Tracer v.1.7 (Rambaut et al. 2018) was used to assess the convergence and effective sampling between all runs; the obtained effective sample size (ESS) values were all greater than 200, indicating that effective sampling occurred. The final trees were visualised in FigTree 1.4.23 and edited in Microsoft Paint.

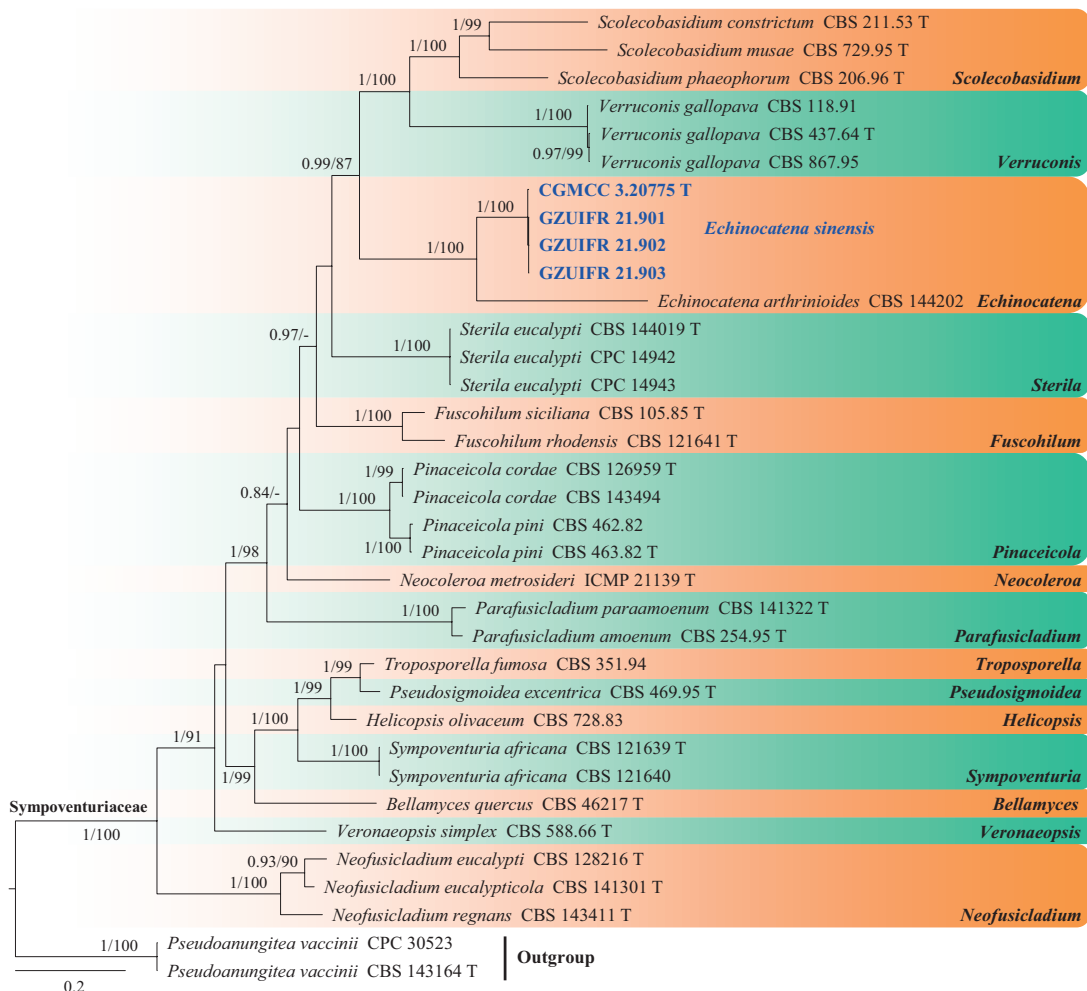


**Figure 1.** Concatenated phylogeny of the ITS, LSU, EF1A, TUB and RPB2 gene regions of species in Sympoventuriaceae. Thirty-five strains are used. The tree is rooted with *Pseudoanungitea vaccinii* (CPC 30523) and *P. vaccinii* (CBS 143164). The tree topology of the BI was similar to the ML analysis. Bayesian posterior probability ( $\geq 0.8$ ) and ML bootstrap values ( $\geq 80\%$ ) are indicated along branches (PP/ML). Novel species are in blue and bold font and "T" indicates type derived sequences.

## Taxonomy

**Dothideomycetes O.E. Erikss. & Winka.**

**Venturiales Yin. Zhang, C.L. Schoch & K.D. Hyde.**

**Sympoventuriaceae Yin. Zhang, C.L. Schoch & K.D. Hyde.**

***Echinocatena* R. Campb. & B. Sutton.**

The establishment of the genus *Echinocatena* dates back to 1977, with *E. arthrinoides* being the only valid species to date. This species was isolated from the apoplastic leaves of an unknown plant (Campbell and Sutton 1977).

***Echinocatena sinensis* Zhi.Y. Zhang, Y.F. Han & Z.Q. Liang, sp. nov.**

Mycobank No: 844151

Fig. 2

**Etymology.** The epithet refers to the locality where the type specimen was found, China.

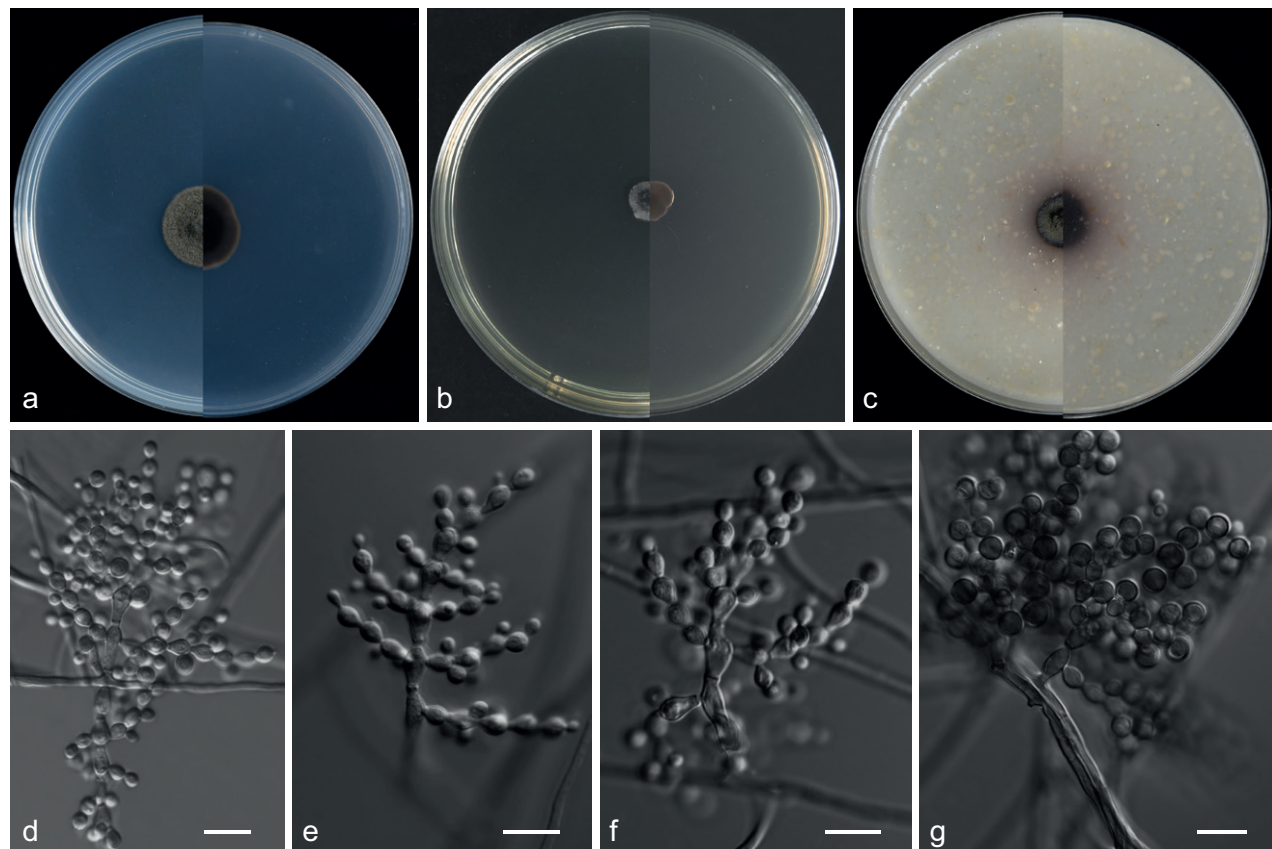


**Figure 2.** *Echinocatena sinensis* (from ex-holotype CGMCC 3.20775) **a–c** upper and reverse views of cultures on PDA, MEA and OA 14 d after inoculation **d–g** phialides and conidia. Scale bars: 10 µm (**d–g**).

**Type.** CHINA: Guangxi Zhuang Autonomous Region, Baise City, Peninsula Park 23°89'96"N, 106°63'29"E, from soil, 30 Aug 2019, Z.Y. Zhang (HMAS 351873 holotype designated here, ex-type living culture CGMCC 3.20775 = GZUIFR 21.900); ibid., GZUIFR 21.901.

**Description. Culture characteristics** (14 days at 25 °C): **Colony on PDA** 16–18 mm diam. after 14 d at 25 °C, dark olive green (2F2), flat, texture velvety, nearly round, margin entire; reverse dark slate grey (3F2). **Colony on MEA** 8–9 mm diam., dark slate grey (3F1), convex, texture velvety, irregularity, margin entire; reverse dark slate grey (3F2). **Colony on OA** 10–12 mm diam., dark slate grey, flat (3F2), texture velvety, nearly round, margin entire, soluble pigments brown to pale red exudates absent; reverse dark pink (12F1).

**Hypphae** branched, septate, hyaline, smooth, 1.0–3.5 µm diam. **Conidiophores** erect or with an acute angle to the axis near the apex, solitary, unbranched, 9.5–49.0 × 1.0–5.0 µm, hyaline, smooth, 1–8-septate, straight to flexuous. **Conidiogenous cells** in simple or branched acropetal chains, 4.0–8.5 × 3.0–5.0 µm, separated by thick, dark brown, refractive septa, appearing like a separating cell, pale brown, doliform to cylindrical, constricted at the septa, polyblastic, integrated with 3–5 conidiogenous loci. **Conidia** solitary, pyriform, sometimes spherical, aseptate, smooth, brown, 3.5–7.0 × 3.5–7.0 µm (av. 4.9 × 5.3 µm, n = 50). **Sexual morph** not observed.

**Additional specimens examined.** CHINA: Guangxi Zhuang Autonomous Region, Baise City, Youjiang Campus of Baise University 23°89'10"N, 106°60'86"E, from soil, 30 Aug 2019, Z.Y. Zhang, GZUIFR 21.902, ibid., GZUIFR 21.903.

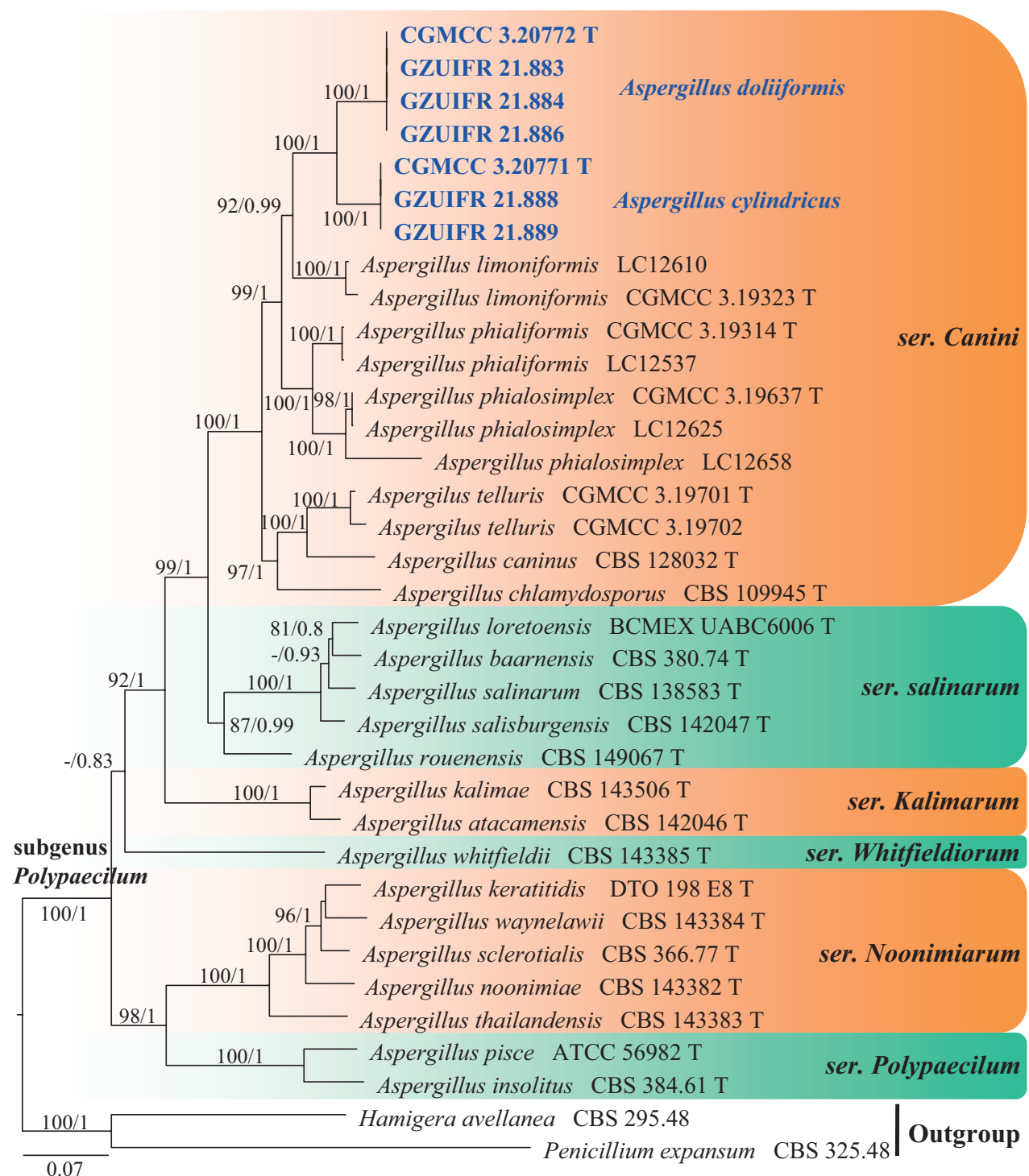


**Figure 3.** Concatenated phylogeny of the ITS, TUB, CaM, RPB2 and TSR1 gene regions of species in *Aspergillus* from subgenus *Polypaecilum*. Thirty-five strains are used. The tree is rooted in *Hamigera avellanea* (CBS 295.48) and *Penicillium expansum* (CBS 325.48). The tree topology of the BI was similar to the ML analysis. Bayesian posterior probability ( $\geq 0.8$ ) and ML bootstrap values ( $\geq 80\%$ ) are indicated along branches (PP/ML). Novel species are in blue and bold font and "T" indicates type derived sequences.

**Notes.** Currently, one species is accepted in *Echinocatena* (Campbell and Sutton 1977; Shen et al. 2020). The phylogenetic analyses, based on the combined ITS, LSU, EF1A, TUB and RPB2 dataset, indicate *Echinocatena sinensis* and *E. arthrinioides* group in a distinct clade (Fig. 1). The morphology of *E. sinensis*

is very similar to *Echinocatena* in having straight to flexuous conidiophores, polyblastic conidiogenous cells, spherical, aseptate conidia (Campbell and Sutton 1977). *Echinocatena sinensis* can be distinguished from *E. arthrinoides* by its conidia that are smooth and pyriform in shape (Campbell and Sutton 1977), as well as by the low sequence similarity between the two species (ITS: 312/403, 77.4% similarity, 25 gaps; LSU: 787/827, 95.2% similarity, 4 gaps).

**Eurotiomycetes O.E. Erikss. & Winka**  
**Eurotiales G.W. Martin ex Benny & Kimbr.**  
**Aspergillaceae Link**  
***Aspergillus* P. Micheli ex Haller**

Micheli (1729) erected the genus *Aspergillus*, whose members can be identified by their aspergillum-like spore-bearing structure (Samson et al. 2014). Currently, the genus *Aspergillus* comprises six subgenera and 27 sections (Houbraken et al. 2020). In this study, two new species are described: *A. cylindricus* and *A. doliformis*.

***Aspergillus cylindricus* Zhi.Y. Zhang, Y.F. Han & Z.Q. Liang, sp. nov.**

Mycobank No: 844152

Fig. 4

**Etymology.** Referring to the cylindrical phialides.

**Type.** CHINA: Shanghai Municipality, Ruijin Hospital, Shanghai Jiao Tong University School of Medicine 31°21'29"N, 121°46'75"E, from soil, 15 Aug 2019, Z.Y. Zhang (HMAS 351868 holotype designated here, ex-type living culture CG-MCC 3.20771 = GZUIFR 21.887); ibid., GZUIFR 21.888.

**Description.** **Culture characteristics** (14 d at 25 °C): **Colony on PDA** 12–13 mm diam., pinkish-white (10A1), velvety to floccose, margin slightly undulate; reverse chrome orange (6A6) to yellowish-white (2A2) from centre to margin. **Colony on MEA** 15–17 mm diam., bluish-white (1A2), felty, margin dentate; reverse mandarin orange (6B8). **Colony on OA** 26–27 mm diam., white (4A1), velvety to floccose, margin slightly undulate; reverse brownish-yellow (5C8) to grey (5C1) from centre to margin.

**Conidiophores** solitary phialides borne laterally or terminally on vegetative hyphae, sometimes occurring in branched hyphal resembling branched conidiophores. **Phialides** mono- to polyphialidic, hyaline, cylindrical to lageniform, sometimes curved irregularly, swollen towards the base or above the mid-section, neck cylindrical or broadly tapering, sometimes extending sympodially from the neck, 2.0–21.0 × 1.0–5.0 µm. **Conidia** borne solitary or in chains with pronounced connectors, hyaline, smooth or roughened, ellipsoid to subglobose, pyriform, 3.0–7.5 × 2.5–5.5 µm (av. 5.3 × 4.5 µm, n = 50). **Sexual morph** not observed.

**Additional specimens examined.** CHINA: Shanghai Municipality, South Campus of Fudan University 31°29'30"N, 121°50'03"E, soil, 16 Aug 2019, Z.Y. Zhang, GZUIFR 21.889.

**Notes.** Phylogenetic and morphological data (Figs 3, 4) support our isolates CGMCC 3.20771, GZUIFR 21.888 and GZUIFR 21.889 as new species of subgenus *Polypaecilum*, series *Canini*. *Aspergillus cylindricus* is phylogenetically

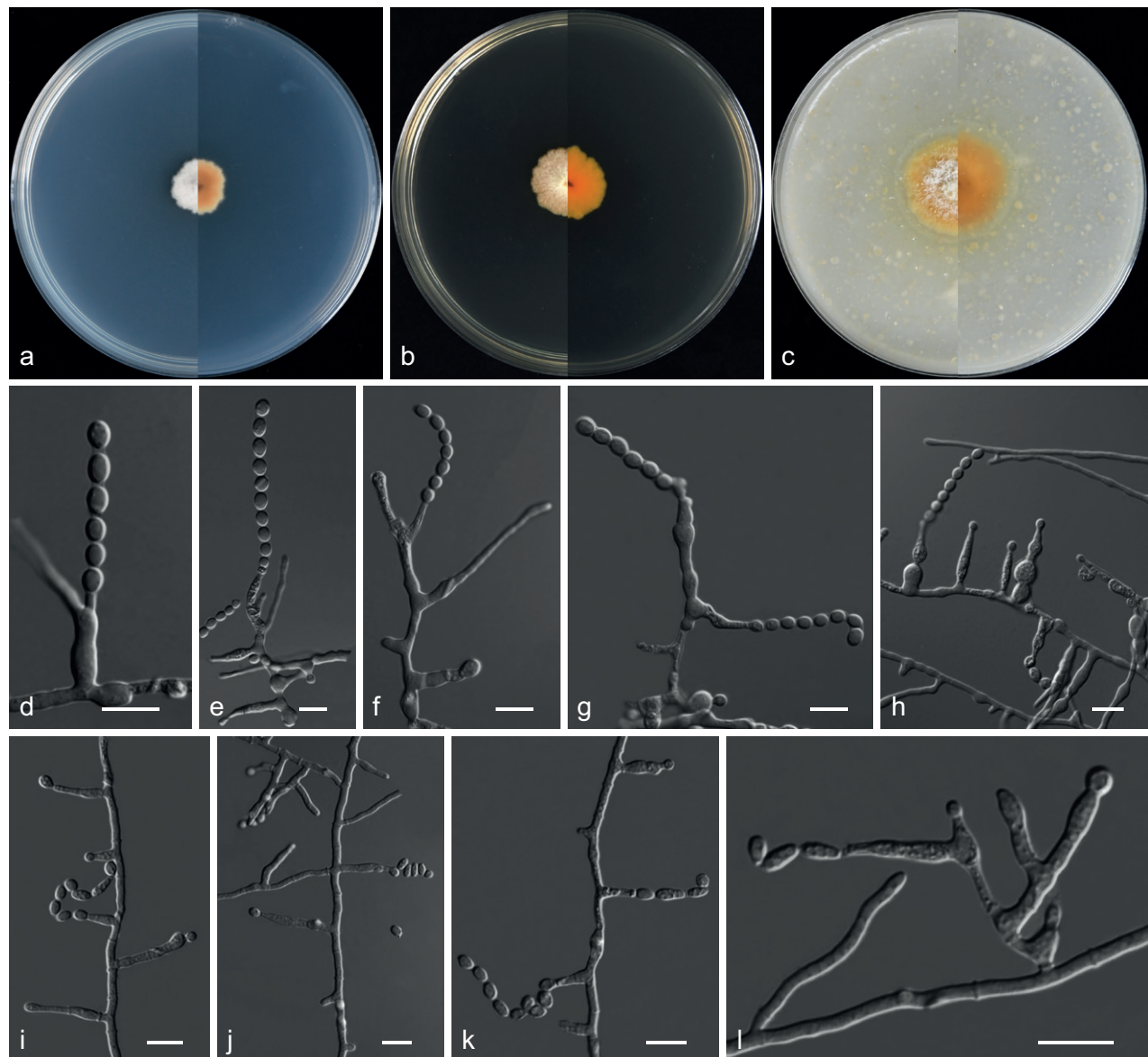


**Figure 4.** *Aspergillus cylindricus* (from ex-holotype CGMCC 3.20771) **a–c** upper and reverse views of cultures on PDA, MEA and OA 14 d after inoculation **d–l** phialides and conidia. Scale bars: 10 µm (**d–l**).

closely related to *A. doliformis* and *A. limoniformis*. However, they can be distinguished by their sequence similarity (94% 498/531; 99% 846/853; 88% 394/448; 92% 767/834; 92% 723/788 similarity of ITS, LSU, TUB, RPB2 and TSR1 in *A. limoniformis* CGMCC 3.19323; 94% 524/554, 99% 1337/1341, 91% 419/458, 94% 1007/1069, 92% 772/843, 91% 629/692 similarity of ITS, LSU, TUB, RPB2, TSR1 and CaM in *A. doliformis* CGMCC 3.20772). Morphologically, the conidia of *A. limoniformis* are limoniform or subglobose, rather than ellipsoid to subglobose, pyriform in *A. cylindricus* (Zhang et al. 2021a). On the other hand, *A. cylindricus* has longer phialides than *A. limoniformis* (2.0–21.0 µm vs. 4.0–10.0 µm) (Zhang et al. 2021a). Furthermore, conidia of *A. doliformis* are lantern, subglobose to globose, obpyriform rather than ellipsoid to subglobose, pyriform in *A. cylindricus*. The conidiophores of *A. cylindricus* are sometimes occurring in branched hyphae resembling branched conidiophores, while the conidiophores of *A. doliformis* are borne laterally or terminally on vegetative hyphae (see description of *A. doliformis*).

***Aspergillus doliiiformis* Zhi.Y. Zhang, Y.F. Han & Z.Q. Liang, sp. nov.**

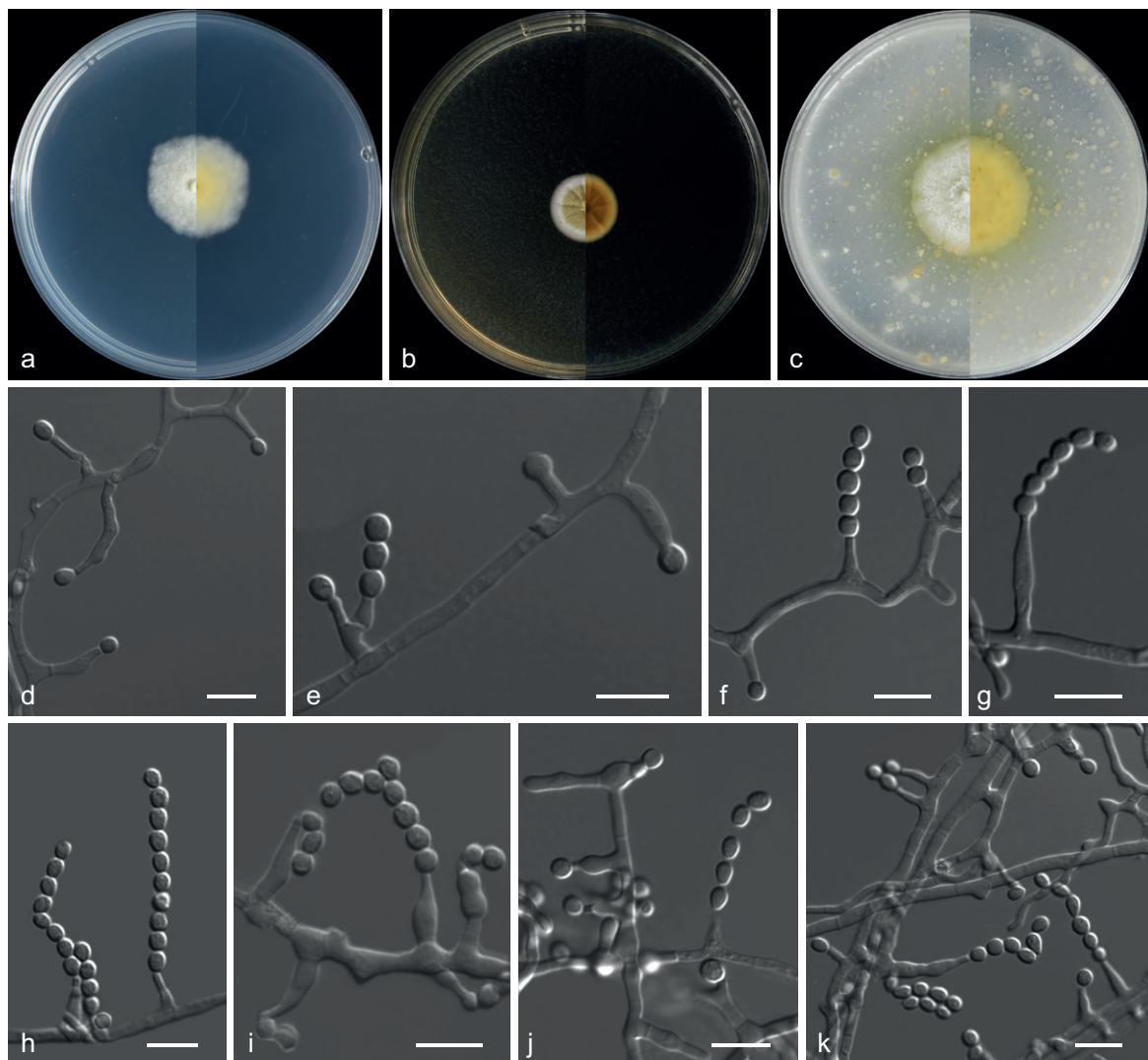
Mycobank No: 844153

Fig. 5

**Etymology.** Referring to the lantern shape of conidia.

**Type.** Hainan Province, Haikou City, Haidian Campus of Hainan University 20°05'76"N, 110°32'91"E, from soil, 28 Aug 2019, Z.Y. Zhang (HMAS 351867 holotype designated here, ex-type living culture CGMCC 3.20772 = GZUIFR 21.885); ibid., GZUIFR 21.883.

**Description. Culture characteristics** (14 d at 25 °C): **Colony on PDA** 23–26 mm diam., white (1A1), felty, fluffy, margin slightly undulate; reverse pale yellow (1A3) to white (1A1) from centre to margin. **Colony on MEA** 16 mm diam., white (1A1) at margin, olive yellow (2D8) at centre, felty, margin entire; reverse oak brown (5D6) to brownish-grey (5D2) from centre to margin. **Colony on OA** 26–27 mm diam., white (1A1), flocculent, margin entire, producing a diffusible faint yellow pigment; reverse greyish-yellow (2B4).



**Figure 5.** *Aspergillus doliiiformis* (from ex-holotype CGMCC 3.20772) **a–c** upper and reverse views of cultures on PDA, MEA and OA 14 d after inoculation **d–k** phialides and conidia. Scale bars: 10 µm (d–k).

**Hyphae** hyaline, septate, smooth, branched, 1.0–3.5 µm wide. **Conidiophores** solitary phialides borne laterally or terminally on vegetative hyphae. **Phialides** mono- to polyphialidic, hyaline, ampulliform, campaniform, cylindrical or tapering with an enlarged base, sometimes curved irregularly, occasionally branched, neck cylindrical or broadly tapering, sometimes extending sympodially from the necks, 2.5–18.0 × 1.0–5.0 µm. **Conidia** borne solitary or formed in long chains, hyaline, smooth or roughened, lantern, subglobose to globose, obpyriform, 3.0–5.0 × 2.5–4.5 µm (av. 4.2 × 3.4 µm, n = 50). **Sexual morph** not observed.

**Additional specimens examined.** CHINA: Hainan Province, Haikou City, Hainan General Hospital 20°00'57"N, 110°28'78"E, from soil, 28 Aug 2019, Z.Y. Zhang, GZUIFR 21.884; Haikou People's Park, soil, 28 Aug 2019, Z.Y. Zhang, GZUIFR 21.886.

**Notes.** *Aspergillus doliformis* represents a new lineage within the subgenus *Polypaecilum*, series *Canini*, forming a fully supported clade (ML = 100%; PP = 1.0). *A. doliformis* is phylogenetically closely related to *A. limoniformis* and *A. cylindricus*. However, *A. doliformis* can be distinguished from *A. limoniformis* by their sequence similarity (93% 502/539; 99% 847/853; 87% 370/423; 91% 762/834; 92% 724/791 similarity of ITS, LSU, TUB, RPB2 and TSR1 in *A. limoniformis* CGMCC 3.19323). Morphologically, the conidia of *A. limoniformis* are limoniform or subglobose, rather than lantern, subglobose to globose, obpyriform in *A. doliformis* (Zhang et al. 2021a). In addition, the distinction between *A. doliformis* and *A. cylindricus* is shown in the notes of *A. cylindricus*.

### ***Penicillium* Link**

The genus *Penicillium* was established in 1809 (Link 1809) and its members are widespread, occurring in abundance in soil, air, indoor environments and contaminated foods (Visagie et al. 2014; Barbosa et al. 2018). Currently, this genus comprises two subgenera and 32 sections (Houbraken et al. 2020). In the present study, one new species is described: *P. fujianense*.

#### ***Penicillium fujianense* Zhi.Y. Zhang, Y.F. Han & Z.Q. Liang, sp. nov.**

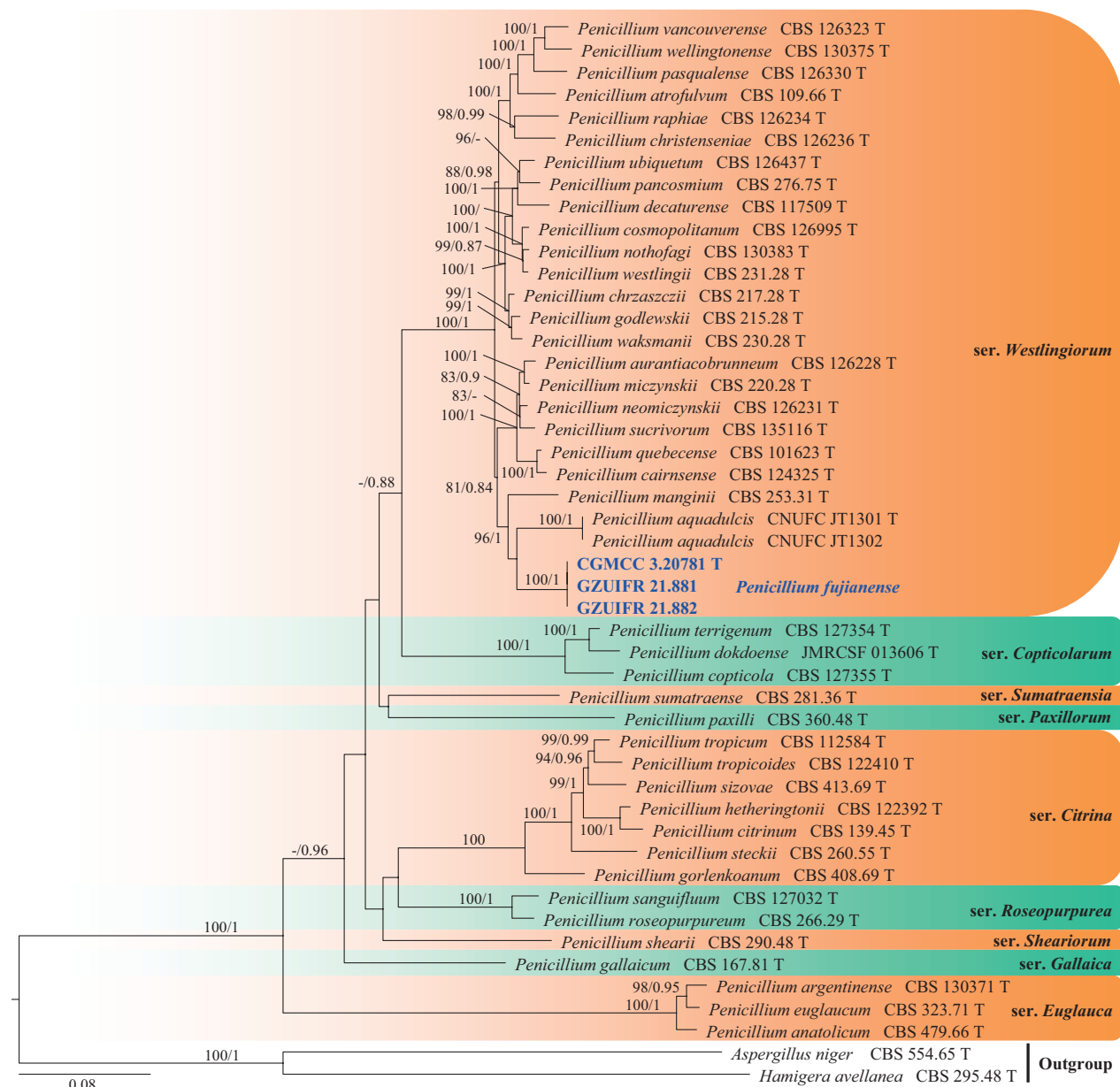
Mycobank No: 844154

Fig. 7

**Etymology.** Referring to its origin, isolated from Fujian Province, China.

**Type.** CHINA: Fujian Province, Xiamen City, Jimei University 24°58'25"N, 118°09'46"E, soil, 18 Aug 2019, Z.Y. Zhang (HMAS 351866 holotype designated here, ex-type living culture CGMCC 3.20781 = GZUIFR 21.880).

**Description. Culture characteristics** (14 d at 25 °C): **Colony on PDA** 18–21 mm diam., white, mycelium inconspicuous, texture velvety, sporulation dense, conidial area dark green (28F8), margin irregular, soluble pigments and exudates absent; reverse milk white (1A2). **Colony on MEA** 18–25 mm diam., white, texture velvety, sporulation dense, conidial area greenish-white (28A2), margin irregular, soluble pigments and exudates absent; reverse orange (5A7). **Colony on OA** 72 mm diam., surrounded by an orange halo, mycelium white, texture velvety, sporulation dense, conidia area masse dark green (26F4), margins entire, soluble pigments light brown, exudates absent; reverse butter yellow (4A5).



**Figure 6.** Concatenated phylogeny of the ITS, TUB, CaM, RPB2 and TSR1 gene regions of species in *Penicillium* from section *Citrina*. Forty-eight strains are used. The tree is rooted in *Aspergillus niger* (CBS 554.65) and *Hamigera avellanea* (CBS 295.48). The tree topology of the BI was similar to the ML analysis. Bayesian posterior probability ( $\geq 0.8$ ) and ML bootstrap values ( $\geq 80\%$ ) are indicated along branches (PP/ML). Novel species are in blue and bold font and “T” indicates type derived sequences.

**Hyphae** hyaline, septate, smooth, branched, 1.0–4.0  $\mu\text{m}$  wide. **Conidiophores** biverticillate and occasionally with an additional divergent branch, stipes variable in length, 10–74  $\mu\text{m}$  long, smooth, 2.0–3.5  $\mu\text{m}$  wide. **Metulae** divergent, 2–6 per stipe, slightly inflated at the apex, 10.5–20  $\times$  2.0–4.0  $\mu\text{m}$ . **Phialides** ampulliform to cylindrical with a short neck, stout, 4.0–11.0  $\times$  2.0–3.5  $\mu\text{m}$ . **Conidia** subglobose to globose, ellipsoidal, finely roughened, 2.0–4.5  $\times$  2.0–3.5  $\mu\text{m}$  (av. 3.8  $\times$  3.2  $\mu\text{m}$ ,  $n = 50$ ). **Sexual morph** not observed.

**Additional specimens examined.** CHINA: Fujian Province, Xiamen City, Wuyuanbay Wetland Park 24°51'52"N, 118°17'48"E, soil, 19 Aug 2019, Z.Y. Zhang, GZUIFR 21.881, ibid., GZUIFR 21.882.

**Notes.** *Penicillium fujianense* represents a new lineage in the subgenus *Aspergilloides*, section *Citrina* and *Westlingiorum* series, forming a strongly supported clade (ML = 100%; PP = 1.0), closely related to *P. manginii* and *P. aquadulcis* (Fig. 6). However, *P. fujianense* distinguished from *P. manginii* by its absent sclerotia (Houbraken et al. 2011a). *P. fujianense* can be distinguished from *P. aquadulcis* by their conidial shape and size (subglobose to globose, ellipsoidal, 3.8 × 3.2 µm in *P. fujianense*; globose to subglobose, 2–2.5 µm in *P. aquadulcis*) (Thuong et al. 2021). Furthermore, in a comparison of ITS, BenA and CaM nucleotides, *P. fujianense* (Type strain CGMCC 3.20781) has 98%, 94% and 92% similarity, in ITS (504/512 bp, one gap), BenA (401/427, no gap) and CaM (516/559, three gaps), which is different from *P. manginii* (Type strain CBS 253.31). Additionally, *P. fujianense* (Type strain CGMCC 3.20781) has 97%, 93% and 91% similarity, in ITS (527/543 bp, four gaps), BenA (410/441, no gap) and CaM (545/598, 15 gaps), which is different from *P. aquadulcis* (Type strain CNUFC JT1301). DNA sequencing and multigene phylogeny provide the most reliable identification of this species.

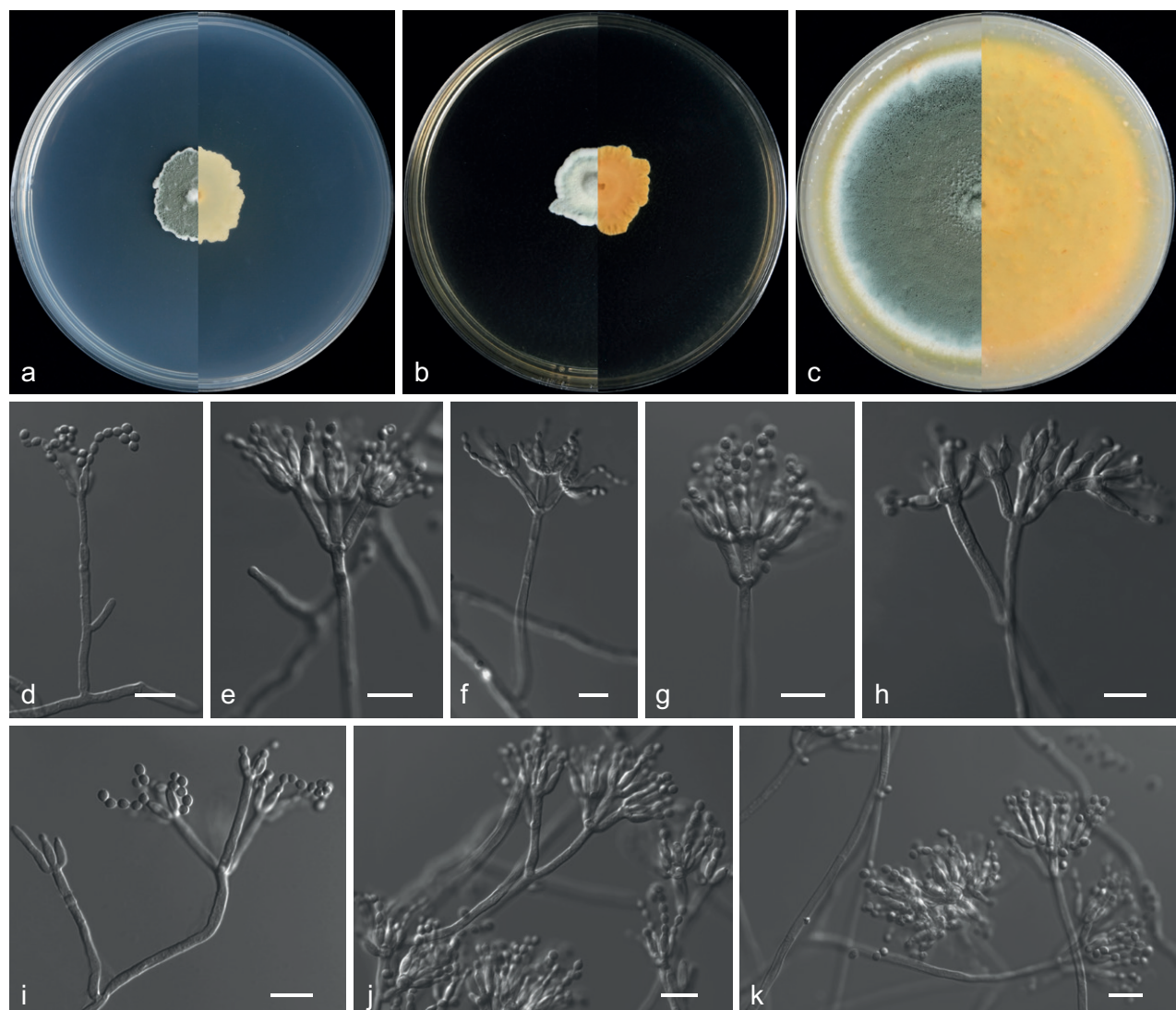


**Figure 7.** *Penicillium fujianense* (from ex-holotype CGMCC 3.20781) **a–c** upper and reverse views of cultures on PDA, MEA and OA 14 d after inoculation **d–k** phialides and conidia. Scale bars: 10 µm (**d–k**).

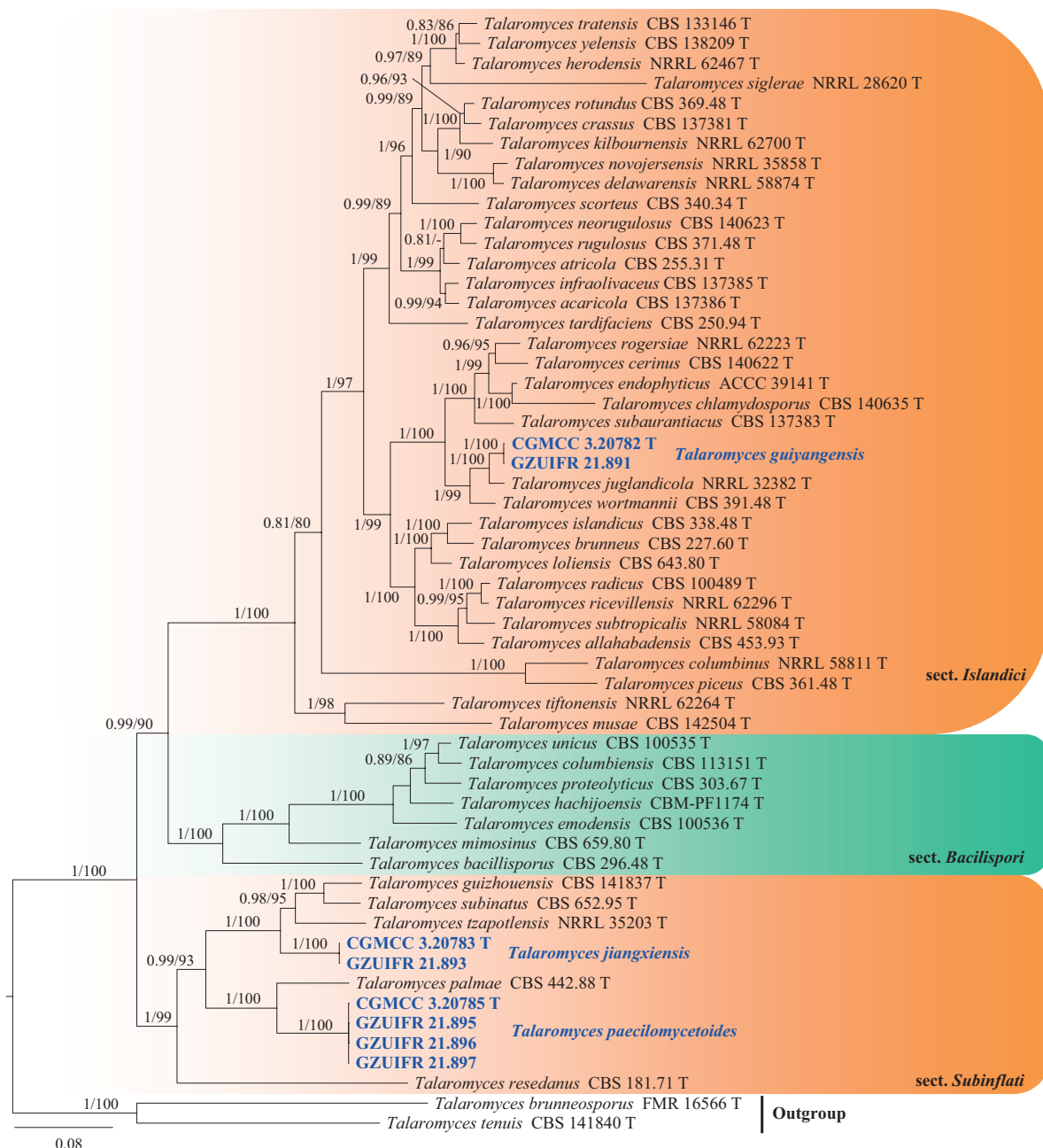


**Figure 8.** Concatenated phylogeny of the ITS, TUB, CaM and RPB2 gene regions of species in *Talaromyces* from sections *Islandici*, *Bacilispori* and *Subinflati*. Fifty-six strains are used. The tree is rooted with *Talaromyces brunneosporus* (FMR 16566) and *T. tenuis* (CBS 141840). The tree topology of the BI was similar to the ML analysis. Bayesian posterior probability ( $\geq 0.8$ ) and ML bootstrap values ( $\geq 80\%$ ) are indicated along branches (PP/ML). Novel species are in blue and bold font and "T" indicates type derived sequences.

#### *Talaromyces* C.R. Benj.

The genus *Talaromyces* was erected in 1955 to accommodate sexual species in the genus *Penicillium* (Benjamin 1955). Members of the genus *Talaromyces* have a worldwide distribution and colonises many substrates, predominantly soil (Sun et al. 2020). Currently, the genus *Talaromyces* includes eight sections, *Bacillispori*, *Helici*, *Islandici*, *Purpurei*, *Tenues*, *Subinflati*, *Talaromyces* and *Trachyspermi* (Yilmaz et al. 2014; Sun et al. 2020). In this study, three new species are described *T. guiyangensis*, *T. jiangxiensis* and *T. paecilomycetoides*.

***Talaromyces guiyangensis* Zhi.Y. Zhang, Y.F. Han & Z.Q. Liang, sp. nov.**

Mycobank No: 844155

Fig. 9

**Etymology.** Referring to its origin, isolated from Guiyang City, China.

**Type.** CHINA: Guizhou Province, Guiyang City, Qianlingshan Park 26°59'03"N, 106°69'57"E, soil, 13 Sept 2019, Z.Y. Zhang (HMAS 351869 holotype designated here, ex-type living culture CGMCC 3.20782 = GZUIFR 21.890).

**Description. Culture characteristics** (14 d at 25 °C): **Colony on PDA** 32–34 mm diam., moderately deep, mycelium white, primrose, velutinous, planar, margins entire and slightly undulate, sporulation dense, conidial area dark green (29F8), soluble pigments and exudates absent; reverse light yellow (4A5) to rust brown (6E8) from margin to the centre. **Colony on MEA** 34–38 mm diam., moderately deep, sunken at the centre, mycelium white, texture velutinous, sporulation dense, conidial area dark green (29F8), soluble pigments and exudates absent; reverse pale green (30A3). **Colony on OA** 32–33 mm diam., moderately deep, mycelium white, margins high, narrow, entire, white (1A1), conidial area grey (29F1), soluble pigments and exudates absent; reverse pastel yellow (1A4).

**Hyphae** hyaline, septate, smooth, branched, 1.0–3.0 µm wide. **Conidiophores** smooth, biverticillate, stipes smooth, bearing terminal biverticillate penicillin.

**Metulae** 3–5, divergent, 8.5–13.5 × 2.0–3.0 µm. **Phialides** 2–5, acerose, 9.0–13.0 × 1.5–2.5 µm, with long gradually tapering collula. **Conidia** spiny, fusiform, pyriform, 3.0–6.0 × 2.5–3.0 µm (av. 4.5 × 2.8 µm, n = 50). **Sexual morph** not observed.

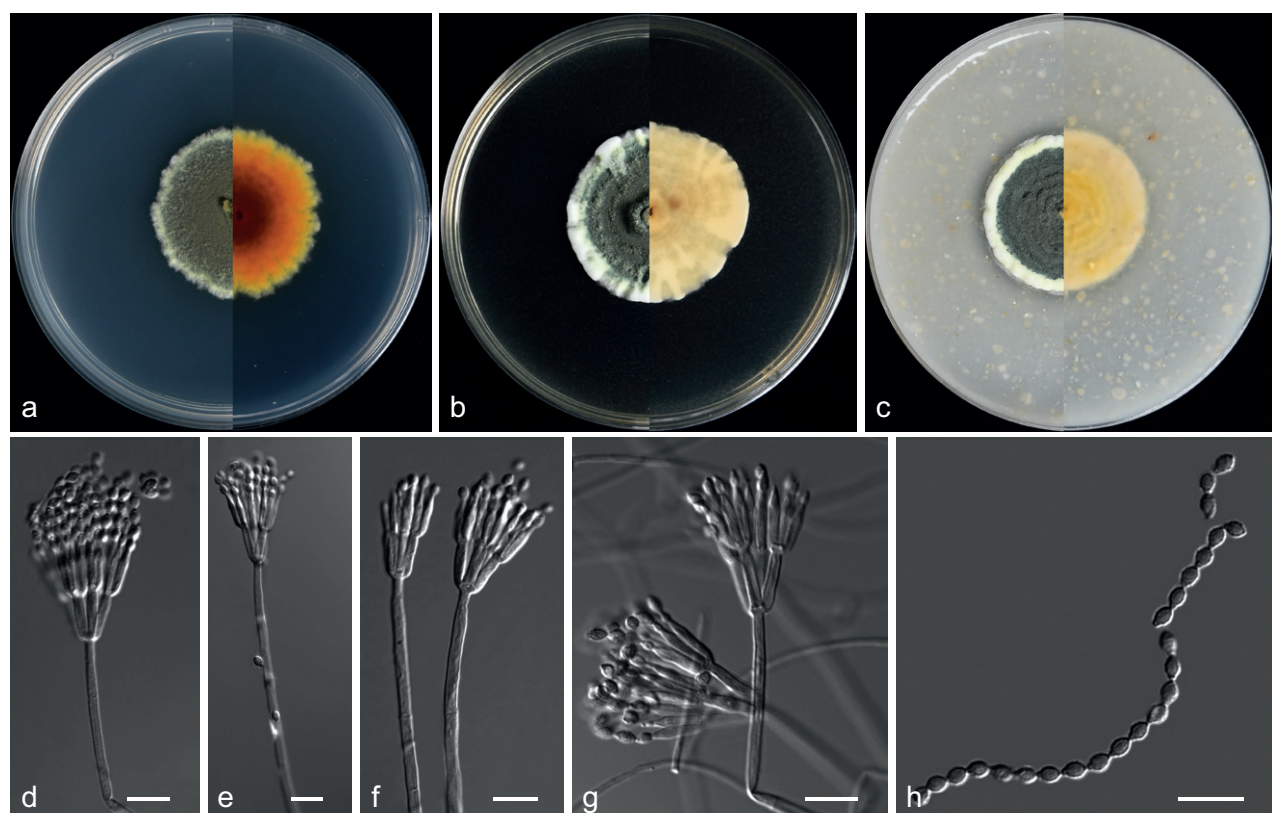


**Figure 9.** *Talaromyces guiyangensis* (from ex-holotype CGMCC 3.20782) **a–c** upper and reverse views of cultures on PDA, MEA and OA 14 d after inoculation **d–g** phialides and conidia **h** conidia chain. Scale bars: 10 µm (d–h).

**Additional specimens examined.** CHINA: Guizhou Province, Guiyang City, North Campus of Guizhou University 26°44'37"N, 106°67'46"E, soil, 13 Sept 2019, Z.Y. Zhang, GZUIFR 21.891.

**Notes.** *Talaromyces guiyangensis* represents a new lineage in the section *Islandici*, forming a strongly-supported clade (ML = 100%; PP = 1.0), closely related to *T. juglandicola* and *T. wortmannii* (Fig. 8). However, *T. guiyangensis* differs from *T. juglandicola* by its fusiform, pyriform conidia and does not produce exudate or droplets on PDA or MEA (Peterson and Jurjević 2017). In addition, *Talaromyces wortmannii* differs from *T. guiyangensis* in the presence of ascocarps and ascospores, which are not observed in *T. guiyangensis*. Furthermore, the conidia of *T. wortmannii* are ellipsoidal, whereas those of *T. guiyangensis* are fusiform or pyriform (Yilmaz et al. 2014).

***Talaromyces jiangxiensis* Zhi.Y. Zhang, Y.F. Han & Z.Q. Liang, sp. nov.**

Mycobank No: 844156

Fig. 10

**Etymology.** Referring to its origin, isolated from Nanchang City, Jiangxi Province, China.

**Type.** CHINA: Jiangxi Province, Nanchang City, Nanchang People's Park 28°68'12"N, 115°91'35"E, soil, 13 Aug 2019, Z.Y. Zhang (HMAS 351870 holotype designated here, ex-type living culture CGMCC 3.20783 = GZUIFR 21.892); ibid., GZUIFR 21.893.

**Description. Culture characteristics** (14 d at 25 °C): **Colony on PDA** 50–51 mm diam., moderately deep, plane, mycelium white, planar, sporulation dense, margins entire, slightly undulate, conidial area dark green (30F3), soluble pigments and exudates absent; reverse white (30A3). **Colony on MEA** 26–33 mm diam., moderately deep, mycelium pale goldenrod at the centre, white at the edge, texture velvety, margins irregular, sporulation dense, conidial area yellowish-white (1A2), soluble pigments and exudates absent; reverse greyish-yellow (2C3). **Colony on OA** 32–33 mm diam., moderately deep, mycelium white, texture velutinous, margins low, narrow, irregular, sporulation moderately dense, conidia masses greenish-grey (30F2), soluble pigments and exudates absent; reverse pastel green (30A4).

**Hyphae** hyaline, septate, smooth, branched, 1.0–4.5 µm wide. **Conidiophores** smooth, biverticillate, stipes smooth, bearing terminal biverticillate penicillin. **Metulae** 3–6, divergent, 8.0–13.5 × 2.0–4.0 µm. **Phialides** 3–6, acerose, 8.0–13.5 × 2.5–4.0 µm, with a long gradually tapering collula. **Conidia** spiny, fusiform to pyriform, sometimes ellipsoidal, 3.0–4.5 × 2.0–3.5 µm (av. 3.7 × 3.3 µm, n = 50). **Sexual morph** not observed.

**Notes.** Currently, five species are accepted in the section *Subinflati* (Houbraken et al. 2020; Sun et al. 2020). *Talaromyces guiyangensis* is classified as a new lineage in the section *Subinflati*, forming a strongly supported clade (ML = 100%; PP = 1.0). *T. guiyangensis* is phylogenetically closely related to *T. guizhouensis*, *T. subinflatus* and *T. tzapotlensis* (Fig. 6). Morphologically, *T. guiyangensis* can be distinguished from *T. guizhouensis* by fusiform to pyriform, sometimes ellipsoidal conidia, rather than subglobose to fusiform conidia of *T. guizhouensis*; whereas the colony of *T. guiyangensis*

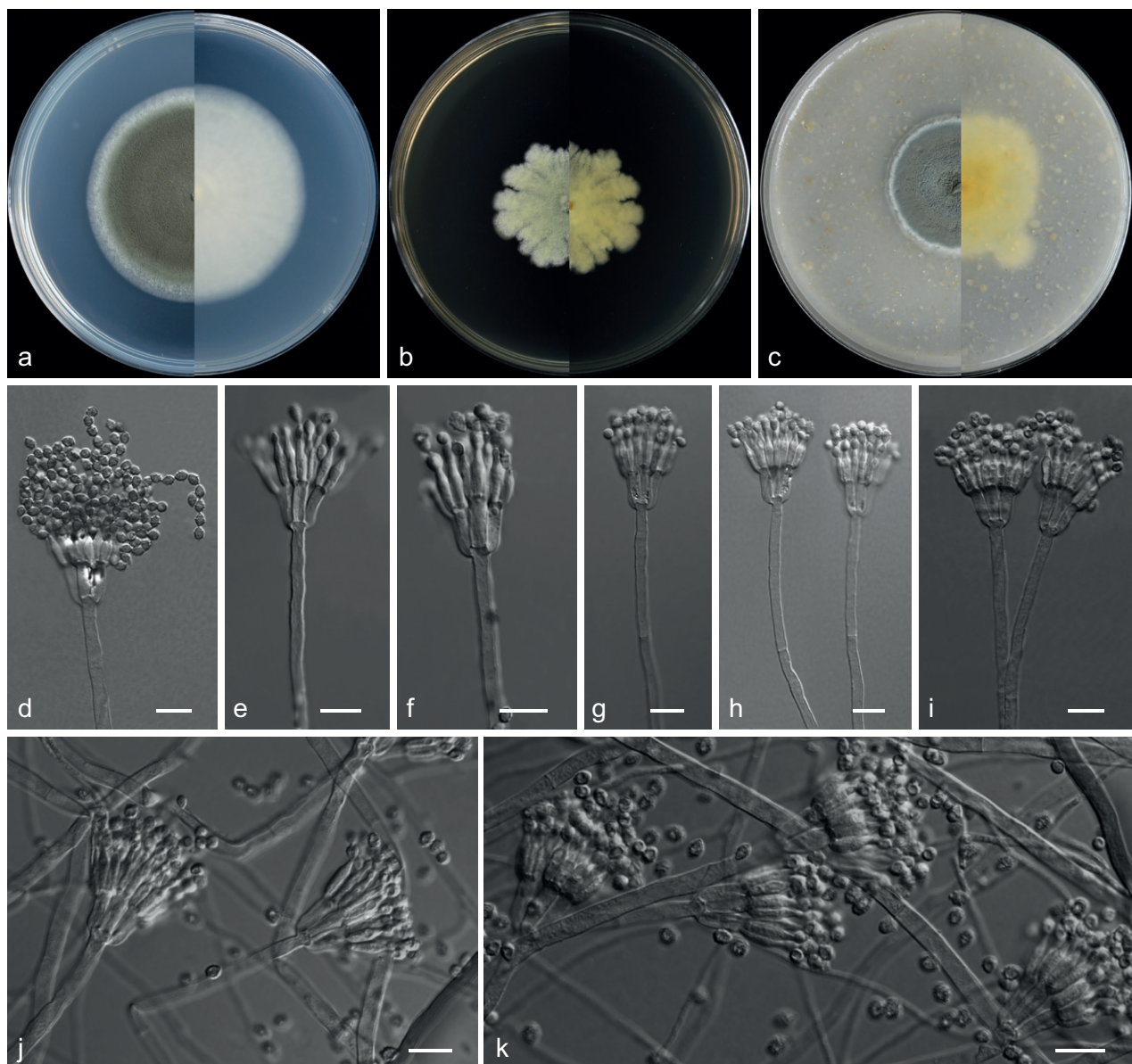


**Figure 10.** *Talaromyces jiangxiensis* (from ex-holotype CGMCC 3.20783) **a–c** upper and reverse views of cultures on PDA, MEA and OA 14 d after inoculation **d–k** phialides and conidia. Scale bars: 10 µm (d–k).

is velvety on MEA, rather than floccose in *T. guizhouensis* (Sun et al. 2020). The conidia of *T. subinflatus* are smooth, ellipsoidal to fusiform, rather than spiny, fusiform to pyriform, sometimes ellipsoidal in *T. guiyangensis* (Yilmaz et al. 2014). Additionally, *T. subinflatus* forms ascocarps, which is not seen in *T. guiyangensis* (Yilmaz et al. 2014). In addition, *T. tzapotlensis* forms smooth to finely roughened, ellipsoidal conidia, whereas *T. guiyangensis* produces spiny, fusiform to pyriform, sometimes ellipsoidal conidia (Peterson and Jurjević 2017).

***Talaromyces paecilomycetoides* Zhi.Y. Zhang, Y.F. Han & Z.Q. Liang, sp. nov.**

Mycobank No: 844157

Fig. 11

**Etymology.** Refers to the production of paecilomyces-like conidiophores.

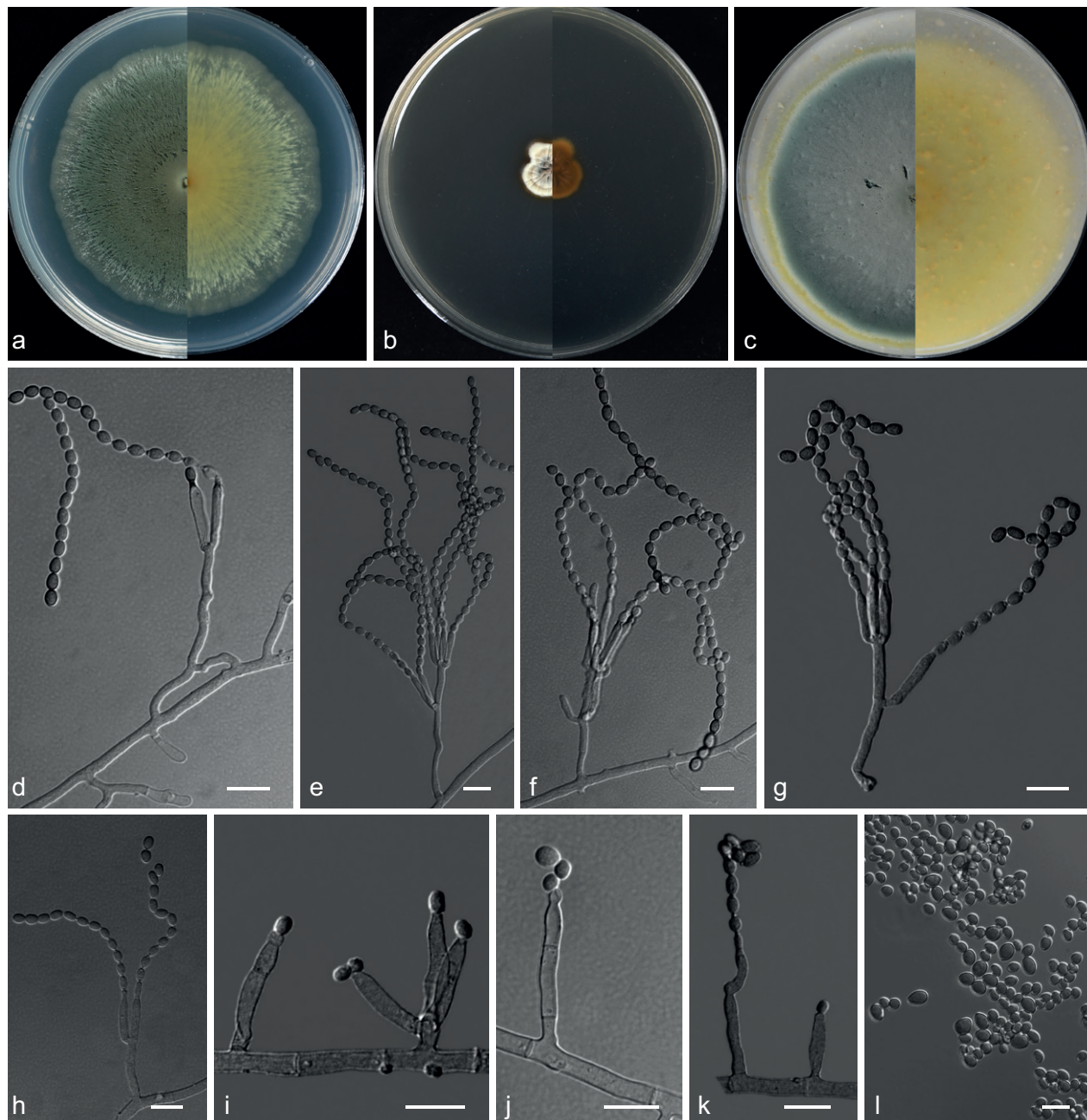


**Figure 11.** *Talaromyces paecilomycetoides* (from ex-holotype CGMCC 3.20785) **a–c** upper and reverse views of cultures on PDA, MEA and OA 14 d after inoculation **d–k** phialides and conidia **l** conidia. Scale bars: 10 µm (d–l).

**Type.** CHINA: Yunnan Province, Dali City, Dali University 25°67'32"N, 100°15'70"E, soil, 2 Sept 2019, Z.Y. Zhang (HMAS 351871 holotype designated here, ex-type living culture CGMCC 3.20785 = GZUIFR 21.894); ibid., GZUIFR 21.895.

**Description. Culture characteristics** (14 d at 25 °C): **Colony on PDA** 63–65 mm diam., mycelium white, planar, margins entire, slightly undulate, sporulation dense, conidia area masse dark green (28F8), soluble pigments and exudates absent; reverse greyish-green (28D5). **Colony on MEA** 11–13 mm diam., moderately deep, sulcate, mycelium white to buff, texture floccose, margins slightly irregular, sporulation moderately dense, conidia area masse orange white (5A2), soluble pigments and exudates absent; reverse raw umber (5F8). **Colony on OA** 68–70 mm diam., mycelium white, plane, texture velvety, margins entire, surrounded

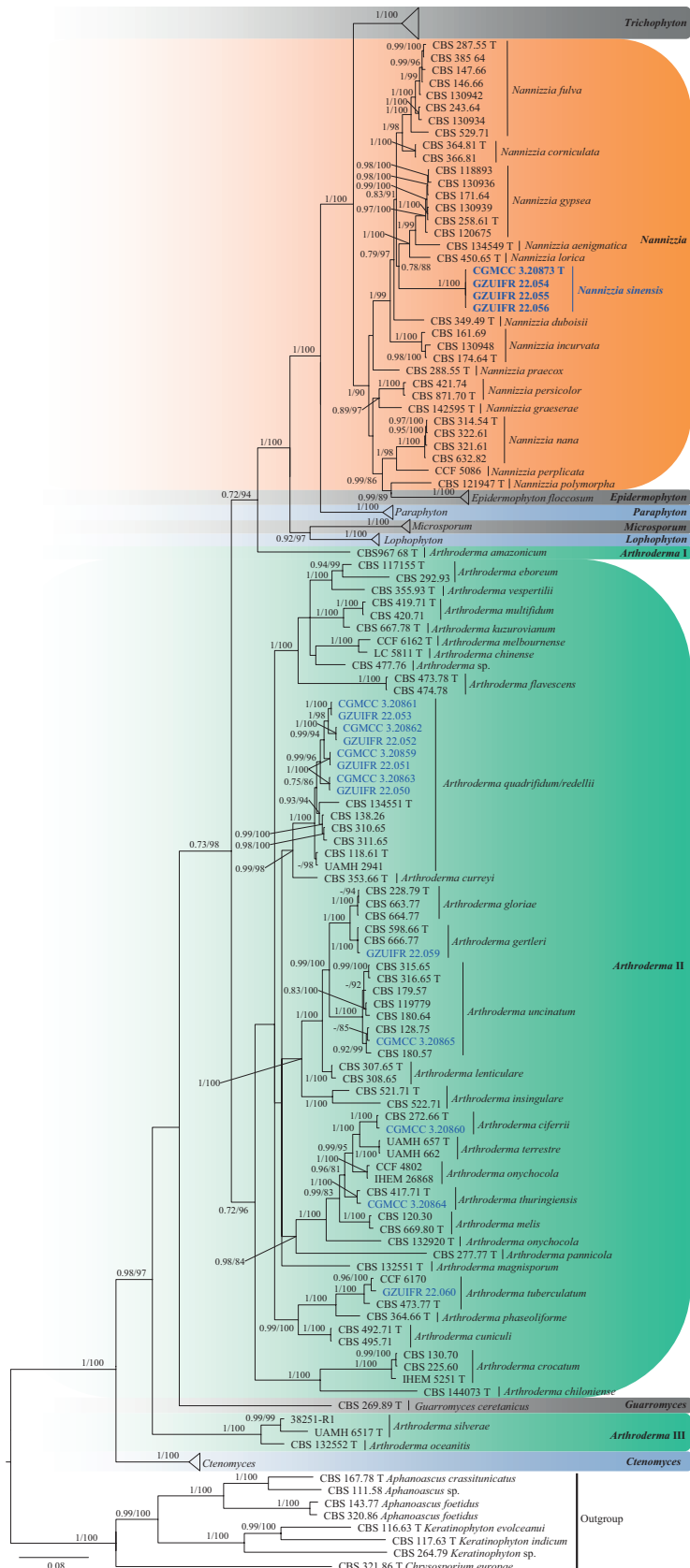


**Figure 12.** Concatenated phylogeny of the ITS, LSU, TUB, TEF3 and RP 60S L1 gene regions of species in Arthrodermataceae. Three hundred and eighteen strains are used. The tree topology of the BI was similar to the ML analysis. Bayesian posterior probability ( $\geq 0.7$ ) and ML bootstrap values ( $\geq 70\%$ ) are indicated along branches (PP/ML). Novel species are in blue and bold font, new isolates are in blue and “T” indicates type derived sequences.

by an orange halo, sporulation dense, conidia area masse dark grey (1F1), soluble pigments light brown, exudates absent; reverse greyish-green (1C4).

**Hyphae** hyaline, septate, smooth, branched, 1.0–5.0 µm wide. **Conidiophores** monoverticillate, smooth, irregular or absent; stipes smooth, 7–20 × 1.5–4.0 µm. **Metulae** 1 or absent, 10.5–14.5 × 2.0–4.0 µm. **Phialides** 1–4, cylindrical, flask-shaped, sometimes borne on hyphae, 10.5–20.0 × 1.5–5.0 µm. **Conidia** smooth, obround, ovoid, subglobose, sometimes cylindrical, 3.0–9.5 × 1.5–5.0 µm (av. 6.5 × 3.6 µm, n = 50), produced in long chains. **Sexual morph** not observed.

**Additional specimens examined.** CHINA: Yunnan Province, Kunming City, Donglu Campus of Yunnan University 25°05'51"N, 102°70'21"E, soil, 31 Aug 2019, Z.Y. Zhang, GZUIFR 21.896, ibid., GZUIFR 21.897.

**Notes.** *Talaromyces paecilomycetoides* is one of several *Talaromyces* species with simple conidiogenous cells (Peterson and Jurjević 2017). Phylogenetically, *Talaromyces paecilomycetoides* belongs to the section *Subinflati* and closely related with *T. palmae* (Fig. 8). Morphologically, they can be distinguished by their conidial shape and size (obround, ovoid, subglobose, sometimes cylindrical, 3.0–9.5 × 1.5–5.0 µm in *T. paecilomycetoides*; subglobose to ellipsoidal 3–4.5 × 2–3.5 µm in *T. palmae*) (Yilmaz et al. 2014).

**Onygenales Cif. ex Benny & Kimbr.**

**Arthrodermataceae Locq. ex Currah**

**Nannizzia Stockdale**

Species of *Nannizzia* are geo- or zoophiles that occasionally infect humans (Dukik et al. 2020). With the newly-proposed taxonomy, the genus *Nannizzia* comprises 13 species (de Hoog et al. 2017; Dukik et al. 2020). However, recent work has shown that the phylogenetic relationship between *Epidermophyton* and *Nannizzia* is unstable (Baert et al. 2020).

***Nannizzia sinensis* Zhi.Y. Zhang, Y.F. Han & Z.Q. Liang, sp. nov.**

Mycobank No: 844162

Fig. 13

**Etymology.** Refers to the country where this fungus was first isolated.

**Type.** CHINA: Guizhou Province, Zunyi City, the affiliated hospital of Zunyi Medical University 27°70'79"N, 106°94'54"E, soil, 5 Jul 2016, Z.Y. Zhang (HMAS 351892 holotype designated here, ex-type living culture CGMCC 3.20873 = GZUIFR 22.012).

**Description. Culture characteristics** (14 d at 25 °C): **Colony on PDA** 76–79 mm diam., yellowishwhite (4A2), floccose, fluffy, edge entire to diffuse; reverse white (4A1). **Colony on MEA** 51–52 mm diam., yellowish-white (4A2), floccose, wavy from centre to margin, edge entire; reverse white (6A1) to brownish-orange (6C8) from margin to centre. **Colony on OA** 52–54 mm diam., white (1A1), fluffy, sparse at the centre, margin irregular; reverse white (1A1).

**Hyphae** hyaline, septate, smooth, branched, 1.0–4.5 µm wide; racquet hyphae and spiral hyphae not observed. **Macroconidia** abundant, thin- or moderately thick-walled, smooth-walled or slightly verrucose, borne individually on short branches alongside hyphae or complex branched conidiophores, fusi-

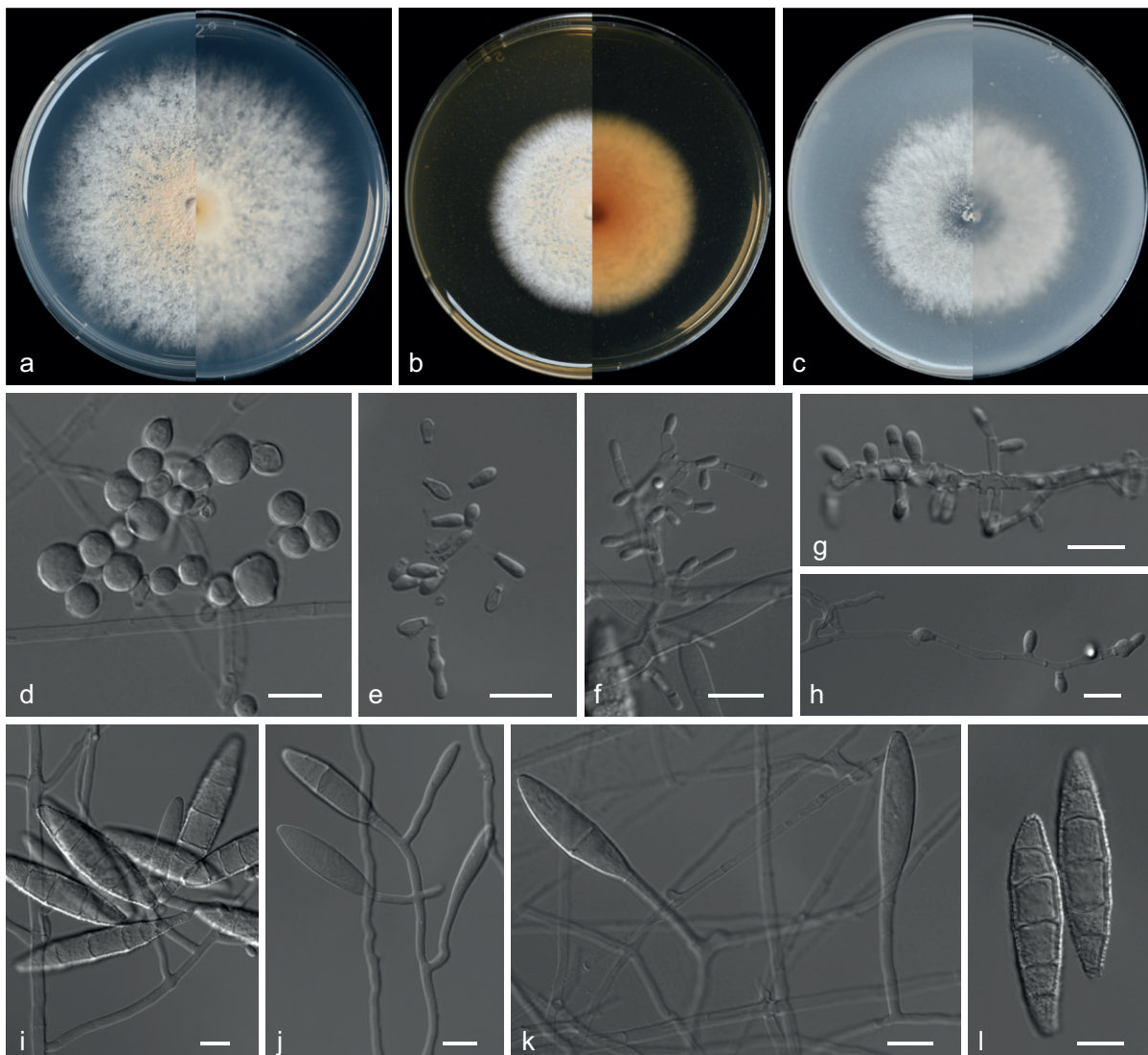


**Figure 13.** *Nannizzia sinensis* (from ex-holotype CGMCC 3.20873) **a–c** upper and reverse views of cultures on PDA, MEA and OA 14 d after inoculation **d** subspherical to spherical microconidia **e–h** conidiophores with sessile or stalked microconidia **i–k** conidiophores and macroconidia **l** macroconidia. Scale bars: 10 µm (**d–l**).

form, 1–5-septate,  $45.0\text{--}51.0 \times 11.5\text{--}12.5 \mu\text{m}$  (av.  $48.6 \times 12.3 \mu\text{m}$ ,  $n = 50$ ).

**Microconidia** scant, sessile or short-stalked, aseptate, smooth-walled. Two types of microconidia are present: subspherical to spherical,  $5.0\text{--}9.0 \times 5.0\text{--}8.0 \mu\text{m}$  (av.  $8.2 \times 6.8 \mu\text{m}$ ,  $n = 50$ ); obovoidal or clavate,  $3.5\text{--}6.5 \times 2.0\text{--}2.5 \mu\text{m}$  (av.  $5.4 \times 2.3 \mu\text{m}$ ,  $n = 50$ ). **Sexual morph** not observed.

**Additional specimens examined.** CHINA: Hainan Province, Haikou City, Haidian Campus of Hainan University  $20^{\circ}05'76''\text{N}$ ,  $110^{\circ}32'91''\text{E}$ , soil, 28 Aug 2019, Z.Y. Zhang, GZUIFR 22.054; Jiangxi Province, Jian City, Jinggangshan University, soil, 22 Aug 2019, Z.Y. Zhang, GZUIFR 22.055, ibid., GZUIFR 22.056.

**Notes.** In the multi-locus phylogenetic analysis, our four isolates form a distinct clade and are closely related to *N. aenigmatica*, *N. gypsea* and *N. lorica* (Fig. 12). However, *N. sinensis* can be distinguished from *N. aenigmatica* by the presence of macroconidia (Dukik et al. 2020). In addition, *N. sinensis* differs from *N. gypsea* and *N. lorica* by the presence of subspherical to spherical microconidia (Dukik et al. 2020).

**Leotiomycetes O.E. Erikss. & Winka**  
**Thelebolales Haeckel**  
**Thelebolaceae Engl.**  
**Pseudogymnoascus Raillo**

The genus *Pseudogymnoascus* was erected by Raillo (1929). However, Raillo did not formally specify a type strain for the genus. Many years later, Samson (1972) designated *P. roseus* Raillo CBS 395.65 as the neotype. Currently, the genus *Pseudogymnoascus* consists of 18 valid species (Villanueva et al. 2021; Zhang et al. 2021b), which belong to 13 clades (Minnis and Lindner 2013).

***Pseudogymnoascus botryoides* Zhi.Y. Zhang, Y.F. Han & Z.Q. Liang, sp. nov.**

MycoBank No: 844164

Fig. 15

**Etymology.** In reference to aleuroconidia and intercalary conidia which are borne together to form a botryoidal-like structure.

**Type.** CHINA: Guangxi Zhuang Autonomous Region, Beihai City 21°48'75"N, 109°12'72"E, soil, 10 Jul 2016, Z.Y. Zhang (HMAS 351904 holotype designated here, ex-type living culture CGMCC 3.20875 = GZUIFR 22.024); ibid., GZUIFR 22.044.

**Description. Culture characteristics** (14 d at 25 °C): **Colony on PDA** 29–30 mm diam., annular, margin aerial hyphae sparse, orange white (5A2) to white (5A1) from centre to margin, flat, compact, exudates and diffusible pigments absent; reverse reddish-orange (7A8) to orange white (5A2) from centre to margin. **Colony on MEA** 28–29 mm diam., white (7A1), flat, compact, nearly round, margin regular, exudates abundant, light red, diffusible pigments absent, reverse brown (7E8) to white (7A1) from centre to margin. **Colony on OA** greyish-orange (5B3) to white (5A1) from centre to margin, 25–28 mm diam., flocculent, granuliform, nearly round, margin slightly undulated, exudates abundant, diffusible pigments absent; reverse light orange (5A5) to white (5A1) from centre to margin.

**Hyphae** branched, septate, hyaline, smooth, 0.5–2.5 µm diam. wide, fertile hyphae bearing aleuroconidia and/or intercalary conidia, sessile. Aleuroconidia and intercalary conidia are borne together to form a botryoidal-like structure.

**Conidiophores** abundant, dense, interwoven into a network, curved, hyaline, rough, usually bearing verticils of two to eight branches, arising from the stipe at an acute angle. **Aleuroconidia** pyriform, obovoid, elongated, with a broad truncated basal scar, 2.0–4.5 × 1.5–2.5 µm (av. 3.8 × 2.3 µm, n = 50). **Intercalary conidia** drum, reniform, 2.5–5.0 × 1.5–2.5 µm, separated by connective cells that undergo rhexolysis, bearing sessile conidia. **Arthroconidia** rare, cylindrical, sometimes slightly curved, 2.5–5.0 × 1.0–2.0 µm (av. 4.4 × 1.6 µm, n = 50).

**Sexual morph** unknown.

**Additional specimens examined.** China: Guangdong Province, Zhanjiang City, the affiliated hospital of Guangdong Medical University 21°19'98"N, 110°40'34"E, soil, 25 Aug 2019, Z.Y. Zhang, GZUIFR 22.045, ibid., GZUIFR 22.046.

**Notes.** *Pseudogymnoascus botryoides* was placed as a member of clade I (Fig. 14). Clade I is composed of *P. antarcticus* and many other isolates that remain unidentified species (Minnis and Lindner 2013; Villanueva et al. 2021).

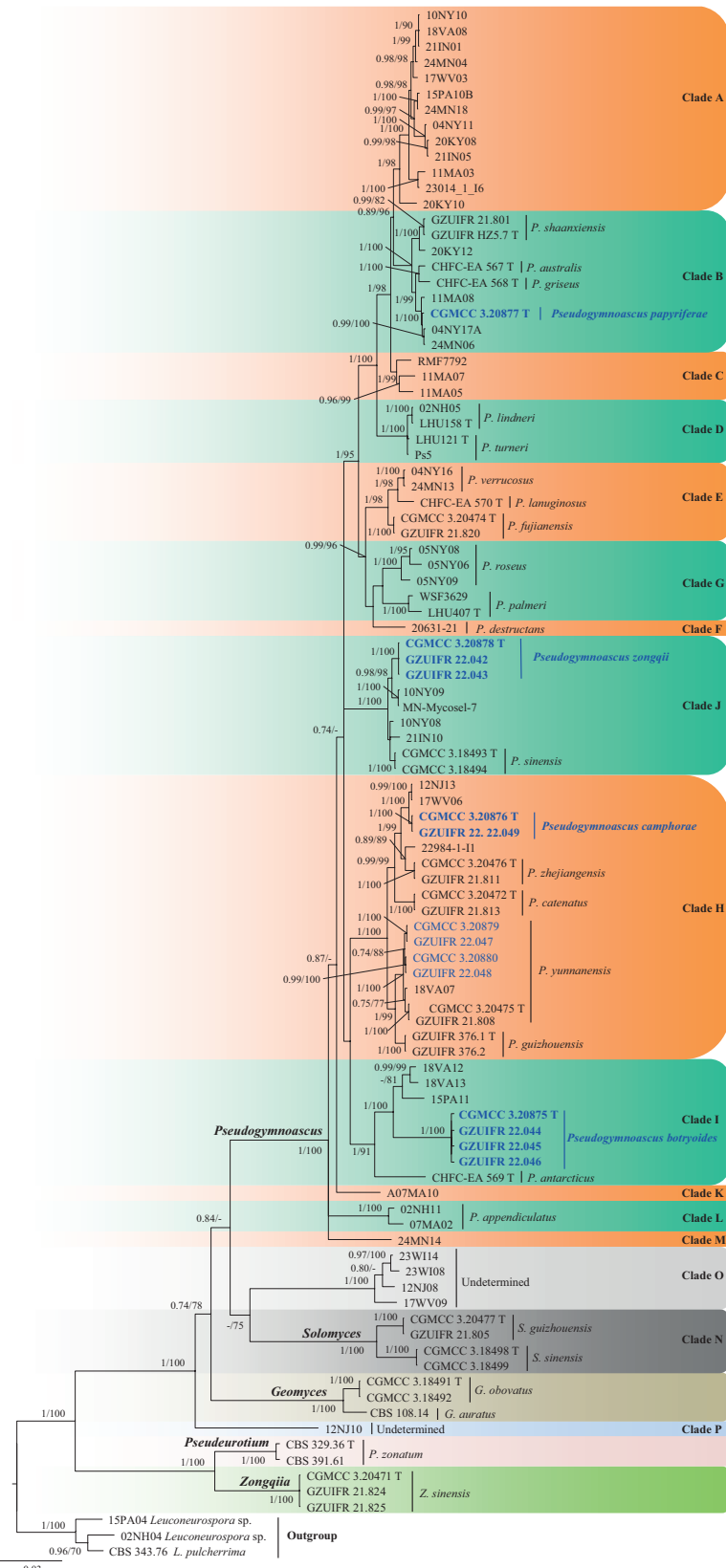


**Figure 14.** Concatenated phylogeny of the ITS, LSU, EF1A, RPB2 and MCM7 gene regions of species in Thelebolaceae. Ninety-nine strains are used. The tree is rooted in *Leuconeurospora pulcherrima* (CBS 343.76) and *Leuconeurospora* sp. (15PA04 and 02NH04). The tree topology of the BI was similar to the ML analysis. Bayesian posterior probability ( $\geq 0.7$ ) and ML bootstrap values ( $\geq 70\%$ ) are indicated along branches (PP/ML). Novel species are in blue and bold font, new isolates are in blue and "T" indicates type derived sequences.

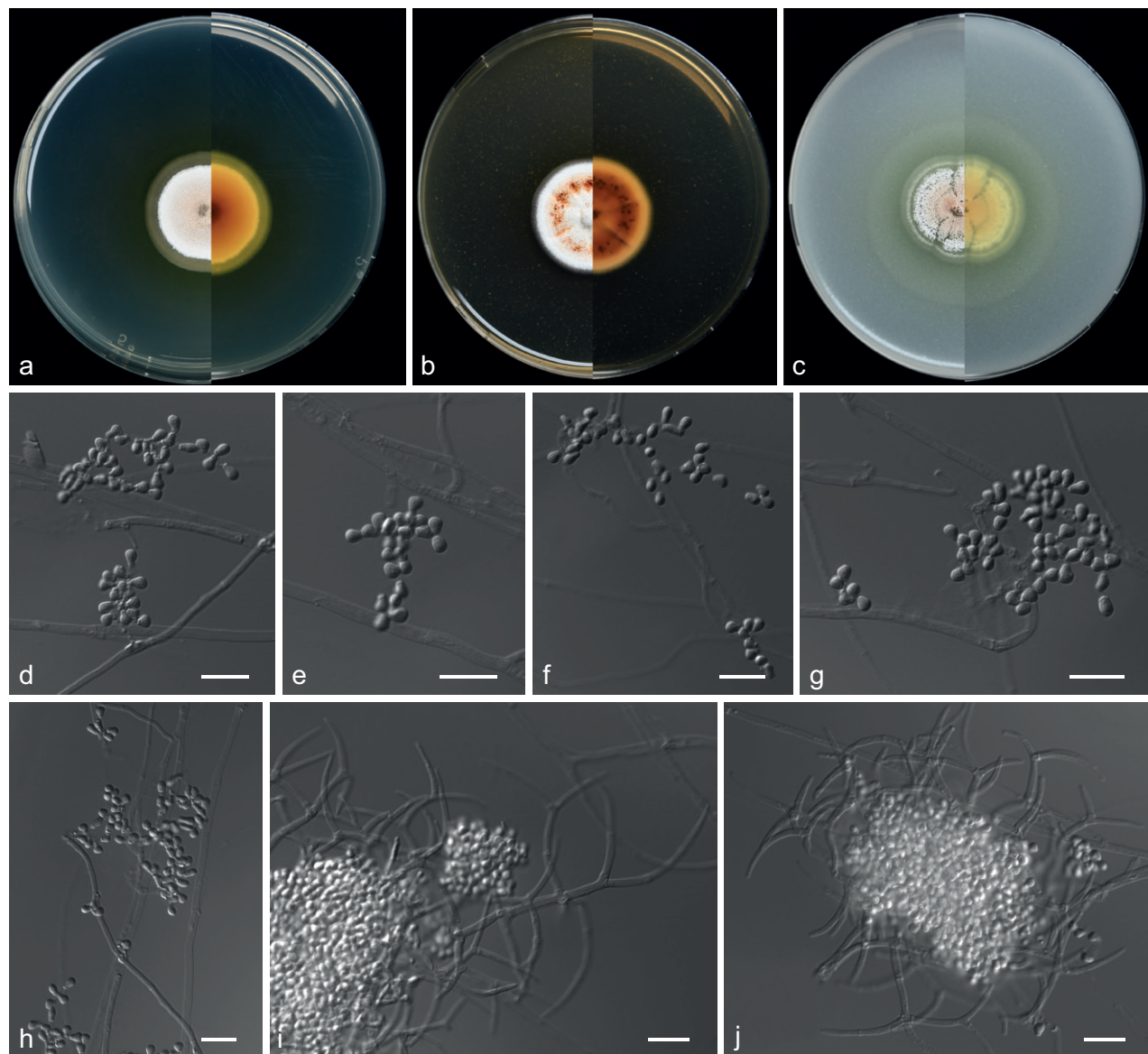


**Figure 15.** *Pseudogymnoascus botryoides* (from ex-holotype CGMCC 3.20875) **a–c** upper and reverse views of cultures on PDA, MEA and OA 14 d after inoculation **d–h** conidiophores and conidia **i, j** cluster conidia. Scale bars: 10 µm (**d–j**).

Phylogenetically, *P. botryoides* forms a distinct lineage with strong support (Fig. 14). Morphologically, *P. botryoides* can be distinguished from other species in the genus *Pseudogymnoascus* by its aleuroconidia and intercalary conidia being borne together to form a botryoidal-like structure.

***Pseudogymnoascus camphorae* Zhi.Y. Zhang, Y.F. Han & Z.Q. Liang, sp. nov.**  
MycoBank No: 844165  
Fig. 16

**Etymology.** Referring to the type strains first isolated from epiphytic soil of *Cinnamomum camphora* (Linn) Presl.

**Type.** CHINA: Guizhou Province, Guiyang City, South Campus of Guizhou University 26°42'21"N, 106°67'13"E, epiphytic soil of *C. camphora*, 8 Jul 2018, Z.Y.

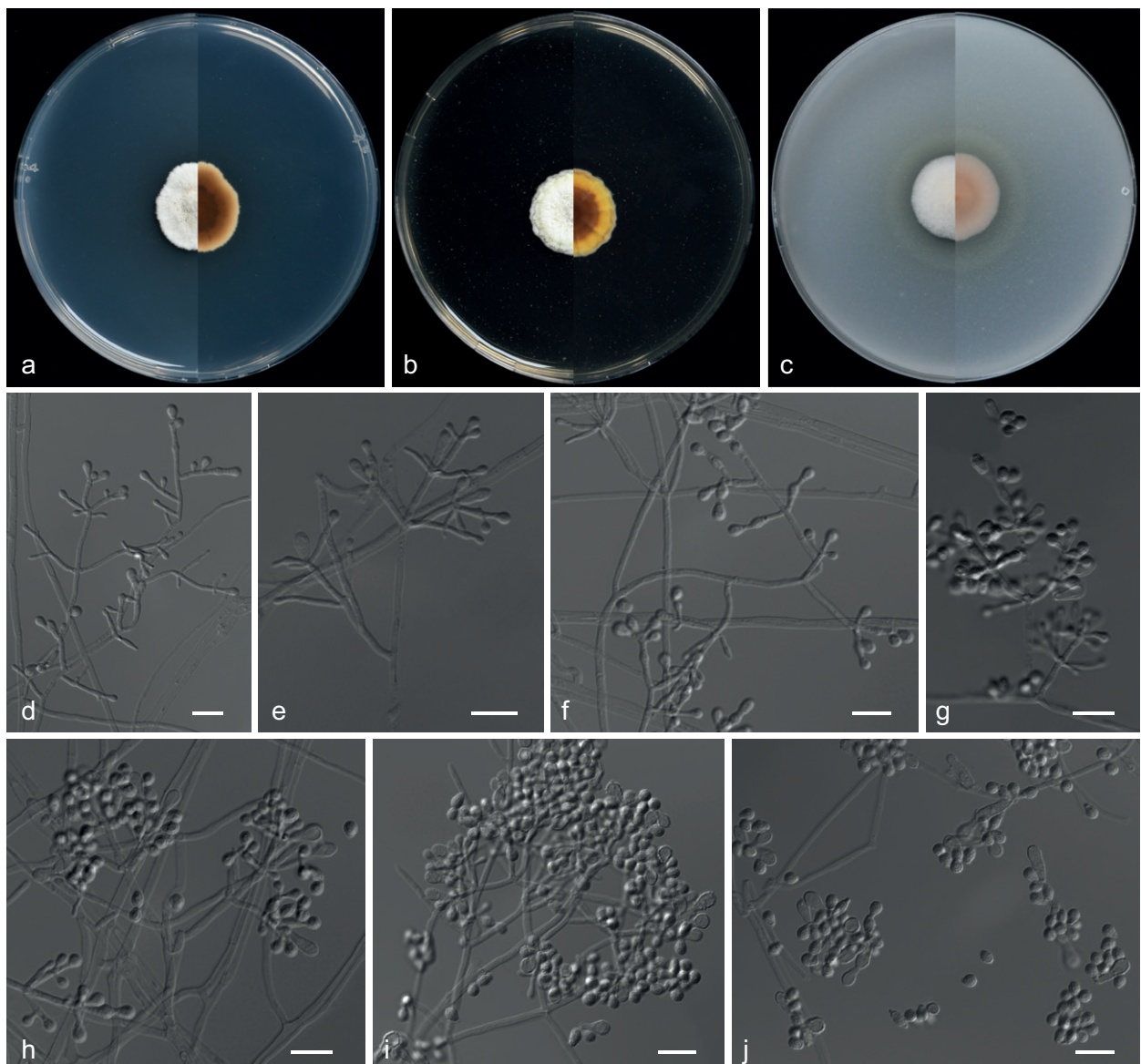


**Figure 16.** *Pseudogymnoascus camphorae* (from ex-holotype CGMCC 3.20876) **a–c** upper and reverse views of cultures on PDA, MEA and OA 14 d after inoculation **d–i** conidiophores and conidia **j** conidia. Scale bars: 10 µm (**d–j**).

Zhang (HMAS 351901 holotype designated here, ex-type living culture CGMCC 3.20876 = GZUIFR 22.021).

**Description. Culture characteristics** (14 d at 25 °C): **Colony on PDA** 20–22 mm diam., white (6A1), slightly raised, flocculent, margin irregular, localised bulge, exudates and diffusible pigments absent; reverse dark brown (6F8) to light brown (6D4) from centre to margin. **Colony on MEA** 20–21 mm diam., white (5A1) to yellowish-white (4A2) from centre to margin, flocculent, nearly round, margin undulated, exudates and diffusible pigments absent; reverse yellowish-brown (5E8) to orange (5A7) from centre to margin. **Colony on OA** 19–20 mm diam., white (13A1), slightly raised, fluffy, nearly round, margin regular, exudates absent, diffusible pigments abundant, pewter; reverse reddish (13A2).

**Hyphae** branched, septate, hyaline, smooth, 1.0–3.0 µm diam. **Conidiophores** abundant, solitary, sometimes minimally differentiated from hyphae, hyaline, smooth, arising from erect hyphae, usually bearing verticils of two to

four branches at an acute angle. **Aleuroconidia** pyriform, obovoid, with a broad truncated basal scar,  $4.0\text{--}5.5 \times 3.0\text{--}3.5 \mu\text{m}$  (av.  $5.2 \times 3.2$ , n = 50). **Terminal aleuroconidia** at the axis obovoid, clavate or irregular, solitary or two in chains,  $6.0\text{--}10.0 \times 3.0\text{--}3.5 \mu\text{m}$  (av.  $8.7 \times 3.2 \mu\text{m}$ , n = 50), with a broad truncated basal scar. Intercalary conidia subglobose, drum, obovoid,  $3.0\text{--}4.0 \times 2.0\text{--}3.0 \mu\text{m}$  (av.  $3.5 \times 2.6 \mu\text{m}$ , n = 50), sometimes separated by connective cells that undergo rhexolysis. **Arthroconidia** absent. **Sexual morph** unknown.

**Additional specimens examined.** China: Fujian Province, Xiamen City, Wuyuanbay Wetland Park  $24^\circ 51' 52''\text{N}$ ,  $118^\circ 17' 48''\text{E}$ , soil, 19 Aug 2019, Z.Y. Zhang, GZUIFR 22. 22.049.

**Notes.** *Pseudogymnoascus camphorae* was placed as a member of clade H (Fig. 14). *P. camphorae* is phylogenetically related to *P. zhejiangensis* and *P. catenatus*; however, *P. camphorae* still forms a single clade. Morphologically, *P. camphorae* can be differentiated from *P. catenatus* by its absent arthroconidia (Zhang et al. 2021b). *P. camphorae* is distinguished from *P. zhejiangensis* by the size and shape of its aleuroconidia (pyriform, obovoid,  $4.0\text{--}5.5 \times 3.0\text{--}3.5 \mu\text{m}$  vs. obovoid to globose,  $2.5\text{--}4.5 \times 2.5\text{--}4.0 \mu\text{m}$ , respectively) and terminal aleuroconidia (obovoid, clavate or irregular, solitary or two in chains,  $6.0\text{--}10.0 \times 3.0\text{--}3.5 \mu\text{m}$  vs. clavate, long obovoid,  $5\text{--}9 \times 2.5\text{--}4 \mu\text{m}$ , respectively) (Zhang et al. 2021b).

***Pseudogymnoascus papyriferae* Zhi.Y. Zhang, Y.F. Han & Z.Q. Liang, sp. nov.**

Mycobank No: 844166

Fig. 17

**Etymology.** Referring to the type strain isolated from epiphytic soil of *Broussonetia papyrifera* L'Heritier ex Ventenat.

**Type.** CHINA: Shaanxi Province, Hanzhong City  $33^\circ 07' 65''\text{N}$ ,  $107^\circ 03' 13''\text{E}$ , from epiphytic soil of *B. papyrifera*, Sep 2018, Z.Y. Zhang (HMAS 351878 holotype designated here, ex-type living culture CGMCC 3.20877 = GZUIFR 22.020).

**Description. Culture characteristics** (14 d at 25 °C): **Colony on PDA** 13–15 mm diam., light orange (6A4) to white (6A1) from centre to margin, slightly raised, cottony, floccose, nearly round, margin slightly undulated, abundant exudates in the form of transparent, cinnamon-colour droplets of large size, diffusible pigments absent; reverse rust brown (6E8) to white (6A1). **Colony on MEA** 13–14 mm diam., white (2A1), hyphae kink into bundles, slightly raised in the centre, nearly round, exudates and diffusible pigments absent; reverse white (2A1) to yellowish-white (2A2) from margin to centre. **Colony on OA** 14–15 mm diam., white (1A1), powdery with dense in the middle with sparse margins, slightly raised at the centre, nearly round, margin slightly undulate, exudates absent, producing a diffusible faint white pigment; reverse white (1A1).

**Hyphae** branched, septate, hyaline, smooth,  $1.0\text{--}2.5 \mu\text{m}$  diam. Sometimes lateral hyphae end in chains of a barrel- or fusiform shape with blunt-ended arthroconidia, sometimes bearing aleuroconidia, sessile or stalked. **Conidiophores** abundant, solitary, erect, arising in acute angles with the main axis, hyaline, smooth, usually bearing verticils of two to four branches arising from the stipe at an acute angle. **Aleuroconidia** obovoid, pyriform to subglobose, with a broad truncated basal scar,  $3.5\text{--}6.0 \times 2.5\text{--}4.0 \mu\text{m}$  (av.  $4.4 \times 3.5 \mu\text{m}$ , n = 50), in

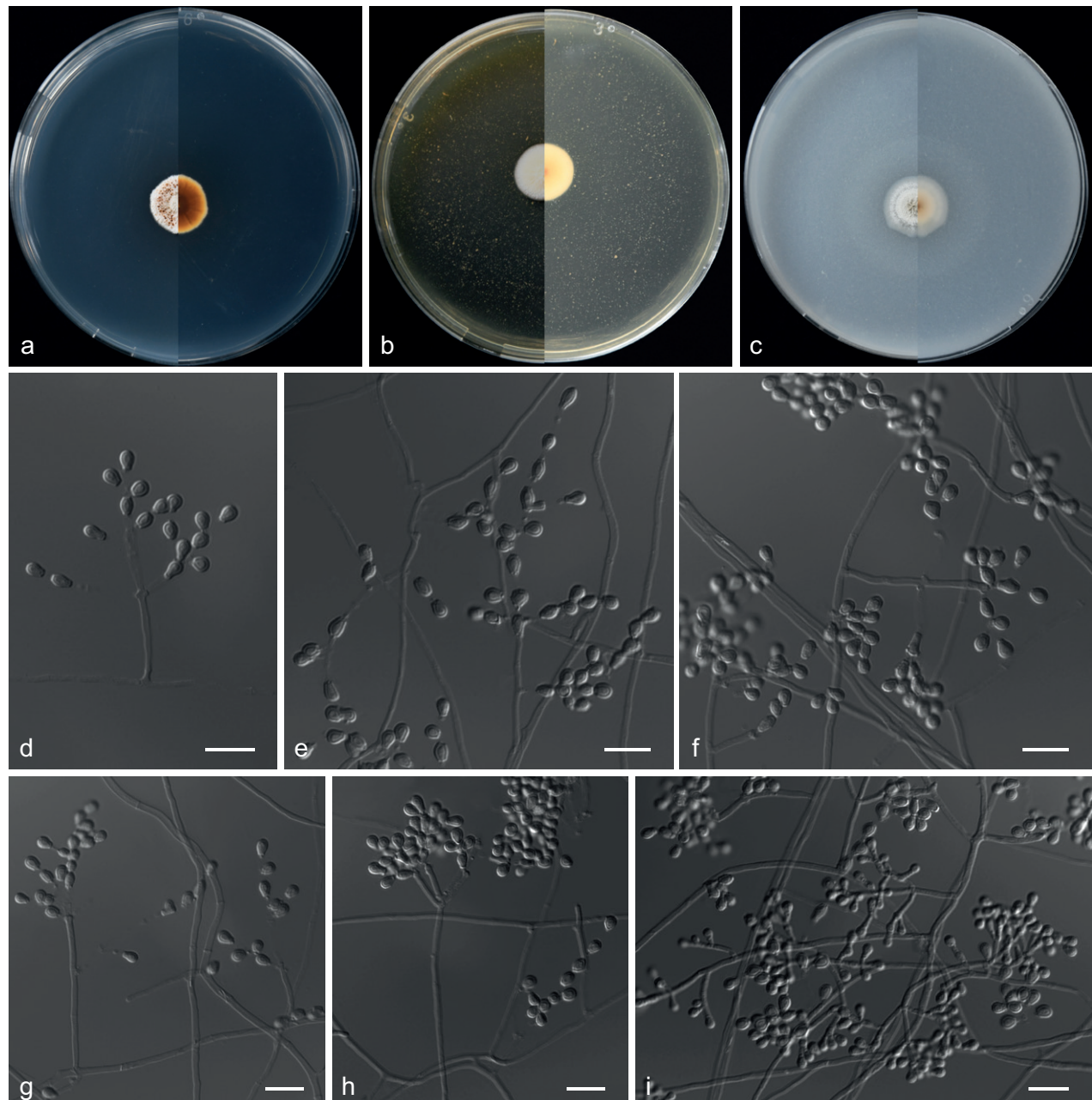


**Figure 17.** *Pseudogymnoascus papyriferae* (from ex-holotype CGMCC 3.20877) **a–c** upper and reverse views of cultures on PDA, MEA and OA 14 d after inoculation **d–i** conidiophore and conidia. Scale bars: 10 µm (**d–i**).

conidiophores separated by connective cells. **Intercalary conidia** drum-shaped, barrel-shaped, pyriform to elongated, with a broad truncated scar at the basal or both ends,  $3.5\text{--}5.5 \times 2.5\text{--}3.5 \mu\text{m}$  (av.  $5.2 \times 3.4 \mu\text{m}$ ,  $n = 50$ ). **Arthroconidia** rare, cylindrical to slightly inflated in the middle,  $2.5\text{--}4.5 \times 2.0\text{--}2.5 \mu\text{m}$  (av.  $3.4 \times 2.2 \mu\text{m}$ ,  $n = 50$ ). Arthroconidia chain or separated by connective cells that undergo rhexolysis, occasionally bearing sessile conidia. **Sexual morph** unknown.

**Notes.** *Pseudogymnoascus papyriferae* is nested in clade B (Fig. 14). Clade B is composed of three species (*P. shaanxiensis*, *P. australis* and *P. griseus*) and six other strains that remain unidentified species (Minnis and Lindner 2013; Zhang et al. 2020b, 2021b; Villanueva et al. 2021). Phylogenetic analysis clearly shows that *P. papyriferae* forms a distinct lineage (Fig. 14). *Pseudogymnoascus papyriferae*

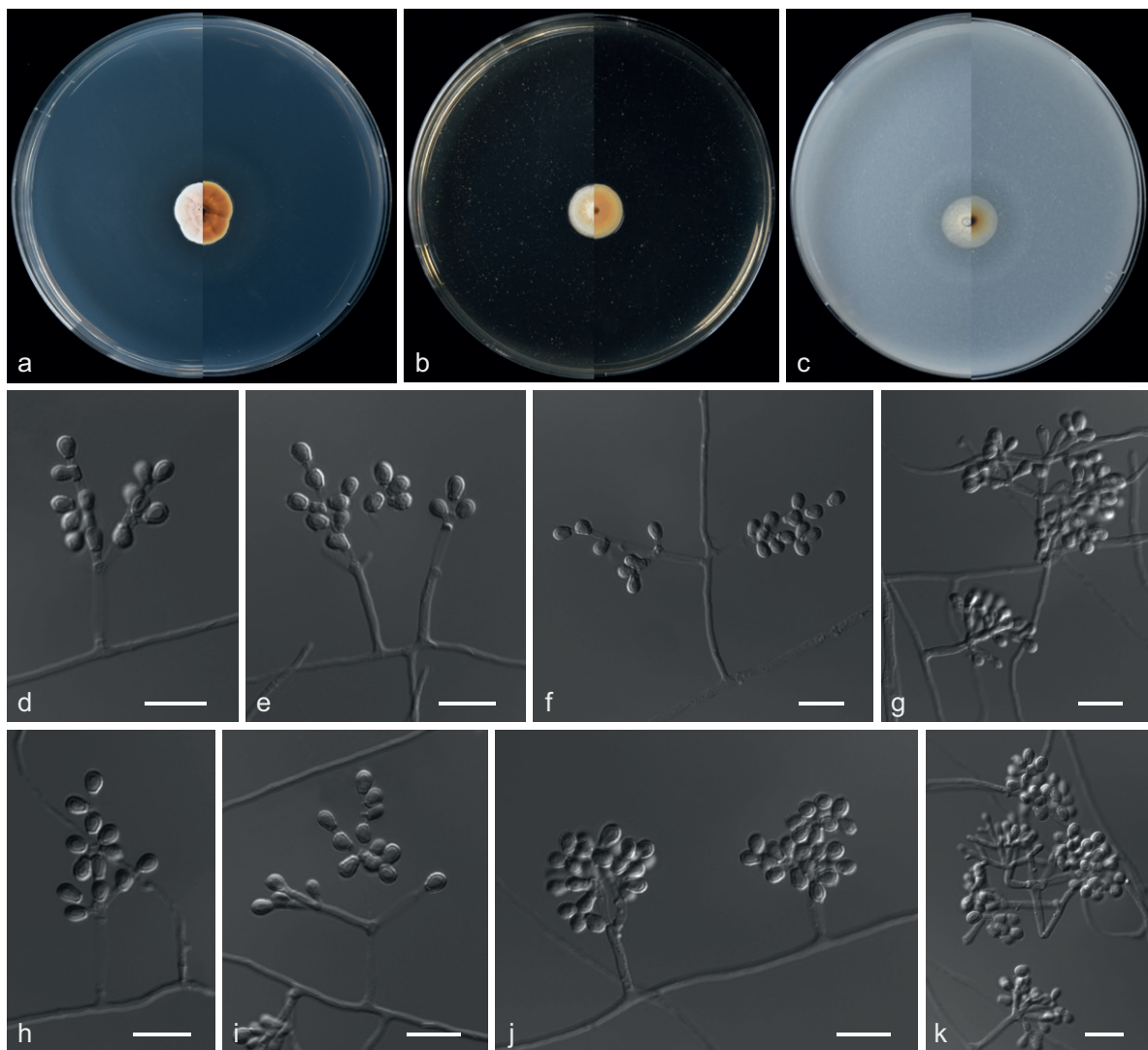
can be distinguished from *P. shaanxiensis* by the presence of arthroconidia (Zhang et al. 2020b). *Pseudogymnoascus papyriferae* can be differentiated from *P. austalis* by the shape of intercalary conidia (drum-shaped, barrel-shaped, pyriform to elongated vs. subglobose to elongated and barrel-shaped, respectively) and rarely arthroconidia (Villanueva et al. 2021). In addition, *P. papyriferae* differs from *P. griseus* in the size and shape of its intercalary conidia ( $3.5\text{--}5.5 \times 2.5\text{--}3.5 \mu\text{m}$ , drum-shaped, barrel-shaped, pyriform to elongated vs.  $3.5\text{--}9.6 \times 1.7\text{--}3.9 \mu\text{m}$ , subglobose to elongated and barrel-shaped, respectively) (Villanueva et al. 2021).

***Pseudogymnoascus zongqii* Zhi.Y. Zhang, Y.F. Han & Z.Q. Liang, sp. nov.**

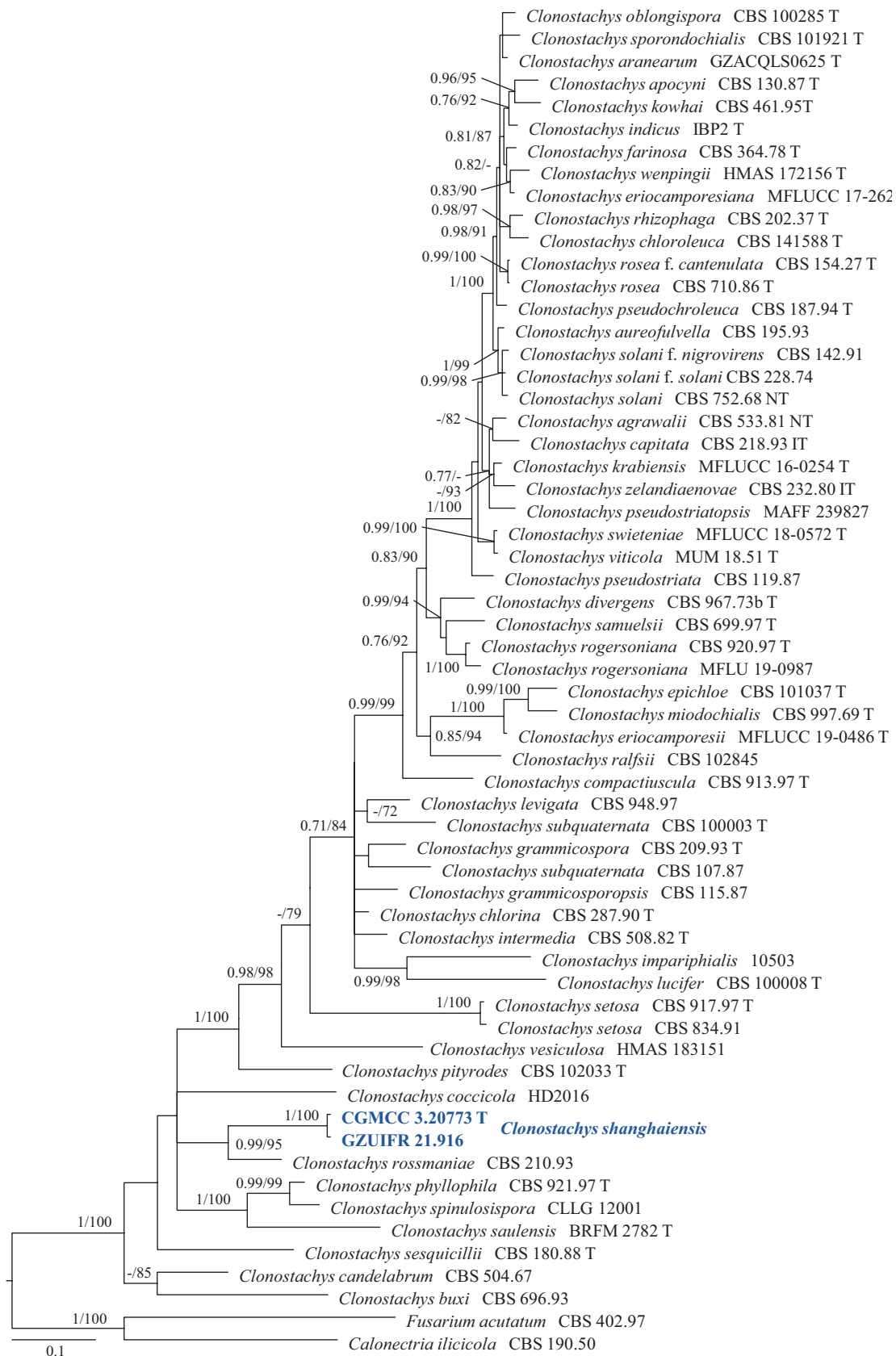
Mycobank No: 844168

Fig. 18

**Etymology.** Refers to the name of Prof. Zong-Qi Liang.



**Figure 18.** *Pseudogymnoascus zongqii* (from ex-holotype CGMCC 3.20878) **a–c** upper and reverse views of cultures on PDA, MEA and OA 14 d after inoculation **d–f, h, i** conidia and intercalary conidia **g–k** conidiophore and conidia. Scale bars: 10  $\mu\text{m}$  (**d–k**).



**Figure 19.** Concatenated phylogeny of the ITS and TUB gene regions of species in *Clonostachys*. Sixty strains are used. The tree is rooted in *Fusarium acutatum* (CBS 402.97) and *Calonectria ilicicola* (CBS 190.50). The tree topology of the BI was similar to the ML analysis. Bayesian posterior probability ( $\geq 0.7$ ) and ML bootstrap values ( $\geq 70\%$ ) are indicated along branches (PP/ML). Novel species are in blue and bold font and "T" indicates type derived sequences.

**Type.** CHINA: Sichuan Province, Chengdu City 30°65'96"N, 104°04'44"E, soil, 8 Aug 2016, Z.Y. Zhang (HMAS 351905 holotype designated here, ex-type living culture CGMCC 3.20878 = GZUIFR 22.025).

**Description.** **Culture characteristics** (14 d at 25 °C): **Colony on PDA** 13–15 mm diam., pale orange (6A3) to white (6A1) from centre to margin, fluffy, flocculent, nearly round, margin slightly sunken, exudates absent, diffusible pigments transparent and inconspicuous; reverse brownish-grey (6C2) to light orange (6A5) from centre to margin. **Colony on MEA** 12–13 mm diam., light yellow (4A4) to white (4A1) from centre to margin, hyphae kink into bundles, raised at the centre, nearly round, margin regular, exudates and diffusible pigments absent; reverse chrome yellow (5B8) to light yellow (4A4) from centre to margin. **Colony on OA** 12 mm diam., grey (5C1) to white (5A1) from centre to margin, flocculent, dense at the centre, sparse at margins, nearly round, margin regular, exudates absent, diffusible pigments transparent and inconspicuous; reverse raw umber (5F8) to grey (5D1) from centre to margin.

**Hyphae** branched, septate, hyaline, smooth, 1.0–3.0 µm diam. wide. **Conidiophores** abundant, solitary, sometimes minimally differentiated from hyphae, hyaline, smooth, arising from the erect hyphae, usually bearing verticils of two to five branches at an acute angle. Aleuroconidia and intercalary conidia are abundant, hyaline, smooth or rough. **Aleuroconidia** pyriform, occasionally ovoid to subglobose, with a broad truncated basal scar, 3.0–5.0 × 2.5–3.5 µm (av. 4.3 × 3.2 µm, n = 50). **Intercalary conidia** pyriform to ovoid, 3.5–5.0 × 2.5–4.5 µm (av. 4.6 × 3.8 µm, n = 50), separated by connective cells that undergo rhexolysis; occasionally bearing sessile conidia. **Arthroconidia** absent. **Sexual morph** unknown.

**Additional specimens examined.** China: Guizhou Province, Zunyi City, the affiliated hospital of Zunyi Medical University 27°70'79"N, 106°94'54"E, soil, 11 Sept 2016, Z.Y. Zhang, GZUIFR 22.042, ibid., GZUIFR 22.043.

**Notes.** *Pseudogymnoascus zongqii* was placed as a member of clade J (Fig. 14). Clade J is composed of *P. sinensis* and many other strains that remain unidentified species (Minnis and Lindner 2013; Zhang et al. 2020b). Phylogenetically, *P. zongqii* forms a distinct lineage with strong support (Fig. 14). Morphologically, *P. zongqii* can be distinguished from *P. sinensis* by its subglobose conidia and absence of drum- or irregularly shaped intercalary conidia (Zhang et al. 2020b).

#### Sordariomycetes O.E. Erikss. & Winka

#### Hypocreales Lindau

#### Bionectriaceae Samuels & Rossman

#### *Clonostachys* Corda

Corda (1839) introduced the genus *Clonostachys*, based on *C. araucaria*. *Clonostachys* species are characterised by penicillate, sporodochial or dimorphic conidiophores and phialidic conidiogenous cells, producing hyaline conidia (Schroers 2001). Rossman et al. (2013) linked the sexual morphic genus *Bionectria* with *Clonostachys* and *Bionectria* was synonymised under *Clonostachys*. *Clonostachys* is a species-rich genus with more than 107 records listed in the Index Fungorum (<http://www.indexfungorum.org>, accessed on 14 May 2022). Members of the genus *Clonostachys* are saprotrophs and are heavily parasitic on fungi and lichens or inhabit recently dead trees and decaying

leaves (Schroers 2001). However, *Clonostachys* spp. are rarely found to be parasitic on myxomycetes, insects, nematodes, flatworms, molluscs or oomyces (Schroers 2001).

***Clonostachys shanghaiensis* Zhi.Y. Zhang, Y.F. Han & Z.Q. Liang, sp. nov.**

Mycobank No: 844171

Fig. 20

**Etymology.** In reference to Shanghai, the city where the type specimen was obtained.

**Type.** CHINA: Shanghai Municipality, Shanghai People's Park 31°23'33"N, 121°47'29"E, soil, 15 Aug 2020, Z.Y. Zhang (HMAS 351878 holotype designated here, ex-type living culture CGMCC 3.20773 = GZUIFR 21.915).

**Description. Culture characteristics** (14 d at 25 °C): **Colony on PDA** 50 mm diam., white (9A1), flat, cottony, annular, dense at the centre, margin slightly undulated; reverse reddish-white (9A2). **Colony on MEA** 66 mm diam., white (5A1), flat, margin undulated, white; reverse orange white (5A2). **Colony on OA** 63 mm diam., white (9A1), surface undulated, margin entire; reverse reddish-white (9A2).

**Hypae** branched, septate, hyaline, smooth, 1.0–5.0 µm diam. **Conidiophores** arising from aerial hyphae, monomorphic, hyaline, smooth-walled, solitary, not sporodochial, monoverticillate or biverticillate, 3.5–9.0 × 1.5–3.0 µm. **Phialides** solitary or in whorls 2–5, broadly flask-shaped, slightly tapering towards the

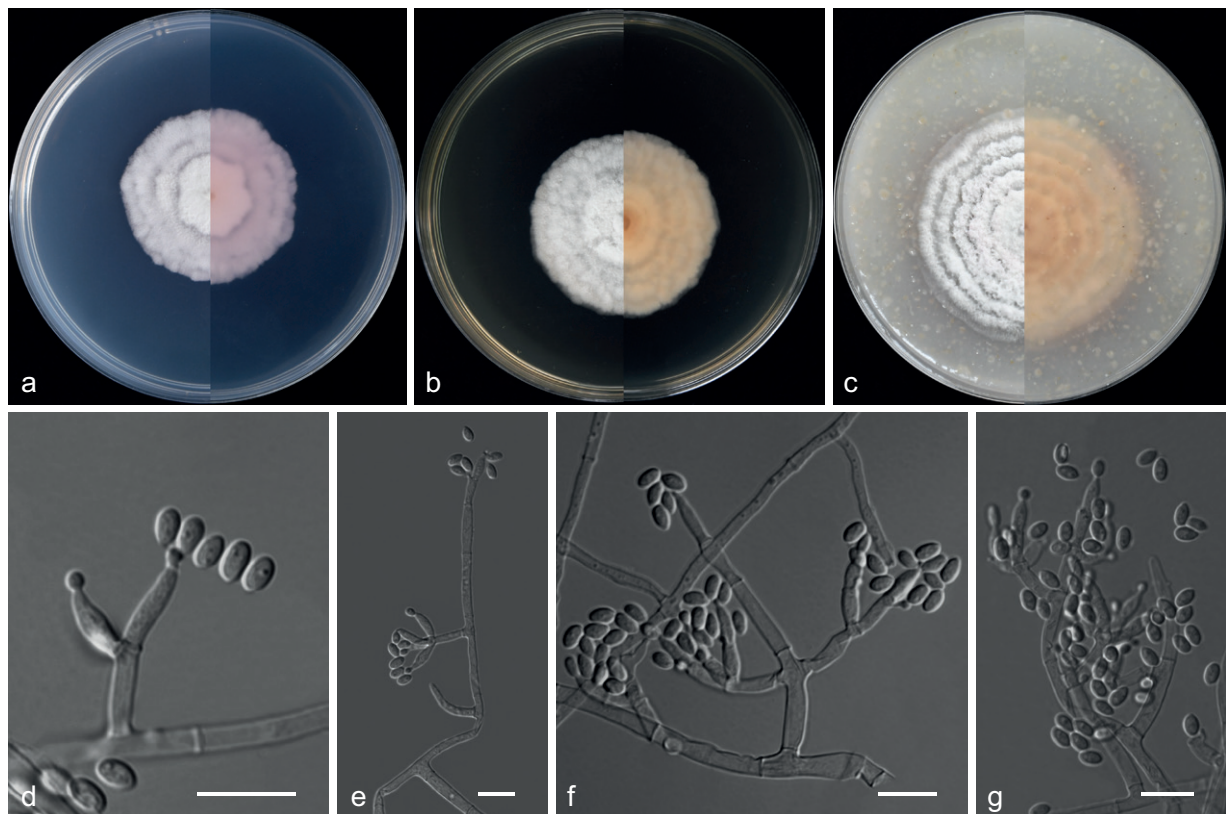


**Figure 20.** *Clonostachys shanghaiensis* (from ex-holotype CGMCC 3.20773) **a–c** upper and reverse views of cultures on PDA, MEA and OA 14 d after inoculation **d–g** conidiophore and conidia. Scale bars: 10 µm (d–g).

apex, with visible periclinal thickening, hyaline, smooth-walled, borne on the tip of hyphae or conidiophores,  $2.5\text{--}10.0 \times 2.0\text{--}3.5 \mu\text{m}$ . **Intercalary phialides** are rarely observed. **Conidia** hyaline, smooth, ellipsoidal, oblong to olivary, from phialides,  $3.0\text{--}5.5 \times 2.0\text{--}3.0 \mu\text{m}$  (av.  $4.8 \times 2.5 \mu\text{m}$ ,  $n = 50$ ). **Sexual morph** not observed.

**Additional specimens examined.** China: Shanghai Municipality, South Campus of Fudan University  $31^{\circ}29'30''\text{N}$ ,  $121^{\circ}50'03''\text{E}$ , soil, 16 Aug 2020, Z.Y. Zhang, GZUIFR 21.916.

**Notes.** Our new isolates (CGMCC 3.20773 and GZUIFR 21.916) formed a single clade and are closely related to *Clonostachys rossmaniae* (CBS 210.93) (Fig. 19). However, the conidia of *C. shanghaiensis* are ellipsoidal, oblong to olivary, rather than ellipsoidal to ovoidal in *C. rossmaniae* (Schroers 2001). Therefore, this species is regarded as a new species, based on morphology and multi-locus phylogeny.

#### Nectriaceae Tul. & C. Tul.

##### *Cyanonectria* Samuels & P. Chaverri

Samuels et al. (2009) established the genus *Cyanonectria*, with the type species *Cyanonectria cyanostoma*. Currently, this genus includes two accepted species (Crous et al. 2021), both are isolated from branches of *Buxus sempervirens* L. (Schroers et al. 2011; Crous et al. 2021).

##### *Cyanonectria bispora* Zhi.Y. Zhang, Y.F. Han & Z.Q. Liang, sp. nov.

Mycobank No: 844172

Fig. 22

**Etymology.** In reference to its production of both macroconidia and microconidia.

**Type.** CHINA: Yunnan Province, Dali City, Dali Bai Autonomous Prefecture People's Hospital  $25^{\circ}57'89''\text{N}$ ,  $100^{\circ}22'16''\text{E}$ , soil, 3 Sep 2019, Z.Y. Zhang (HMAS 351875 holotype designated here, ex-type living culture CGMCC 3.20774 = GZUIFR 21.908).

**Description. Culture characteristics** (14 d at 25 °C): **Colony on PDA** 42–46 mm diam., grey (29B1), flocculent, aerial mycelium sparse, substrate mycelium abundant, fimbriate; reverse grey (29C1). **Colony on MEA** 15–19 mm diam., grey (29B1) to white (29A1) from centre to margin, fluffy, margin dentate; reverse grey (29F1) to white (29A1) from centre to margin. **Colony on OA** 63 mm diam., yellowish-white (4A2), felty, rounded, margin regular; reverse pale yellow (4A3).

**Hyphae** branched, septate, hyaline, smooth,  $1.0\text{--}5.0 \mu\text{m}$  diam. **Conidiophores** mononematous (aerial conidiophores) or grouped on sporodochia. **Monophialides** arising from aerial hyphae, hyaline, smooth-walled, solitary or connected by pronounced connectors, sometimes septate, cylindrical, sometimes curved irregularly, neck broadly tapering towards the apex,  $5.5\text{--}39.0 \mu\text{m}$  long,  $1.0\text{--}3.5 \mu\text{m}$  wide at the base, ca.  $1.0\text{--}2.5 \mu\text{m}$  near the aperture. **Sporodochia** of branched conidiophores with solitary or whorls of 2–3 terminal monophialides. **Phialides** of sporodochia cylindrical or bottle-shaped,  $13.5\text{--}29 \mu\text{m}$  long,  $2.0\text{--}3.5 \mu\text{m}$  wide at the base,  $2.5\text{--}4.0 \mu\text{m}$  in middle,  $1.0\text{--}2.0 \mu\text{m}$  wide near the conidiogenous aperture. **Microconidia**

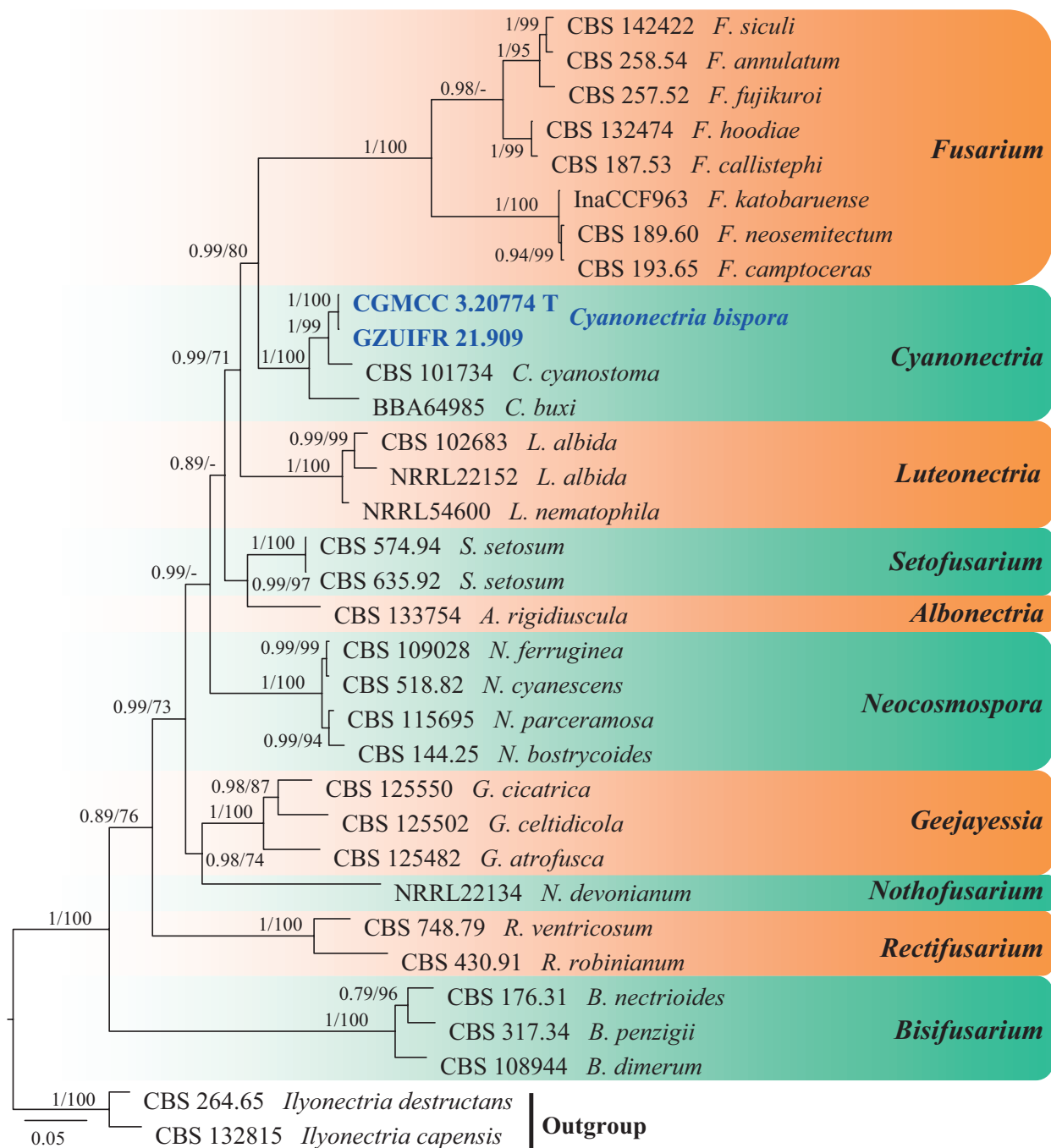


**Figure 21.** Concatenated phylogeny of the ITS, LSU, RPB2 and EF1A gene regions of species in *Cyanonectria* and its allied genera. Thirty-three strains are used. The tree is rooted in *Ilyonectria destructans* (CBS 264.65) and *I. capensis* (CBS 132815). The tree topology of the BI was similar to the ML analysis. Bayesian posterior probability ( $\geq 0.7$ ) and ML bootstrap values ( $\geq 70\%$ ) are indicated along branches (PP/ML). Novel species are in blue and bold font and "T" indicates type derived sequences.

hyaline, smooth, aseptate, cylindrical, fusiform, sometimes irregular,  $5.0 - 14.5 \times 2.5 - 6.0 \mu\text{m}$  (av.  $10.4 \times 4.6 \mu\text{m}$ ,  $n = 50$ ). **Macroconidia** hyaline, smooth, typically with the central and basal part nearly straight, rarely gently curved throughout, with a more or less pronounced pedicellate foot cell and an inequilateral fusoid or hooked apical cell, aseptate or 1–3(–4) septate,  $23.5 - 40.5 \times 3.0 - 5.5 \mu\text{m}$  (av.  $38.6 \times 4.8 \mu\text{m}$ ,  $n = 50$ ). **Chlamydospores** not observed. **Sexual morph** not observed.

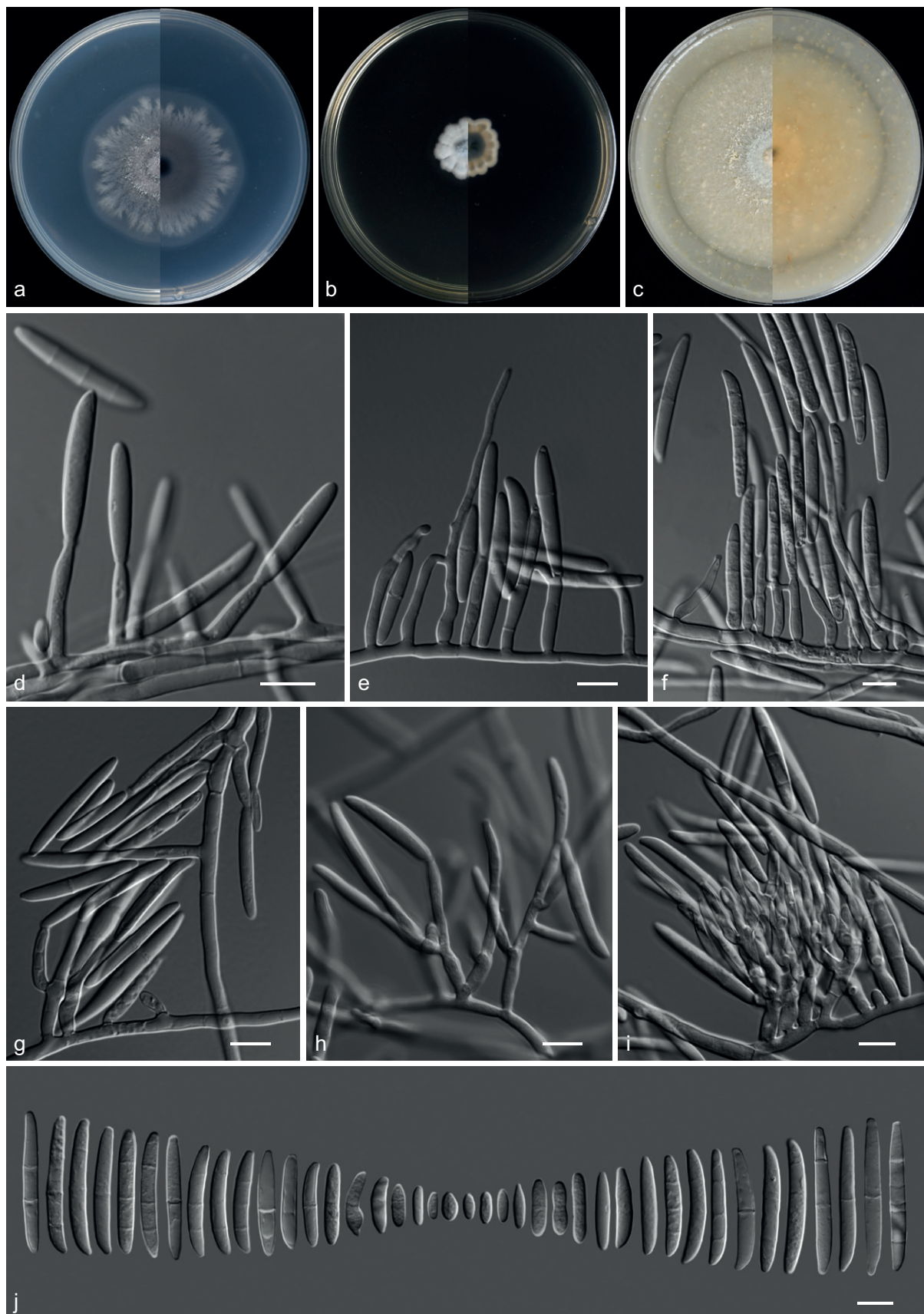


**Figure 22.** *Cyanonectria bispora* (from ex-holotype CGMCC 3.20774) **a–c** upper and reverse views of cultures on PDA, MEA and OA 14 d after inoculation **d–f** monophialide and conidia **g, h** polyphialides with multiple conidiogenous loci **i** sporodochial conidiophore and conidiogenous cells **j** conidia. Scale bars: 10 µm (d–j).

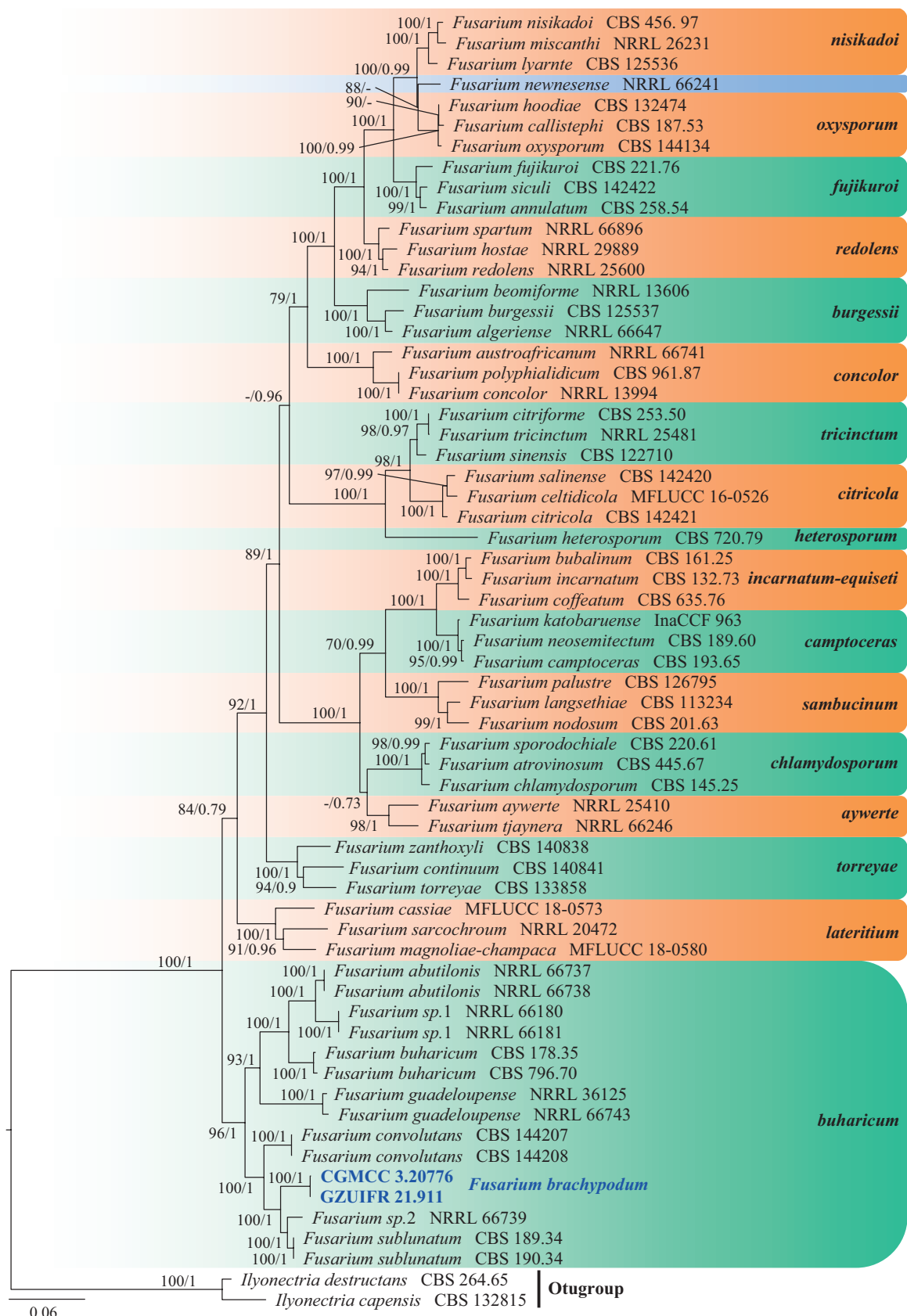


**Figure 23.** Concatenated phylogeny of the ITS, LSU, RPB2 and EF1A gene regions of species in *Fusarium*. Sixty-three strains are used. The tree is rooted in *Ilyonectria destructans* (CBS 264.65) and *I. capensis* (CBS 132815). The tree topology of the BI was similar to the ML analysis. Bayesian posterior probability ( $\geq 0.7$ ) and ML bootstrap values ( $\geq 70\%$ ) are indicated along branches (PP/ML). Novel species are in blue and bold font and "T" indicates type derived sequences.

**Additional specimens examined.** China: Guangxi Zhuang Autonomous Region, Guilin City, Yucai Campus of Guangxi Normal University 25°26'64"N, 110°32'70"E, soil, 30 Aug 2019, Z.Y. Zhang, GZUIFR 21.909.

**Notes.** The species is described here, based on its morphology of the asexual morph. In the phylogenetic analysis (Fig. 21), *Cyanonectria bispora* is nested in the genus *Cyanonectria* and sister to *C. cyanostoma* and *C. buxi*. Morphologically, *C. bispora* can be distinguished from *C. cyanostoma* and *C. buxi* by the production of macroconidia and microconidia (Samuels et al. 2009). In addition, *C. cyanostoma* and *C. buxi* are reported from Europe (Belgium, France, Germany and Slovenia) and associated with *B. sempervirens*, while *C. bispora* was isolated from soil in China.

### ***Fusarium* Link**

The genus *Fusarium* was established in 1809 by Link. Currently, *Fusarium* consists of 18 species complexes (Sandoval-Denis et al. 2018a; Lombard et al. 2019; Crous et al. 2021) with over 100 species. While the current classification of *Fusarium* relies on molecular phylogeny, it is important to note that morphology remains an essential component of the definition of fungal genus and species and should not be disregarded (Crous et al. 2021).

#### ***Fusarium brachypodium* Zhi.Y. Zhang, Y.F. Han & Z.Q. Liang, sp. nov.**

Mycobank No: 844173

Fig. 24

**Etymology.** Refers to the sporodochial conidia connected by 1–3 short-stalks.

**Type.** CHINA: Guizhou Province, Guiyang City, Qianlingshan Park 26°59'03"N, 106°69'57"E, soil, 13 Sep 2019, Z.Y. Zhang (HMAS 351876 holotype designated here, ex-type living culture CGMCC 3.20776 = GZUIFR 21.910).

**Description. Culture characteristics** (14 d at 25 °C): **Colony on PDA** 79 mm diam., milk white (1A2), flat, velvety, with scant and short aerial mycelium, rounded, margins irregular; reverse white (1A1). **Colony on MEA** 63 mm diam., white (1A1), flat, cottony, rounded, margins regularly; reverse white (1A1). **Colony on OA** 58 mm diam., white (1A1), flat, surface khaki granular, rounded, margin entire; reverse white (1A1).

**Hyphae** abundant, branched, septate, hyaline, smooth, 1.0–4.0 µm diam. **Conidiophores** arising from aerial hyphae, straight or flexuous, hyaline, smooth-walled, unbranched or sparingly branched, bearing terminal or monopodialides, often reduced to single phialides. **Phialides** subcylindrical to cylindrical, straight or flexuous, smooth, 12–22 µm long, 3.5–4.0 µm at the widest point. **Aerial conidia** forming small false heads on the tips of the phialides, hyaline, subcylindrical to cylindrical, straight or flexuous, smooth-walled, aseptate, 11.5–34.0 × 2.5–4.5 µm (av. 24.5 × 3.6 µm, n = 50). **Sporodochia** abundant. **Conidiophores** in sporodochia verticillately branched, consisting of a short, smooth-walled stipe, phialides cylindrical to lageniform, or irregular, 12.5–18.5 × 2.5–4.5 µm, bearing apical whorls of 2–3 monopodialides or as single lateral monopodialide. **Sporodochial conidia** smooth-walled, lunate to falcate, curved or somewhat straight, robust, with an elongated or whip-like curved apical cell and papillate to elong-

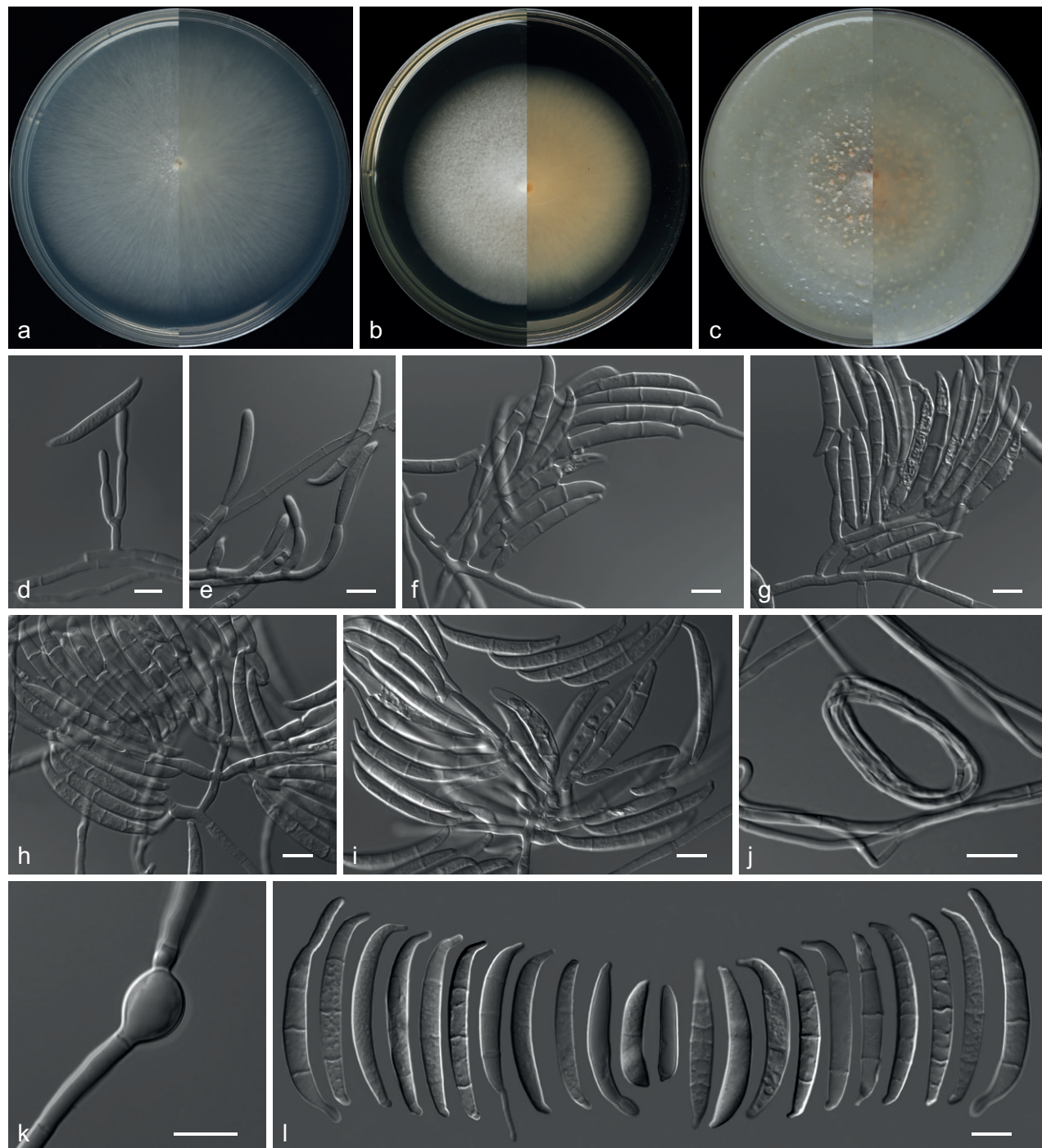


**Figure 24.** *Fusarium brachypodium* (from ex-holotype CGMCC 3.20776) **a–c** upper and reverse views of cultures on PDA, MEA and OA 14 d after inoculation **d, e** conidiophores and phialides on aerial mycelium **f–i** sporodochia, sporodochial conidiophores and conidia **j** spiral hyphae **k** chlamydospores **l** conidia. Scale bars: 10 µm (**d–l**).

gate, well-developed foot-shaped, sometimes poorly development basal cell, always aggregated, with connected by 1–3 short-stalked; 1–3 septate, sometimes aseptate, 1–septate conidia:  $26.5\text{--}29 \times 3.5\text{--}6.0 \mu\text{m}$  (av.  $28.2 \times 4.6 \mu\text{m}$ ,  $n = 50$ ), 2–septate conidia:  $38.0\text{--}45.0 \times 4.5\text{--}6.0 \mu\text{m}$  (av.  $41.7 \times 5.5 \mu\text{m}$ ,  $n = 50$ ), 3–septate conidia:  $32.5\text{--}61.0 \times 4.0\text{--}6.0 \mu\text{m}$  (av.  $46.0 \times 4.3 \mu\text{m}$ ,  $n = 50$ ), aseptate conidia:  $24.5\text{--}45.0 \times 3.5\text{--}6.0 \mu\text{m}$  (av.  $34.7 \times 4.0 \mu\text{m}$ ,  $n = 50$ ). **Chlamydospores** rare, subglobose to globose, hyaline, smooth-walled, intercalary, solitary, 9.0–

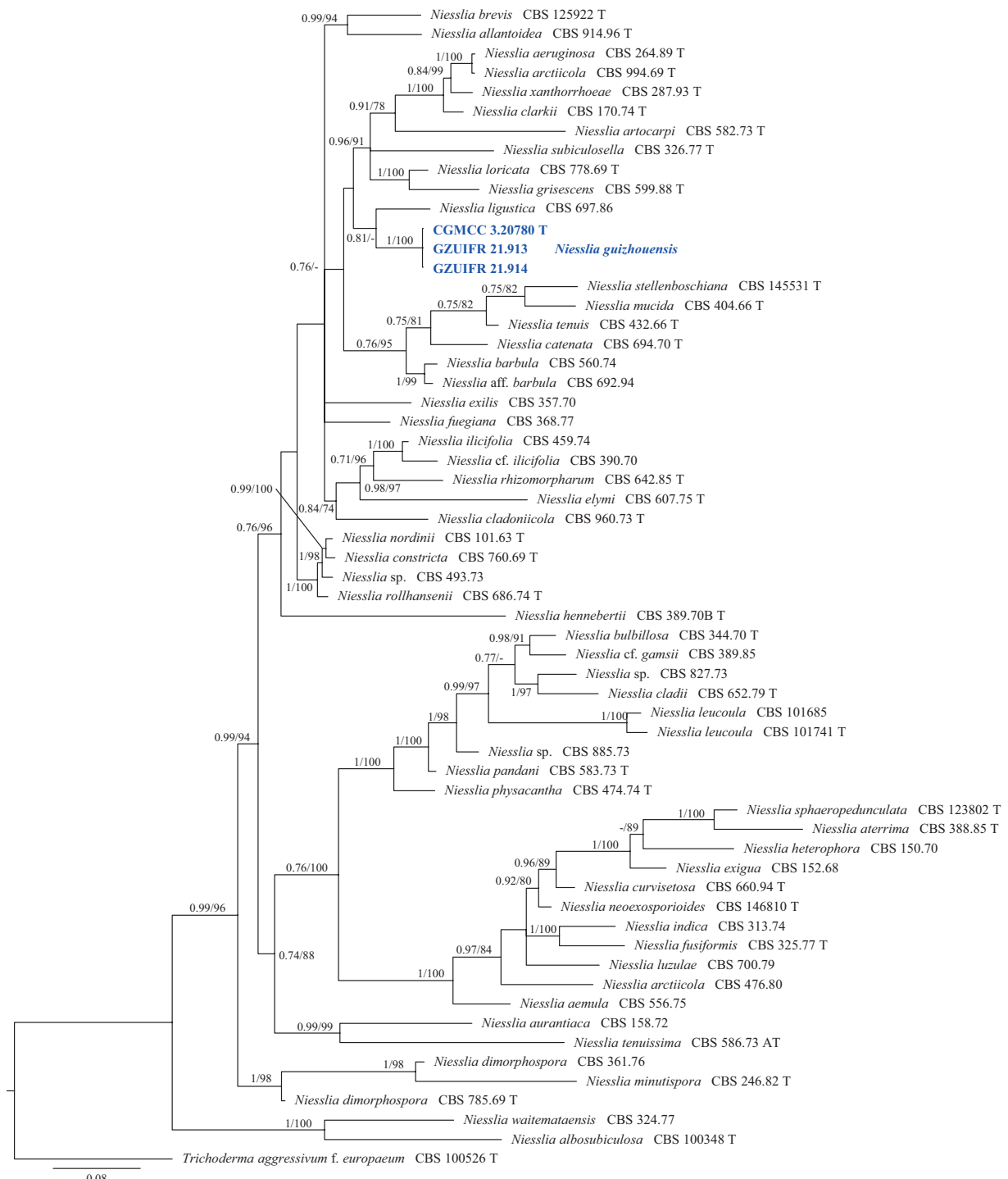


**Figure 25.** Concatenated phylogeny of the ITS, LSU, EF1A and ACT gene regions of species in *Niesslia*. Sixty strains are used. The tree is rooted in *Trichoderma aggressivum* f. *europaeum* (CBS 100526). The tree topology of the BI was similar to the ML analysis. Bayesian posterior probability ( $\geq 0.7$ ) and ML bootstrap values ( $\geq 70\%$ ) and are indicated along branches (PP/ML). Novel species are in blue and bold font and "T" indicates type derived sequences.

13.5  $\mu\text{m}$  (av. 11.8  $\mu\text{m}$ ,  $n = 5$ ) diam. **Coiled** sometimes from the substrate and aerial mycelium. **Microconidia** not observed. **Sexual morph** unknown.

**Additional specimens examined.** CHINA: Jiangxi Province, Jian City, Jinggangshan University 27°11'30"N, 115°03'19"E, soil, 22 Aug 2019, Z.Y. Zhang, GZUIFR 21.911.

**Notes.** *Fusarium brachypodium* was introduced as a new species while adding one more species to the *Fusarium buharicum* species complex (FBSC; Geiser et al. 2013; O'Donnell et al. 2013). Our isolates formed a single clade nested in FBSC (Fig. 23), which comprise *F. abutilonis*, *F. buharicum*, *F. convolutans*, *F. guadeloupense* and *F. sublunatum*. However, *Fusarium brachypodium* differs from members of FBSC in its presence of hyphae coiled, chlamydospores, absent microconidia and sporodochial conidia connected by 1–3 short stalks (Gerlach and Nirenberg 1982; Sandoval-Denis et al. 2018b).

**Niessliaceae Kirschst.**

***Niesslia* Auersw.**

The genus *Niesslia* was established in 1869, with the type species *N. chaetomium* (Auerswald 1869). *Niesslia* is characterised by tuberculate perithecia, surrounded by brown, septate setae, clavate ascii and filiform ascospores (Auerswald 1869). This genus is one of the more species-rich genera of ascomycetes, but has received relatively little taxonomic attention. Members of the genus are mostly saprophytic and globally distributed (Gams et al. 2019).

***Niesslia guizhouensis* Zhi.Y. Zhang, Y.F. Han & Z.Q. Liang, sp. nov.**

Mycobank No: 844174

Fig. 26

**Etymology.** In reference to Guizhou, the Province where the type specimen was obtained.

**Type.** CHINA: Guizhou Province, Guiyang City, North Campus of Guizhou University 26°44'37"N, 106°67'46"E, soil, 13 Sep 2019, Z.Y. Zhang (HMAS 351877 holotype designated here, ex-type living culture CGMCC 3.20780 = GZUIFR 21.912); ibid., GZUIFR 21.913.

**Description.** **Culture characteristics** (14 d at 25 °C): **Colony on PDA** 26–27 mm diam., white (1A1), texture velvety, nearly round, margin entire; reverse white (1A1). **Colony on MEA** 14–16 mm diam., orange white (5A2), aerial mycelia sparse, compact, rugged, cracked, margin undulated; reverse brownish-yellow (5C8) to white (5A1) from centre to margin. **Colony on OA** 36 mm diam., white (1A1), with a light-coloured margin, felty, compact, plicated, convex, margin entire to undulate; reverse white (1A1).

**Hypae** branched, septate, hyaline, smooth, 0.5–2.0 µm diam. **Sporulation** abundant, nematogenous to synnematogenous. **Phialides** from hyphae, hyphal coils, fertile, acerose at the moderately thick-walled base, sometimes bending, hardly widening above and tapering to 0.5–1 µm at the tip, 10.5–79.0 × 1.0–3.0 µm. **Conidia** adhering to slimy heads, cylindrical, smooth- and thin-walled, 3.0–7.5 × 1.0–2.5 µm (av. 5.3 × 1.9 µm, n = 50). **Chlamydospores** not observed. **Sexual morph** unknown.

**Additional specimens examined.** CHINA: Guizhou Province, Guiyang City, Qianlingshan Park 26°59'03"N, 106°69'57"E, soil, 13 Sep 2019, Z.Y. Zhang, GZUIFR 21.914.

**Notes.** *Niesslia guizhouensis* is phylogenetically related to *N. ligustica*, as demonstrated in Fig. 25, but can be differentiated from it by the absence of

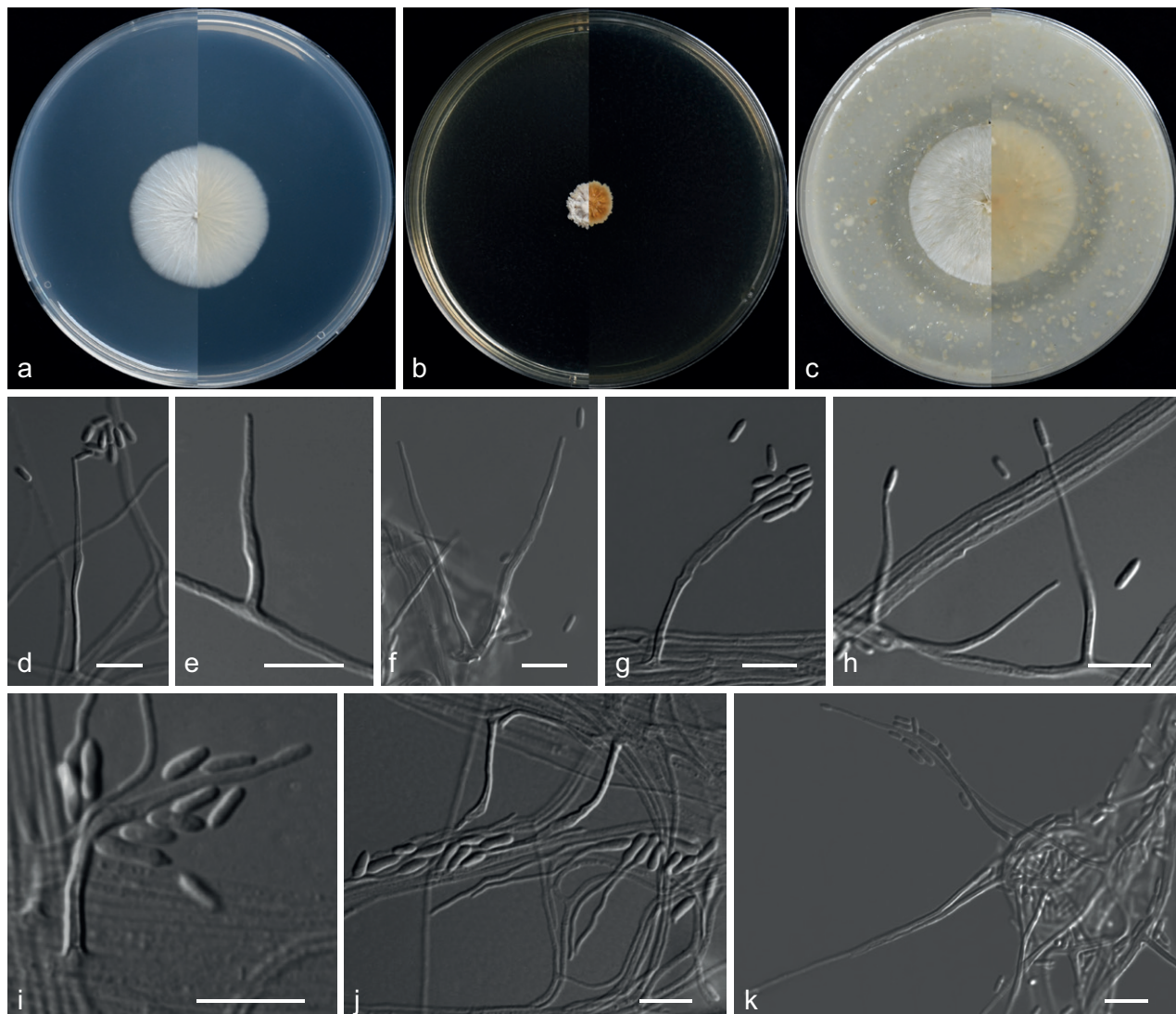


**Figure 26.** *Niesslia guizhouensis* (from ex-holotype CGMCC 3.20780) **a–c** upper and reverse views of cultures on PDA, MEA and OA 14 d after inoculation **d–j** monocillium-like conidiophores and conidia **k** hyphal coil with conidiophores. Scale bars: 10 µm (**d–k**).

pigmented cells (Gams et al. 2019). In addition, the colony of *N. guizhouensis* on MEA are white with a white reverse, whereas those of *N. ligustica* are white or sometimes pale orange with a pale luteous to ochraceous reverse (Gams et al. in 2019).

**Xylariales Nannf.**

**Microdochiaeae Hern.-Restr., Crous & J.Z. Groenew.**

***Idriella* P.E. Nelson & S. Wilh.**

*Idriella* comprises soil-inhabiting hyphomycetes and terrestrial species worldwide (Hyde et al. 2020b). The genus is characterised by brown, aseptate conidiophores and polyblastic conidiogenous cells with hyaline, unicellular, smooth, lunate, curved conidia in the heads (Hernández-Restrepo et al. 2016). Although the genus *Idriella* includes 30 species, molecular data are available for only four species and, based on the results of phylogenetic analyses, three of these species

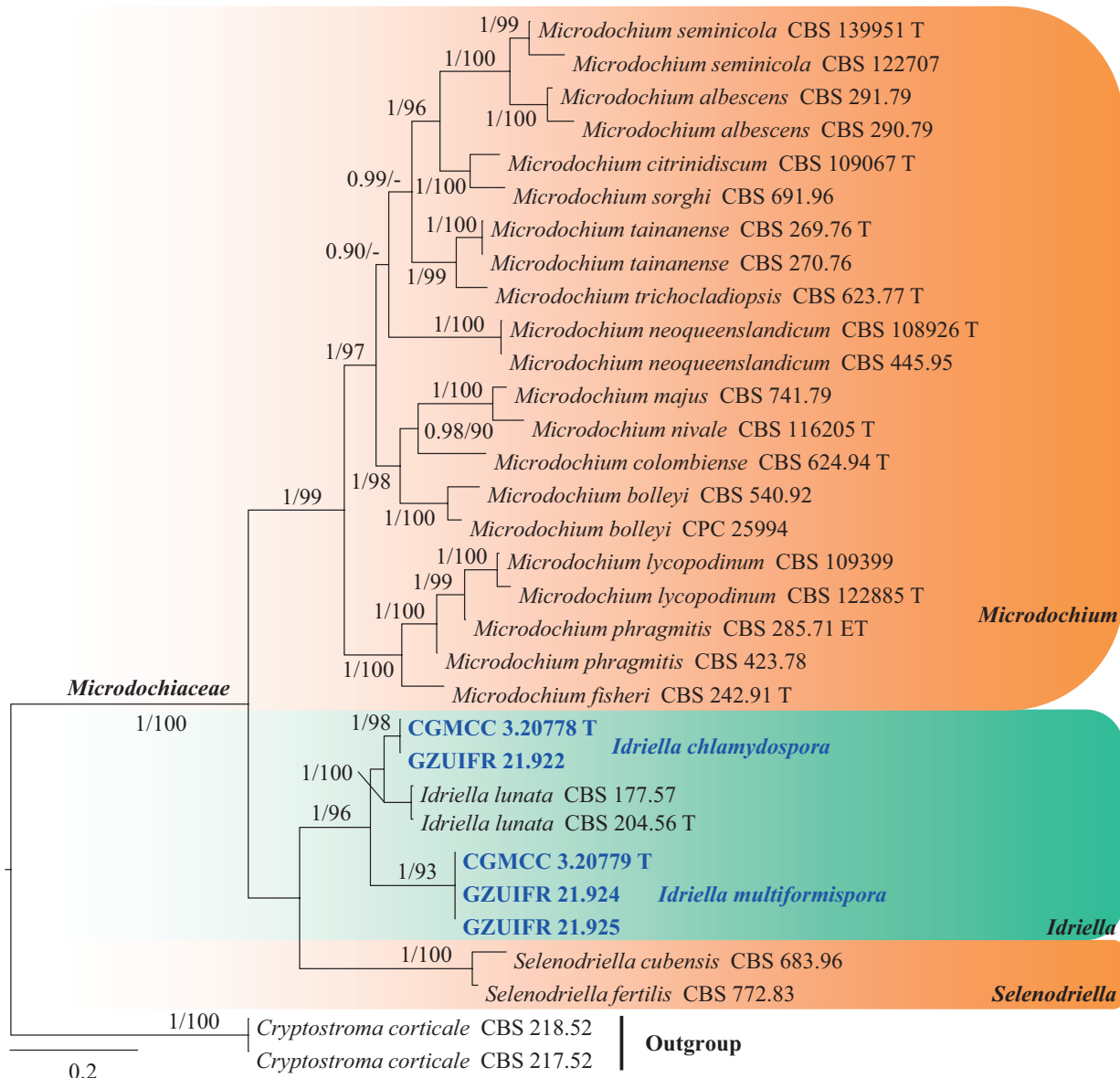


**Figure 27.** Concatenated phylogeny of the ITS, LSU, TUB and RPB2 gene regions of species in Microdochiaeae. Thirty-two strains are used. The tree is rooted in *Cryptostroma corticale* (CBS 218.52 and CBS 217.52). The tree topology of the BI was similar to the ML analysis. Bayesian posterior probability ( $\geq 0.8$ ) and ML bootstrap values ( $\geq 80\%$ ) are indicated along branches (PP/ML). Novel species are in blue and bold font, and “T” indicates type derived sequences.

have been moved out as type species and new genera have been established (Castañeda-Ruiz and Kendrick 1991; Hernández-Restrepo et al. 2016). The taxonomic status of species morphologically similar to these three species is debatable (Castañeda-Ruiz and Kendrick 1991; Hernández-Restrepo et al. 2016).

***Idriella chlamydospora* Zhi.Y. Zhang, Y.F. Han & Z.Q. Liang, sp. nov.**

Mycobank No: 844175

Fig. 28

**Etymology.** Refers to the species that only produces chlamydospores.

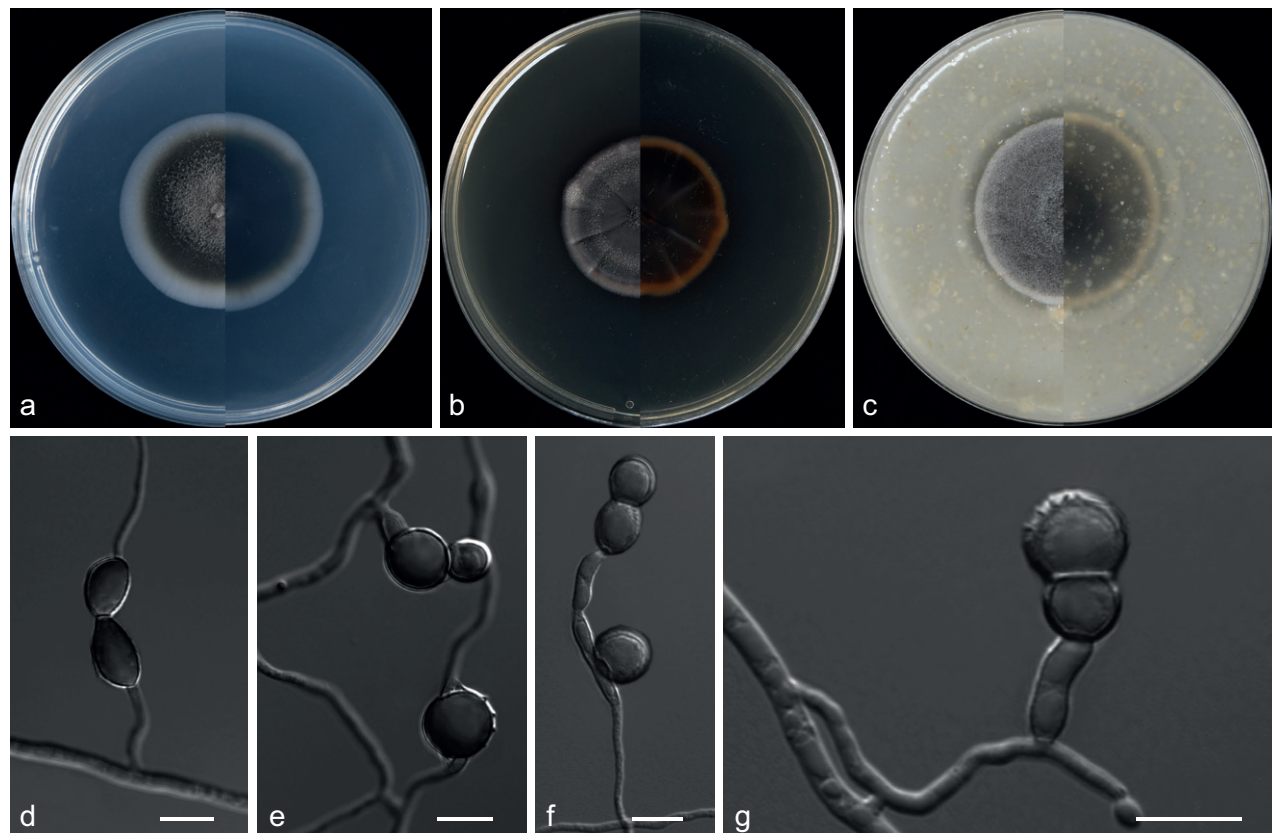


**Figure 28.** *Idriella chlamydospora* (from ex-holotype CGMCC 3.20778) **a–c** upper and reverse views of cultures on PDA, MEA and OA 14 d after inoculation **d–g** chlamydospores. Scale bars: 10 µm (**d–g**).

**Type.** CHINA: Guangdong Province, Guangzhou City, Nanfang Hospital of Southern Medical University 23°19'14"N, 113°32'93"E, soil, 24 Aug 2019, Z.Y. Zhang (HMAS 351879 holotype designated here, ex-type living culture CGMCC 3.20778 = GZUIFR 21.921).

**Description. Culture characteristics** (14 d at 25 °C): **Colony on PDA** 40–41 mm diam., grey (30F1–30E1), flat, felty to pulverulent, nearly round, margin entire; reverse grey (29F1). **Colony on MEA** 31–33 mm diam., grey (6F1), compact, plicated, nearly round, margin entire; reverse soot brown (5F5) from centre to margin. **Colony on OA** 38 mm diam., grey (30F1) with a white circle, plicated, nearly round, margin entire; reverse greenish-grey (30E2).

**Hyphae** branched, septate, hyaline, smooth, 1.0–3.0 µm diam. **Chlamydospores** arising in axenic culture on PDA, MEA and OA, moniliform, 1–2-septate, brown, 7.5–20.0 × 6.5–11.0 µm (av. 18.5 × 8.6 µm, n = 50). **Conidia** were not observed. **Sexual morph** unknown.

**Additional specimens examined.** China: Guangdong Province, Guangzhou City, South Campus of Sun Yat-sen University 23°10'04"N, 113°29'95"E, soil, 24 Aug 2019, Z.Y. Zhang, GZUIFR 21.922.

**Notes.** *Idriella chlamydospora* was isolated from soil in China. Phylogenetically, the new isolates CGMCC 3.20778 and GZUIFR 21.922 formed a single clade with a strongly-supported value and were nested in the genus *Idriella* (Fig. 27). However, morphologically, *I. chlamydospora* differs from other species in the genus *Idriella* in that it only produces chlamydospores.

***Idriella multiformispora* Zhi.Y. Zhang, Y.F. Han & Z.Q. Liang, sp. nov.**

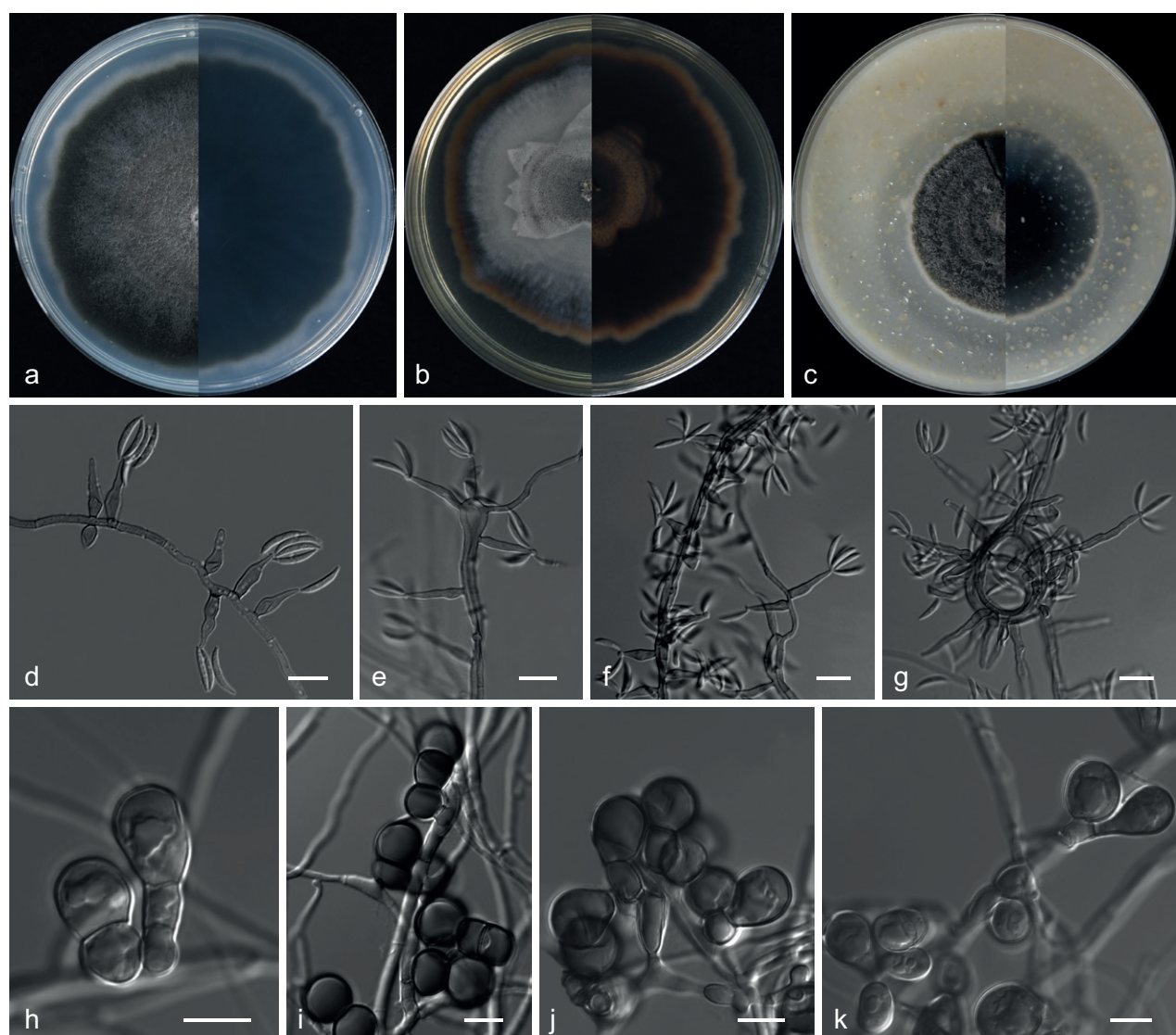
Mycobank No: 844176

Fig. 29

**Etymology.** Referring to the multiform conidia.

**Type.** CHINA: Jiangxi Province, Nanchang City, Nanchang People's Park 28°68'12"N, 115°91'35"E, soil, 13 Aug 2019, Z.Y. Zhang (HMAS 351880 holotype designated here, ex-type living culture CGMCC 3.20779 = GZUIFR 21.923).

**Description. Culture characteristics** (14 d at 25 °C): **Colony on PDA** 51 mm diam., grey (30F1) to dark green (30F4), felty, compact, margin entire to undulated; reverse dark green (30F4). **Colony on MEA** 27–30 mm diam., greenish-grey (30E2), flat, stellate striate with grey, margin entire to undulated; reverse dark green (30F4). **Colony on OA** 33–38 mm diam., greenish-grey (30E2), aerial mycelia dense, plicated, sectorisation, nearly round; reverse greenish-grey (30E2).



**Figure 29.** *Idriella multiformispora* (from ex-holotype CGMCC 3.20779) **a–c** upper and reverse views of cultures on PDA, MEA and OA 14 d after inoculation **d–f** conidiogenous cells and conidia **g** hyphal coil with phialides **h–k** chlamydospores. Scale bars: 10 µm (d–k).

**Hyphae** branched, septate, hyaline, smooth, 1.0–4.0 µm diam. **Conidiophores** reduced to conidiogenous cells. **Conidiogenous cells** numerous, borne on hyphae or hyphal coil, erect, straight or flexuous, lageniform, 9.5–25.5 µm long, 1.0–3.0 µm wide at the base, apex inflated or globose and 1.0–2.5 µm diam. **Conidia** lunate, sometimes acerose, pointed at each end, non-septate, smooth-walled, colourless, 8.5–13.5 × 1.0–2.0 µm (av. 11.6 × 1.7 µm, n = 50). **Chlamydospores** are borne on hyphae, moniliform or branched, 1–2-septate, brown, 12.5–22.5 × 6.5–11.5 µm (av. 21.4 × 10.5 µm, n = 50). **Sexual morph** unknown.

**Additional specimens examined.** CHINA: Jiangxi Province, Nanchang City, Qianhu Campus of Nanchang University 28°65'68"N, 115°80'12"E, soil, 13 Aug 2019, Z.Y. Zhang, GZUIFR 21.924, ibid., GZUIFR 21.925.

**Notes.** According to Castañeda-Ruiz and Kendrick (1991), *Idriella multiformispora* and *I. acerosa* share similarities in terms of their lunate conidia and moniliiform or branched chlamydospores. While introducing *I. acerosa*, Castañeda-Ruiz and Kendrick (1991) also noted that it bears a resemblance to *I. desertorum*. However, molecular data on *I. acerosa* are not available. Later, Hernández-Restrepo et al. (2016) established the genus *Neoidriella*, based on the molecular analysis of *I. desertorum* and removed it from the genus *Idriella* as the type species. In this study, *I. multiformispora* was phylogenetically categorised within the genus *Idriella* (Fig. 27). Morphologically, *I. multiformispora* can be differentiated from *I. acerosa* by its fewer septate chlamydospores (Castañeda-Ruiz and Kendrick in 1991).

## Acknowledgements

We greatly appreciate Dr. Bensch for her advice on the new species names.

## Additional information

### Conflict of interest

The authors have declared that no competing interests exist.

### Ethical statement

No ethical statement was reported.

### Funding

The work was supported by the National Natural Science Foundation of China (no. 32060011, 32160007, 31860002), "Hundred" Talent Projects of Guizhou Province (Qian Ke He [2020] 6005), Key Areas of Research and Development Program of Guangdong Province (no. 2018B020205003), Construction Program of Biology First-class Discipline in Guizhou (GNYL [2017] 009), and Scientific Research Project of Introduction of Talents in Guizhou University (Gui Da Ren Ji He Zi (2018) 10).

### Author contributions

Sampling, molecular biology analysis: Zhi-Yuan Zhang and Wan-Hao Chen; fungal isolation: Zhi-Yuan Zhang and Xin Li; description and phylogenetic analysis: Zhi-Yuan Zhang, Wan-Hao Chen and Jian-Dong Liang; microscopy: Zhi-Yuan Zhang Xin Li and Yan-Feng Han; writing—original draft preparation: Zhi-Yuan Zhang and Yan-Feng Han; writing—review and editing, Zhi-Yuan Zhang, Xin Li, Wan-Hao Chen, Jian-Dong Liang and Yan-Feng Han. All authors read and approved the final manuscript.

## Author ORCIDs

- Zhi-Yuan Zhang  <https://orcid.org/0000-0003-2031-7518>  
Xin Li  <https://orcid.org/0000-0001-7910-1469>  
Wan-Hao Chen  <https://orcid.org/0000-0001-7240-6841>  
Jian-Dong Liang  <https://orcid.org/0000-0002-3939-3900>  
Yan-Feng Han  <https://orcid.org/0000-0002-8646-3975>

## Data availability

All of the data that support the findings of this study are available in the main text or Supplementary Information.

## References

- Antrop M (2004) Landscape change and the urbanization process in Europe. *Landscape and Urban Planning* 67(1–4): 9–26. [https://doi.org/10.1016/S0169-2046\(03\)00026-4](https://doi.org/10.1016/S0169-2046(03)00026-4)
- Auerswald B (1869) Synopsis pyrenomycetum europaeorum. In: Gonnerman W, Rabenhorst GL (Eds) *Mycologia Europaea*.
- Baert F, Stubbe D, D'hooge E, Packeu A, Hendrickx M (2020) Updating the taxonomy of dermatophytes of the BCCM/IHEM collection according to the new standard: A phylogenetic approach. *Mycopathologia* 185: 161–168. <https://doi.org/10.1007/s11046-019-00338-7>
- Barbosa RN, Bezerra JDP, Souza-Motta CM, Frisvad JC, Samson RA, Oliveira NT, Houbraken J (2018) New *Penicillium* and *Talaromyces* species from honey, pollen and nests of stingless bees. *Antonie van Leeuwenhoek* 111(10): 1883–1912. <https://doi.org/10.1007/s10482-018-1081-1>
- Benjamin CR (1955) Ascocarps of *Aspergillus* and *Penicillium*. *Mycologia* 47(5): 669–687. <https://doi.org/10.1080/00275514.1955.12024485>
- Berry BJL (2008) Urbanization. In: Marzluff JM, Bradley G, Schulenberger E, Ryan C, Endlicher W, Simon U, Alberti M, Zumbrunnen C (Eds) *Urban Ecology: an International Perspective on the Interaction Between Humans and Nature*. Springer, New York, 25–48. [https://doi.org/10.1007/978-0-387-73412-5\\_3](https://doi.org/10.1007/978-0-387-73412-5_3)
- Campbell R, Sutton BC (1977) Conidial ontogeny in *Echinocatena arthrinoides* gen. et sp. nov. (Deuteromycotina: Hyphomycetes). *Transactions of the British Mycological Society* 69(1): 125–131. [https://doi.org/10.1016/S0007-1536\(77\)80123-X](https://doi.org/10.1016/S0007-1536(77)80123-X)
- Carbone I, Kohn LM (1999) A method for designing primer sets for speciation studies in filamentous ascomycetes. *Mycologia* 91(3): 553–556. <https://doi.org/10.1080/00275514.1999.12061051>
- Castañeda-Ruiz RF, Kendrick B (1991) Ninety-nine conidial fungi from Cuba and three from Canada. *University of Waterloo Biology Series* 35: 1–132.
- Chen CJ, Chen H, Zhang Y, Thomas HR, Frank MH, He Y, Xia R (2020) TBtools: An integrative toolkit developed for interactive analyses of big biological data. *Molecular Plant* 13(8): 1194–1202. <https://doi.org/10.1016/j.molp.2020.06.009>
- Corda ACJ (1839) Pracht – Flora. *Europaeischer Schimmel-Bildungen*.
- Crous PW, Lombard L, Sandoval-Denis M, Seifert KA, Schroers HJ, Chaverri P, Gené J, Guarro J, Hirooka Y, Bensch K, Kema GHJ, Lamprecht SC, Cai L, Rossman AY, Stadler M, Summerbell RC, Taylor JW, Ploch S, Visagie CM, Yilmaz N, Frisvad JC, Abdel-Azeem AM, Abdollahzadeh J, Abdolrasouli A, Akulov A, Alberts JF, Araújo JPM, Ariyawansa HA, Bakhshi M, Bendiksby M, Ben Hadj Amor A, Bezerra JDP, Boekhout T, Câmara MPS, Carbia M, Cardinali G, Castañeda-Ruiz RF, Celis A, Chaturvedi V, Collemare J, Croll D, Damm U, Decock CA, de Vries RP, Ezekiel CN, Fan XL, Fernández NB, Gaya E, González

- CD, Gramaje D, Groenewald JZ, Grube M, Guevara-Suarez M, Gupta VK, Guarnaccia V, Haddaji A, Hagen F, Haelewaters D, Hansen K, Hashimoto A, Hernández-Restrepo M, Houbraken J, Hubka V, Hyde KD, Iturriaga T, Jeewon R, Johnston PR, Jurjević Ž, Karaltı ī, Korsten L, Kuramae EE, Kušan I, Labuda R, Lawrence DP, Lee HB, Lechat C, Li HY, Litovka YA, Maharachchikumbura SSN, Marin-Felix Y, Matto Kemkuignou B, Matočec N, McTaggart AR, Mičoch P, Mugnai L, Nakashima C, Nilsson RH, Noumeur SR, Pavlov IN, Peralta MP, Phillips AJL, Pitt JI, Polizzi G, Quaedvlieg W, Rajeshkumar KC, Restrepo S, Rhaiem A, Robert J, Robert V, Rodrigues AM, Salgado-Salazar C, Samson RA, Santos ACS, Shivas RG, Souza-Motta CM, Sun GY, Swart WJ, Szoke S, Tan YP, Taylor JE, Taylor PWJ, Tiago PV, Váczky KZ, van de Wiele N, van der Merwe NA, Verkley GJM, Vieira WAS, Vizzini A, Weir BS, Wijayawardene NN, Xia JW, Yáñez-Morales MJ, Yurkov A, Zamora JC, Zare R, Zhang CL, Thines M (2021) *Fusarium*: More than a node or a foot-shaped basal cell. *Studies in Mycology* 98: 1–184. <https://doi.org/10.1016/j.simyco.2021.100116>
- de Hoog GS, Dukik K, Monod M, Packeu A, Stubbe D, Hendrickx M, Kupsch C, Stielow JB, Freeke J, Göker M, Rezaei-Matehkolaie A, Mirhendi H, Gräser Y (2017) Toward a novel multilocus phylogenetic taxonomy for the dermatophytes. *Mycopathologia* 182(1–2): 5–31. <https://doi.org/10.1007/s11046-016-0073-9>
- Dukik K, de Hoog GS, Stielow JB, Freeke J, van den Ende BG, Vicente VA, Menken SGJ (2020) Molecular and phenotypic characterization of *Nannizzia* (Arthrodermataceae). *Mycopathologia* 185: 9–35. <https://doi.org/10.1007/s11046-019-00336-9>
- El-Gendi H, Saleh AK, Badierah R, Redwan EM, El-Maradny YA, El-Fakharany EM (2022) A comprehensive insight into fungal enzymes: Structure, classification, and their role in mankind's challenges. *Journal of Fungi* 8(1): 1–23. <https://doi.org/10.3390/jof8010023>
- Fisher MC, Henk DA, Briggs CJ, Brownstein JS, Madoff LC, McCraw SL, Gurr SJ (2012) Emerging fungal threats to animal, plant and ecosystem health. *Nature* 484: 186–194. <https://doi.org/10.1038/nature10947>
- Fisher MC, Gurr SJ, Cuomo CA, Blehert DS, Jin H, Stukenbrock EH, Stajich JE, Kahmann R, Boone C, Denning DW, Gow NAR, Klein BS, Kronstad JW, Sheppard DC, Taylor JW, Wright GD, Heitman J, Casadevall A, Cowen LE (2020) Threats posed by the fungal kingdom to humans, wildlife, and agriculture. *mBio* 11(3): e00449–e20. <https://doi.org/10.1128/mBio.00449-20>
- Fones HN, Bebber DP, Chaloner TM, Kay WT, Steinberg G, Gurr SJ (2020) Threats to global food security from emerging fungal and oomycete crop pathogens. *Nature Food* 1(6): 332–342. <https://doi.org/10.1038/s43016-020-0075-0>
- Gams W, Stielow B, Gräfenhan T, Schroers HJ (2019) The ascomycete genus *Niesslia* and associated monocillium-like anamorphs. *Mycological Progress* 18(1–2): 5–76. <https://doi.org/10.1007/s11557-018-1459-5>
- Geiser DM, Aoki T, Bacon CW, Baker SE, Bhattacharyya MK, Brandt ME, Brown DW, Burgess LW, Chulze S, Coleman JJ, Correll JC, Covert SF, Crous PW, Cuomo CA, de Hoog GS, Pietro AD, Elmer WH, Epstein L, Frandsen RJN, Freeman S, Gagkaeva T, Glenn AE, Gordon TR, Gregory NF, Hammond-Kosack KE, Hanson LE, del Mar Jímenez-Gasco M, Kang S, Kistler HC, Kulda GA, Leslie JF, Logrieco A, Lu G, Lysøe E, Ma LJ, McCormick SP, Micheli Q, Moretti A, Munaut F, O'Donnell K, Pfenning L, Ploetz RC, Proctor RH, Rehner SA, Robert VARG, Rooney AP (2013) One fungus, one name: Defining the genus *Fusarium* in a scientifically robust way that preserves longstanding use. *Phytopathology* 103(5): 400–408. <https://doi.org/10.1094/PHYTO-07-12-0150-LE>
- Gerlach W, Nirenberg HI (1982) The genus *Fusarium* – a pictorial atlas. *Mitteilungen der Biologischen Bundesanstalt für Land- und Forstwirtschaft Berlin-Dahlem* 209: 1–406.

- Glass NL, Donaldson GC (1995) Development of primer sets designed for use with the PCR to amplify conserved genes from filamentous ascomycetes. *Applied and Environmental Microbiology* 61(4): 1323–1330. <https://doi.org/10.1128/aem.61.4.1323-1330.1995>
- Grimm NB, Faeth SH, Golubiewski NE, Redman CL, Wu J, Bai X, Briggs JM (2008) Global change and the ecology of cities. *Science* 319(5864): 756–760. <https://doi.org/10.1126/science.1150195>
- Hebert PD, Ratnasingham S, De Waard JR (2003) Barcoding animal life: Cytochrome c oxidase subunit 1 divergences among closely related species. *Proceedings of the Royal Society of London, Series B, Biological Sciences* 270: S96–S99. <https://doi.org/10.1098/rsbl.2003.0025>
- Heeger F, Bourne EC, Baschien C, Yurkov A, Bunk B, Spröer C, Overmann J, Mazzoni CJ, Monaghan MT (2018) Long-read DNA metabarcoding of ribosomal RNA in the analysis of fungi from aquatic environments. *Molecular Ecology Resources* 18(6): 1500–1514. <https://doi.org/10.1111/1755-0998.12937>
- Hernández-Restrepo M, Groenewald JZ, Crous PW (2016) Taxonomic and phylogenetic re-evaluation of *Microdochium*, *Monographella* and *Idriella*. *Persoonia* 36(1): 57–82. <https://doi.org/10.3767/003158516X688676>
- Hoffmeister D, Keller NP (2007) Natural products of filamentous fungi: Enzymes, genes, and their regulation. *Natural Product Reports* 24(2): 393–416. <https://doi.org/10.1039/B603084J>
- Hou LW, Giraldo A, Groenewald JZ, Rämä T, Summerbell RC, Huang GZ, Cai L, Crous PW (2023) Redisposition of acremonium-like fungi in Hypocreales. *Studies in Mycology* 105: 23–203. <https://doi.org/10.3114/sim.2023.105.02>
- Houbraken J, Frisvad JC, Samson RA (2011a) Taxonomy of *Penicillium* section *Citrina*. *Studies in Mycology* 70: 53–138. <https://doi.org/10.3114/sim.2011.70.02>
- Houbraken J, Spierenburg H, Frisvad JC (2011b) *Rasamonia*, a new genus comprising thermotolerant and thermophilic *Talaromyces* and *Geosmithia* species. *Antonie van Leeuwenhoek* 101(2): 403–421. <https://doi.org/10.1007/s10482-011-9647-1>
- Houbraken J, Kocsubé S, Visagie CM, Yilmaz N, Wang XC, Meijer M, Kraak B, Hubka V, Bensch K, Samson RA, Frisvad JC (2020) Classification of *Aspergillus*, *Penicillium*, *Talaromyces* and related genera (Eurotiales): An overview of families, genera, subgenera, sections, series and species. *Studies in Mycology* 95: 5–169. <https://doi.org/10.1016/j.simyco.2020.05.002>
- Hoyt H (1939) The Structure and Growth of Residential Neighborhoods in American Cities. Nabu Press, Atlanta.
- Hyde KD, Jeewon R, Chen YJ, Bhunjun CS, Calabon MS, Jiang HB, Lin CG, Norphanphoun C, Sysouphanthong P, Pem D, Tibpromma S, Zhang Q, Doilom M, Jayawardena RS, Liu J-K, Maharachchikumbura SSN, Phukhamsakda C, Phookamsak R, Al-Sadi AM, Thongklang N, Wang Y, Gafforov Y, Gareth Jones EB, Lumyong S (2020a) The numbers of fungi: Is the descriptive curve flattening? *Fungal Diversity* 103(1): 219–271. <https://doi.org/10.1007/s13225-020-00458-2>
- Hyde KD, Norphanphoun C, Maharachchikumbura SSN, Bhat DJ, Jones EBG, Bundhun D, Chen YJ (2020b) Refined families of Sordariomycetes. *Mycosphere: Journal of Fungal Biology* 11(1): 305–1059. <https://doi.org/10.5943/mycosphere/11/1/7>
- Jewell LE, Hsiang T (2013) Multigene differences between *Microdochium niveale* and *Microdochium majus*. *Botany* 91(2): 99–106. <https://doi.org/10.1139/cjb-2012-0178>
- Kalyaanamoorthy S, Minh BQ, Wong TKF, von Haeseler A, Jermiin LS (2017) ModelFinder: Fast model selection for accurate phylogenetic estimates. *Nature Methods* 14(6): 587–589. <https://doi.org/10.1038/nmeth.4285>

- Katoh K, Standley DM (2013) MAFFT multiple sequence alignment software version 7: Improvements in performance and usability. *Molecular Biology and Evolution* 30(4): 772–780. <https://doi.org/10.1093/molbev/mst010>
- Kornerup A, Wanscher JH (1978) Methuen handbook of colour (3<sup>rd</sup> edn.). Eyre Methuen Ltd., London.
- Li X, Zhang ZY, Chen WH, Liang JD, Huang JZ, Han YF, Liang ZQ (2022a) A new species of *Arthrographis* (Eremomycetaceae, Dothideomycetes), from the soil in Guizhou, China. *Phytotaxa* 538(3): 175–181. <https://doi.org/10.11646/phytotaxa.538.3.1>
- Li X, Zhang ZY, Chen WH, Liang JD, Liang ZQ, Han YF (2022b) *Keratinophyton chongqinense* sp. nov. and *Keratinophyton sichuanense* sp. nov., from soil in China. *International Journal of Systematic and Evolutionary Microbiology* 72(8): e005468. <https://doi.org/10.1099/ijsem.0.005468>
- Link HF (1809) *Observationes in ordines plantarum naturales. Dissertatio I. Magazin der Gesellschaft Naturforschenden Freunde Berlin* 3: 1–31.
- Liu YJ, Whelen S, Hall BD (1999) Phylogenetic relationships among Ascomycetes: Evidence from an RNA polymerase II subunit. *Molecular Biology and Evolution* 16(12): 1799–1808. <https://doi.org/10.1093/oxfordjournals.molbev.a026092>
- Lombard L, Sandoval-Denis M, Lamprecht SC, Crous PW (2019) Epitypification of *Fusarium oxysporum*—clearing the taxonomic chaos. *Persoonia* 43(1): 1–47. <https://doi.org/10.3767/persoonia.2019.43.01>
- Mapook A, Hyde KD, Hassan K, Kemkuignou BM, Čmoková A, Surup F, Kuhnert E, Pao-mephan P, Cheng T, de Hoog S, Song Y, Jayawardena RS, Al-Hatmi AMS, Mahmoudi T, Ponts N, Studt-Reinhold L, Richard-Forget F, Chethana KWT, Harishchandra DL, Mortimer PE, Li H, Lumyong S, Aidiang W, Kumla J, Suwannarach N, Bhunjun CS, Yu FM, Zhao Q, Schaefer D, Stadler M (2022) Ten decadal advances in fungal biology leading towards human well-being. *Fungal Diversity* 116(1): 547–614. <https://doi.org/10.1007/s13225-022-00510-3>
- McDonnell MJ, Pickett ST (1990) Ecosystem structure and function along urban-rural gradients: An unexploited opportunity for ecology. *Ecology* 71(4): 1232–1237. <https://doi.org/10.2307/1938259>
- Micheli PA (1729) *Nova plantarvm genera ivxta Tovrnefortii methodvm disposita.* Florence.
- Minh BQ, Nguyen MAT, von Haeseler A (2013) Ultrafast approximation for phylogenetic bootstrap. *Molecular Biology and Evolution* 30(5): 1188–1195. <https://doi.org/10.1093/molbev/mst024>
- Minnis AM, Lindner DL (2013) Phylogenetic evaluation of *Geomyces* and allies reveals no close relatives of *Pseudogymnoascus destructans*, comb. nov., in bat hibernacula of eastern North America. *Fungal Biology* 117(9): 638–649. <https://doi.org/10.1016/j.funbio.2013.07.001>
- Nguyen LT, Schmidt HA, von Haeseler A, Minh BQ (2015) IQ-TREE: A fast and effective stochastic algorithm for estimating maximum-likelihood phylogenies. *Molecular Biology and Evolution* 32(1): 268–274. <https://doi.org/10.1093/molbev/msu300>
- O'Donnell K, Kistler HC, Cigelnik E, Ploetz R (1998) Multiple evolutionary origins of the fungus causing Panama disease of banana: Concordant evidence from nuclear and mitochondrial gene genealogies. *Proceedings of the National Academy of Sciences of the United States of America* 95(5): 2044–2049. <https://doi.org/10.1073/pnas.95.5.2044>
- O'Donnell K, Nirenberg HI, Aoki T, Cigelnik E (2000) A multigene phylogeny of the *Gibberella fujikuroi* species complex: Detection of additional phylogenetically distinct species. *Mycoscience* 41(1): 61–78. <https://doi.org/10.1007/BF02464387>

- O'Donnell K, Rooney AP, Proctor RH, Brown DW, McCormick SP, Ward TJ, Frandsen RJP, Lysøe E, Rehner SA, Aoki T, Robert VARG, Crous PW, Groenewald JZ, Kang S, Geiser DM (2013) Phylogenetic analyses of RPB1 and RPB2 support a middle Cretaceous origin for a clade comprising all agriculturally and medically important fusaria. *Fungal Genetics and Biology* 52: 20–31. <https://doi.org/10.1016/j.fgb.2012.12.004>
- Orr MC, Ascher JS, Bai M, Chesters D, Zhu CD (2020) Three questions: How can taxonomists survive and thrive worldwide? *Megataxa* 001(1): 019–027. <https://doi.org/10.11646/megataxa.1.1.4>
- Peng L, Zhang YW, Wang HY, Dong CB, Chen WH, Liang JD, Han YF (2023) Taxonomy and phylogeny of eight new *Acrophialophora* species (Sordariales, Chaetomiaceae) from China. *Journal of Fungi* 9(6): e645. <https://doi.org/10.3390/jof9060645>
- Peterson SW, Jurjević Ž (2017) New species of *Talaromyces* isolated from maize, indoor air, and other substrates. *Mycologia* 109(4): 537–556. <https://doi.org/10.1080/00275514.2017.1369339>
- Peterson SW, Vega FE, Posada F, Nagai C (2005) *Penicillium coffeae*, a new endophytic species isolated from a coffee plant and its phylogenetic relationship to *P. fellutanum*, *P. thiersii* and *P. brocae* based on parsimony analysis of multilocus DNA sequences. *Mycologia* 97(3): 659–666. <https://doi.org/10.1080/15572536.2006.11832796>
- Raillo A (1929) Beiträge zur kenntnis der boden-pilze. *Zentralblatt für Bakteriologie, Parasitenkunde, Infektionskrankheiten und Hygiene. Zweite Naturwissenschaftliche Abt.: Allgemeine, Landwirtschaftliche und Technische Mikrobiologie* 78: 515–524.
- Rambaut A, Drummond AJ, Xie D, Baele G, Suchard MA (2018) Posterior summarization in bayesian phylogenetics using Tracer 1.7. *Systematic Biology* 67(5): 901–904. <https://doi.org/10.1093/sysbio/syy032>
- Reeb V, Lutzoni F, Roux C (2004) Contribution of RPB2 to multilocus phylogenetic studies of the euascomycetes (Pezizomycotina, Fungi) with special emphasis on the lichen-forming Acarosporaceae and evolution of polyspority. *Molecular Phylogenetics and Evolution* 32(3): 1036–1060. <https://doi.org/10.1016/j.ympev.2004.04.012>
- Rehner SA, Buckley E (2005) A *Beauveria* phylogeny inferred from nuclear ITS and EF1-a sequences: Evidence for cryptic diversification and links to *Cordyceps* teleomorphs. *Mycologia* 97(1): 84–98. <https://doi.org/10.3852/mycologia.97.1.84>
- Ronquist F, Teslenko M, van der Mark P, Ayres DL, Darling A, Höhna S, Larget B, Liu L, Suchard MA, Huelsenbeck JP (2012) MrBayes 3.2: Efficient bayesian phylogenetic inference and model choice across a large model space. *Systematic Biology* 61(3): 539–542. <https://doi.org/10.1093/sysbio/sys029>
- Rossman AY, Seifert KA, Samuels GJ, Minnis AM, Schroers HJ, Lombard L, Crous PW, Pöldmaa K, Cannon PF, Summerbell RC, Geiser DM, Zhuang W, Hirooka Y, Herrera C, Salgado-Salazar C, Chaverri P (2013) Genera in Bionectriaceae, Hypocreaceae, and Nectriaceae (Hypocreales) proposed for acceptance or rejection. *IMA Fungus* 4(1): 41–51. <https://doi.org/10.5598/imafungus.2013.04.01.05>
- Rydin Y, Bleahu A, Davies M, Dávila JD, Friel S, De Grandis G, Groce N, Hallal PC, Hamilton I, Howden-Chapman P, Lai K-M, Lim CJ, Martins J, Osrin D, Ridley I, Scott I, Taylor M, Wilkinson P, Wilson J (2012) Shaping cities for health: Complexity and the planning of urban environments in the 21<sup>st</sup> century. *Lancet* 379(9831): 2079–2108. [https://doi.org/10.1016/S0140-6736\(12\)60435-8](https://doi.org/10.1016/S0140-6736(12)60435-8)
- Samson RA (1972) Notes on *Pseudogymnoascus*, *Gymnoascus* and related genera. *Acta Botanica Neerlandica* 21(5): 517–527. <https://doi.org/10.1111/j.1438-8677.1972.tb00804.x>

- Samson RA, Visagie CM, Houbraken J, Hong SB, Hubka V, Klaassen CHW, Perrone G, Seifert KA, Susca A, Tanney JB, Varga J, Kocsimbé S, Szigeti G, Yaguchi T, Frisvad JC (2014) Phylogeny, identification and nomenclature of the genus *Aspergillus*. Studies in Mycology 78(1): 141–173. <https://doi.org/10.1016/j.simyco.2014.07.004>
- Samuels GJ, Lu BS, Chaverri P, Candoussau F, Fournier J, Rossman AY (2009) *Cyanonectria*, a new genus for *Nectria cyanostoma* and its *Fusarium* anamorph. Mycological Progress 8(1): 49–58. <https://doi.org/10.1007/s11557-008-0577-x>
- Sandoval-Denis M, Guarnaccia V, Polizzi G, Crous PW (2018a) Symptomatic *Citrus* trees reveal a new pathogenic lineage in *Fusarium* and two new *Neocosmospora* species. Persoonia 40(1): 1–25. <https://doi.org/10.3767/persoonia.2018.40.01>
- Sandoval-Denis M, Swart WJ, Crous PW (2018b) New *Fusarium* species from the Kruger National Park, South Africa. MycoKeys 34: 63–92. <https://doi.org/10.3897/mycokes.34.25974>
- Schmitt I, Crespo A, Divakar PK, Fankhauser JD, Herman-Sackett E, Kalb K, Nelsen MP, Nelson NA, Rivas-Plata E, Shimp AD, Widholm T, Lumbsch HT (2009) New primers for promising single-copy genes in fungal phylogenetics and systematics. Persoonia 23(1): 35–40. <https://doi.org/10.3767/003158509X470602>
- Schoch CL, Seifert KA, Huhndorf S, Robert V, Spouge JL, Levesque CA, Chen W, Bolchacova E, Voigt K, Crous PW, Miller AN, Wingfield MJ, Aime MC, An KD, Bai FY, Barreto RW, Begerow D, Bergeron MJ, Blackwell M, Boekhout T, Bogale M, Boonyuen N, Burgaz AR, Buyck B, Cai L, Cai Q, Cardinali G, Chaverri P, Coppins BJ, Crespo A, Cubas P, Cummings C, Damm U, de Beer ZW et al. (2012) Nuclear ribosomal internal transcribed spacer (ITS) region as a universal DNA barcode marker for Fungi. Proceedings of the National Academy of Sciences of the United States of America 109(16): 6241–6246. <https://doi.org/10.1073/pnas.1117018109>
- Schroers HJ (2001) A monograph of Bionectria (Ascomycota, Hypocreales, Bionectriaceae) and its *Clonostachys* anamorphs. Studies in Mycology 46: 1–214.
- Schroers HJ, Gräfenhan T, Nirenberg HI, Seifert KA (2011) A revision of *Cyanonectria* and *Geejayessia* gen. nov., and related species with *Fusarium*-like anamorphs. Studies in Mycology 68: 115–138. <https://doi.org/10.3114/sim.2011.68.05>
- Shen M, Zhang JQ, Zhao LL, Groenewald JZ, Crous PW, Zhang Y (2020) Venturiales. Studies in Mycology 96: 185–308. <https://doi.org/10.1016/j.simyco.2020.03.001>
- Stielow JB, Lévesque CA, Seifert KA, Meyer W, Irinyi L, Smits D, Renfum R, Verkley GJM, Groenewald M, Chaduli D, Lomascolo A, Welti S, Lesage-Meessen L, Favel A, Al-Hatmi AMS, Damm U, Yilmaz N, Houbraken J, Lombard L, Quaedvlieg W, Binder M, Vaas LAI, Vu D, Yurkov A, Begerow D, Roehl O, Guerreiro M, Fonseca A, Samerpitak K, van Diepeningen AD, Dolatabadi S, Moreno LF, Casaregola S, Mallet S, Jacques N, Roscini L, Egidi E, Bizet C, Garcia-Hermoso D, Martín MP, Deng S, Groenewald JZ, Boekhout T, de Beer ZW, Barnes I, Duong TA, Wingfield MJ, de Hoog GS, Crous PW, Lewis CT, Hambleton S, Moussa TAA, Al-Zahrani HS, Almaghrabi OA, Louis-Seize G, Assabgui R, McCormick W, Omer G, Dukik K, Cardinali G, Eberhardt U, de Vries M, Robert V (2015) One fungus, which genes? Development and assessment of universal primers for potential secondary fungal DNA barcodes. Persoonia 35(1): 242–263. <https://doi.org/10.3767/003158515X689135>
- Sun BD, Chen AJ, Houbraken J, Frisvad JC, Wu WP, Wei HL, Zhou Y-G, Jiang X-Z, Samson RA (2020) New section and species in *Talaromyces*. MycoKeys 68: 75–113. <https://doi.org/10.3897/mycokes.68.52092>
- Tamura K, Stecher G, Peterson D, Filipski A, Kumar S (2013) MEGA6: Molecular evolutionary genetics analysis version 6.0. Molecular Biology and Evolution 30(12): 2725–2729. <https://doi.org/10.1093/molbev/mst197>

- Tautz D, Arctander P, Minelli A, Thomas RH, Vogler AP (2003) A plea for DNA taxonomy. *Trends in Ecology & Evolution* 18(2): 70–74. [https://doi.org/10.1016/S0169-5347\(02\)00041-1](https://doi.org/10.1016/S0169-5347(02)00041-1)
- Thuong TTN, Kyo JKN, Hyang BL (2021) New species and eight undescribed species belonging to the families Aspergillaceae and Trichocomaceae in Korea. *Mycobiology* 49(6): 534–550. <https://doi.org/10.1080/12298093.2021.1997461>
- Uchida R, Imasato R, Yamaguchi Y, Masuma R, Shiomi K, Tomoda H, Ōmura S (2005) New insecticidal antibiotics, Hydroxyfungerins A and B, produced by *Metarhizium* sp. FKI-1079. *The Journal of Antibiotics* 58(12): 804–809. <https://doi.org/10.1038/ja.2005.107>
- Vilgalys R, Hester M (1990) Rapid genetic identification and mapping of enzymatically amplified ribosomal DNA from several *Cryptococcus* species. *Journal of Bacteriology* 172(8): 4238–4246. <https://doi.org/10.1128/jb.172.8.4238-4246.1990>
- Villanueva P, Vásquez G, Gil-Durán C, Oliva V, Díaz A, Henríquez M, Álvarez E, Laich F, Chávez R, Vaca I (2021) Description of the first four species of the genus *Pseudogymnoascus* from Antarctica. *Frontiers in Microbiology* 12: e713189. <https://doi.org/10.3389/fmicb.2021.713189>
- Visagie CM, Houbraken J, Frisvad JC, Hong SB, Klaassen CHW, Perrone G, Seifert KA, Varga J, Yaguchi T, Samson RA (2014) Identification and nomenclature of the genus *Penicillium*. *Studies in Mycology* 78(1): e343371. <https://doi.org/10.1016/j.simyco.2014.09.001>
- Vu D, Groenewald M, Szöke S, Cardinali G, Eberhardt U, Stielow B, de Vries M, Verkleij GJM, Crous PW, Boekhout T, Robert V (2016) DNA barcoding analysis of more than 9000 yeast isolates contributes to quantitative thresholds for yeast species and genera delimitation. *Studies in Mycology* 85(1): 91–105. <https://doi.org/10.1016/j.simyco.2016.11.007>
- Vu D, Groenewald M, de Vries M, Gehrman T, Stielow B, Eberhardt U, Al-Hatmi A, Groenewald JZ, Cardinali G, Houbraken J, Boekhout T, Crous PW, Robert V, Verkley GJM (2019) Large-scale generation and analysis of filamentous fungal DNA barcodes boosts coverage for kingdom fungi and reveals thresholds for fungal species and higher taxon delimitation. *Studies in Mycology* 92(1): 135–154. <https://doi.org/10.1016/j.simyco.2018.05.001>
- Wang LY, Xiao Y, Rao EM, Jiang L, Xiao Y, Ouyang ZY (2018) An assessment of the impact of urbanization on soil erosion in Inner Mongolia. *International Journal of Environmental Research and Public Health* 15(3): e550. <https://doi.org/10.3390/ijerph15030550>
- Wang XW, Bai FY, Bensch K, Meijer M, Sun BD, Han YF, Crous PW, Samson RA, Yang FY, Houbraken J (2019) Phylogenetic re-evaluation of *Thielavia* with the introduction of a new family Podosporaceae. *Studies in Mycology* 93(1): 155–252. <https://doi.org/10.1016/j.simyco.2019.08.002>
- White TJ, Bruns T, Lee S, Taylor J (1990) Amplification and direct sequencing of fungal ribosomal RNA genes for phylogenetics. In: Innis MA, Gelfand DH, Sninsky JJ, White TJ (Eds) *PCR Protocols: a Guide to Methods and Applications*, Academic Press, San Diego, 315–322. <https://doi.org/10.1016/b978-0-12-372180-8.50042-1>
- Woudenberg JHC, Aveskamp MM, de Gruyter J, Spiers AG, Crous PW (2009) Multiple *Didymella* teleomorphs are linked to the *Phoma clematidina* morphotype. *Persoonia* 22(1): 56–62. <https://doi.org/10.3767/003158509X427808>
- Yilmaz N, Visagie CM, Houbraken J, Frisvad JC, Samson RA (2014) Polyphasic taxonomy of the genus *Talaromyces*. *Studies in Mycology* 78: 175–341. <https://doi.org/10.1016/j.simyco.2014.08.001>

- Zhang ZY, Chen WH, Zou X, Han YF, Huang JZ, Liang ZQ, Deshmukh SK (2019a) Phylogeny and taxonomy of two new *Plectosphaerella* (Plectosphaerellaceae, Glomerellales) species from China. MycoKeys 57: 47–60. <https://doi.org/10.3897/mycokes.57.36628>
- Zhang ZY, Han YF, Chen WH, Liang ZQ (2019b) *Gongronella sichuanensis* (Cunninghamellaceae, Mucorales), a new species isolated from soil in China. Phytotaxa 416: 167–174. <https://doi.org/10.11646/phytotaxa.416.2.4>
- Zhang ZY, Han YF, Chen WH, Liang ZQ (2019c) Phylogeny and taxonomy of three new *Ctenomyces* (Arthrodermataceae, Onygenales) species from China. MycoKeys 47: 1–16. <https://doi.org/10.3897/mycokes.47.30740>
- Zhang D, Gao FL, Jakovlić I, Zou H, Zheng J, Li WX, Wang GT (2020a) PhyloSuite: An integrated and scalable desktop platform for streamlined molecular sequence data management and evolutionary phylogenetics studies. Molecular Ecology Resources 20(1): 348–355. <https://doi.org/10.1111/1755-0998.13096>
- Zhang Z, Dong C, Chen W, Mou Q, Lu X, Han YF, Huang JZ, Liang Z (2020b) The enigmatic Thelebolaceae (Thelebolales, Leotiomycetes): One new genus *Solomyces* and five new species. Frontiers in Microbiology 11: e572596. <https://doi.org/10.3389/fmicb.2020.572596>
- Zhang ZY, Zhao YX, Shen X, Chen WH, Han YF, Huang JZ, Liang ZQ (2020c) Molecular phylogeny and morphology of *Cunninghamella guizhouensis* sp. nov. (Cunninghamellaceae, Mucorales), from soil in Guizhou, China. Phytotaxa 455: 031–039. <https://doi.org/10.11646/phytotaxa.455.1.4>
- Zhang ZF, Zhou SY, Eurwilaichitr L, Ingsriswang S, Raza M, Chen Q, Zhao P, Liu F, Cai L (2021a) Culturable mycobiota from Karst caves in China II, with descriptions of 33 new species. Fungal Diversity 106(1): 29–136. <https://doi.org/10.1007/s13225-020-00453-7>
- Zhang ZY, Shao QY, Li X, Chen WH, Liang JD, Han YF, Huang JZ, Liang Z-Q (2021b) Culturable fungi from urban soils in China I: Description of 10 new taxa. Microbiology Spectrum 9(2): e00867–e21. <https://doi.org/10.1128/Spectrum.00867-21>
- Zhang ZY, Han YF, Chen WH, Tao G (2023a) Additions to Thelebolales (Leotiomycetes, Ascomycota): *Pseudogeomyces lindneri* gen. et sp. nov. and *Pseudogymnoascus campensis* sp. nov. MycoKeys 95: 47–60. <https://doi.org/10.3897/mycokes.95.97474>
- Zhang ZY, Feng Y, Tong SQ, Ding CY, Tao G, Han YF (2023b) Morphological and phylogenetic characterisation of two new soil-borne fungal taxa belonging to Clavicipitaceae (Hypocreales, Ascomycota). MycoKeys 98: 113–132. <https://doi.org/10.3897/mycokes.98.106240>

## Supplementary material 1

### Strain numbers and sequence accession numbers of new isolates

Authors: Zhi-Yuan Zhang, Xin Li, Wan-Hao Chen, Jian-Dong Liang, Yan-Feng Han

Data type: table (word document)

Copyright notice: This dataset is made available under the Open Database License (<http://opendatacommons.org/licenses/odbl/1.0/>). The Open Database License (ODbL) is a license agreement intended to allow users to freely share, modify, and use this Dataset while maintaining this same freedom for others, provided that the original source and author(s) are credited.

Link: <https://doi.org/10.3897/mycokes.98.102816.suppl1>

## Supplementary material 2

### Strains used in this study

Authors: Zhi-Yuan Zhang, Xin Li, Wan-Hao Chen, Jian-Dong Liang, Yan-Feng Han

Data type: table (excel document)

Copyright notice: This dataset is made available under the Open Database License (<http://opendatacommons.org/licenses/odbl/1.0/>). The Open Database License (ODbL) is a license agreement intended to allow users to freely share, modify, and use this Dataset while maintaining this same freedom for others, provided that the original source and author(s) are credited.

Link: <https://doi.org/10.3897/mycokeys.98.102816.suppl2>

## Supplementary material 3

### The concatenated sequences dataset

Authors: Zhi-Yuan Zhang, Xin Li, Wan-Hao Chen, Jian-Dong Liang, Yan-Feng Han

Data type: .zip file

Copyright notice: This dataset is made available under the Open Database License (<http://opendatacommons.org/licenses/odbl/1.0/>). The Open Database License (ODbL) is a license agreement intended to allow users to freely share, modify, and use this Dataset while maintaining this same freedom for others, provided that the original source and author(s) are credited.

Link: <https://doi.org/10.3897/mycokeys.98.102816.suppl3>